

Editors: Tasman, William; Jaeger, Edward A.

Title: *Duane's Ophthalmology, 2009 Edition*

Copyright ©2008 Lippincott Williams & Wilkins

> Table of Contents > Duane's Foundations of Clinical Ophthalmology > Volume 2 > Physiology of the Eye and Visual System >
Chapter 4 - Cornea and Sclera

Chapter 4

Cornea and Sclera

Daniel G. Dawson

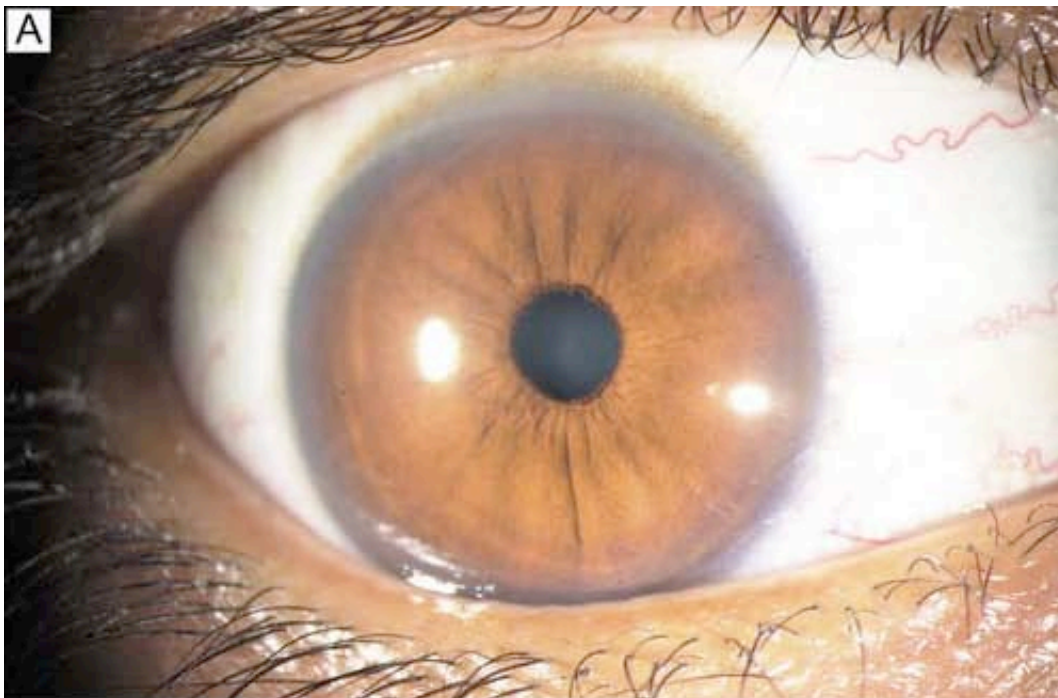
Mitchell A. Watsky

Dayle H. Geroski

Henry F. Edelhauser

CORNEA

The cornea covers the anterior one-sixth of the total circumference of the globe (Fig. 1), whereas the sclera covers the remaining five-sixths. The cornea is a clear, transparent, colorless avascular structure richly supplied with sensory nerve endings that generally subserve touch and pain. There are no lymph vessels or other channels for bulk fluid flow. The interface between the corneal tear film and the ambient atmosphere provides roughly two-thirds of the refractive power of the human eye. The cornea itself is resilient, yet is described as viscoelastic in its response to stretching forces.



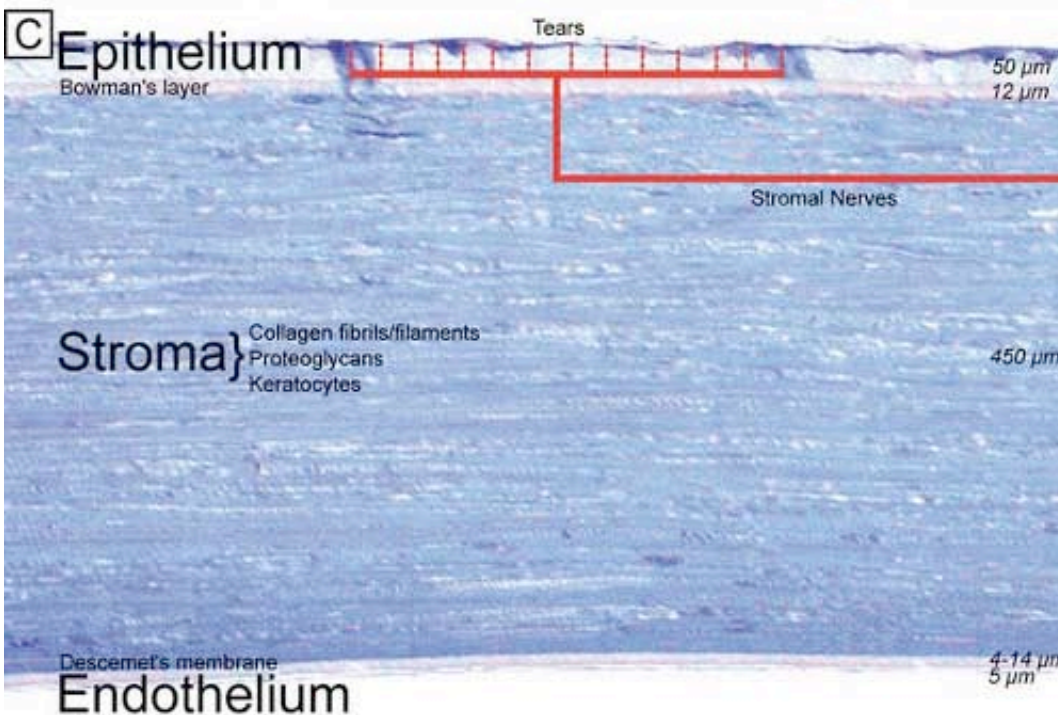


Figure 1. (A) Diffuse illumination slit-lamp view of the human cornea. (B) Slit-beam illumination slit-lamp view of the human cornea shows an optical section of the tissue. Notice the slight light scattering that occurs in the tissue, mainly from cellular components in cornea. (C) Histologic diagram of the major cellular and extracellular matrix components of the human cornea (toluidine blue 25 \times).

Due to the avascular nature of the cornea, much of its oxygen requirement for metabolic activities comes from atmospheric oxygen dissolved in the tear film. When the eyelids are closed, oxygen can also predominantly enter the tear film from the superficial conjunctival capillaries. Most nutrients such as carbohydrates, vitamins, amino acids, and other substrates are primarily delivered to the cornea through the leaky corneal endothelial barrier with a minor contribution from the vascular arcades of the limbus. Certain growth factors, immune constituents, and other substrates like retinol are also secreted by the lacrimal gland and delivered to the cornea by the tears. Carbon dioxide and other metabolic end products are removed across the corneal endothelium to the aqueous humor, by the tear film, or through the limbal capillaries.

EMBRYOLOGY AND DEVELOPMENT

Following lens vesicle formation, which occurs between 4 to 5 weeks of gestation (27 to 36 days), surface ectodermal cells cover the defect left by lens vesicle invagination and become the primitive corneal epithelium composed initially of two cell layers. Similar to the avian cornea, the primitive epithelium of the primate cornea appears to be responsible for forming a prominent primary acellular corneal stroma, also known as the Bowman's layer, which becomes detectable around 20 weeks of gestation. It should be noted, however, that the primate cornea's ectodermal phase (primary acellular stroma) is de-emphasized compared to the mesodermal phase (secondary cellular stroma) and is less well organized in ultrastructure compared to that of the avian cornea.

Sometime between when the eyelids fuse together (8 weeks gestation) and by the time the eyelids open (26 weeks gestation), the epithelium stratifies to four to five cell layers thick. The basal epithelial cells, which secrete an underlying basement membrane called the basal lamina, are cuboidal to columnar. Above this layer are interdigitating wing cells and, most superficially, a layer of flattened squamous epithelial cells. Early in gestation, adhesion complexes (hemidesmosomes, anchoring fibrils, and anchoring plaques) on the basal surface of the epithelium are absent. Rudimentary adhesion complexes only become detectable by 19 weeks of gestation. With further development in utero, the number of hemidesmosomes increases, anchoring fibril penetration into the Bowman's layer increases, and Bowman's layer thickens.

A first wave of neural crest-derived mesodermal cells begins to extend beneath the corneal epithelial cells from the limbus around 5 weeks of gestation (33 days); these cells form the primitive endothelium. The primitive endothelium is initially composed of two cell layers, which by 8 weeks of gestation become a monolayer that starts to produce Descemet's membrane. The epithelium and endothelium remain closely opposed until 7 weeks of gestation (49 days) when a second wave of mesoderm begins to grow centrally from the limbus between the epithelium and endothelium. This tissue forms the secondary cellular corneal stroma, and extracellular collagen is produced within a few days. During the third month of gestation, Descemet's membrane is secreted by the endothelial cells and can be recognized in histologic sections. By the seventh month of gestation, the cornea resembles that of the adult in most structural characteristics other than size.

At birth in the full-term infant, the horizontal diameter of the cornea is only around 9.8 mm (surface area 102 mm²), or approximately 75% to 80% of the size of the adult human cornea. (Note that the posterior segment is less than 50% of adult size at birth.) Additionally, at birth, the cross-sectional thickness of the epithelium averages 50 µm, the Bowman's layer averages 12 µm, the central cellular corneal stroma averages 450 µm, Descemet's membrane averages 4 µm, and the endothelium averages 5-µm thick.

During infancy, the cornea continues to grow over the first years of life, reaching adult size at 2 years old with a horizontal diameter of 11.7 mm (surface area 138 mm²) and changes very little in size, shape, and optical properties thereafter. The only significant structure in the cornea that thickens with age is the Descemet's membrane, which gradually increases an additional 6 to 11 µm from birth to senescence.

OPTICAL PROPERTIES

The average index of refraction of the cornea and tear film taken as a whole is about 1.376. The refractive power for the anterior surface of the cornea may be computed by the following formula:

$$D = n' - n / r = D = 1.376 - 1.000 / 0.0078 = 48.2$$

where D equals diopters of optical power, n is the index of refraction of air (1.000), n' is the index of refraction of the whole cornea, and r is the radius of curvature of the anterior corneal surface in meters.

The posterior surface of the cornea is bathed with aqueous humor. By applying the same formula, we arrive at the following value for the optical power of the posterior corneal surface, where n' is the refractive index of aqueous humor (1.336):

$$D = n' - n/r = 1.336 - 1.376 / 0.0065 = -6.2$$

Therefore, the total optical power of the cornea is $48.2 - 6.2$, or approximately 42.0 D, which is about two-thirds of the 60.0 D total optical power of the human eye. Because the cornea is thinner in the center than in the periphery, it should act as a minus lens but functions as a plus lens because the aqueous humor neutralizes most of the minus optical power on the posterior corneal surface. If we compute the power of the posterior corneal surface in air, we would find the following:

$$D = 1.000 - 1.375 / 0.0065 = -96.0$$

By subtracting the plus power of the anterior surface, the resulting net power for the cornea in air becomes -96.0 D + 42.0 D = -54.0 D, a powerful minus lens.

From the previous calculations, it is obvious that the most important refracting surface is that of the anterior cornea. However, if a large air bubble is placed in the anterior chamber so that it contacts the corneal endothelium or if the anterior surface of the cornea is submerged in water—thereby destroying the corneal-air interface—tremendous changes in the refractive power of the eye occur. When the eye is open underwater, the optical imagery is extremely blurred; the index of refraction of water is quite similar to that of the cornea and most of the optical power of the anterior corneal surface is lost. If the tear film-air interface is maintained by the use of a mask or goggles, then underwater mask vision is as sharp and clear as normal terrestrial vision.

A contact lens placed on the corneal surface is an efficient way of correcting optical errors in the dioptic system of the eye. This is particularly true for errors that are caused by abnormalities of corneal curvature. The contact lens placed upon the corneal surface has the same index of refraction as the cornea and becomes covered immediately with the normal corneal tear film. Therefore, the contact lens becomes, in effect, a new part of the cornea.

Several surgical procedures have also been developed to permanently alter the curvature of the cornea, thereby reducing nonpathologic refractive errors. The procedures most commonly performed today include laser-assisted in situ keratomileusis (LASIK), photorefractive keratectomy (PRK), and astigmatic keratotomy (AK). LASIK and PRK are surgical techniques that use an excimer laser (193 nm) to ablate the anterior corneal stroma with submicron accuracy and create a new refractive surface. LASIK is different from PRK in that it involves a mechanical or laser created lamellar keratectomy step before the excimer ablation step, which is applied to the underlying residual mid-stromal bed. PRK ablation directly occurs on the surface of the cornea (Bowman's layer and anterior stroma). Both procedures have been used on myopic and hyperopic eyes with up to a mild degree of astigmatism and produce similar visual outcomes. AK is an incisional keratotomy technique that cuts up to 90% depth arcs in the peripheral cornea using a scalpel to reduce astigmatism by flattening the cornea in the visual axis over the area of the cut. AK is usually performed in association with cataract surgery.

GROSS ANATOMY

When viewed anteriorly in the living eye, the adult human cornea is somewhat elliptical; the largest measurement is typically in the horizontal meridian (mean 11.7 mm) and the smallest is in the vertical meridian (mean 10.6 mm). The elliptical configuration is brought about by an anterior extension of the opaque scleral structure superiorly and inferiorly. When viewed from the posterior surface of the dissected eye, the cornea is circular, with an average horizontal and vertical measurement of 11.7 mm. The average radius of curvature of the anterior corneal surface is 7.8 mm, which is significantly less than the 11.5 mm average radius of curvature of the sclera. This results in a small, 1.5- to 2-mm wide transition zone that forms an external and internal surface groove, or *scleral sulci*, where the steeper cornea meets that of the flatter sclera. These sulcus typically are not as obvious to see clinically because they are filled in by overlying episclera and conjunctiva or trabecular meshwork.

The tissue in this transition zone is known as the limbus and is important because it is used as surgical landmark for various anterior segment surgeries, contains corneal epithelial stem cells, contains the conventional outflow

pathway for the aqueous humor, is the inciting site of pathology in a few immunologic or cancerous diseases, and possibly contains stem-like corneal endothelial cells (Fig. 2). The limbus is a definite anatomic landmark, or geographical reference, used for planning surgical entry into the anterior segment because it appears clinically as a blue transition zone. Therefore, an incision placed anterior to blue zone is anatomically in the peripheral cornea, safely inside the trabecular meshwork.

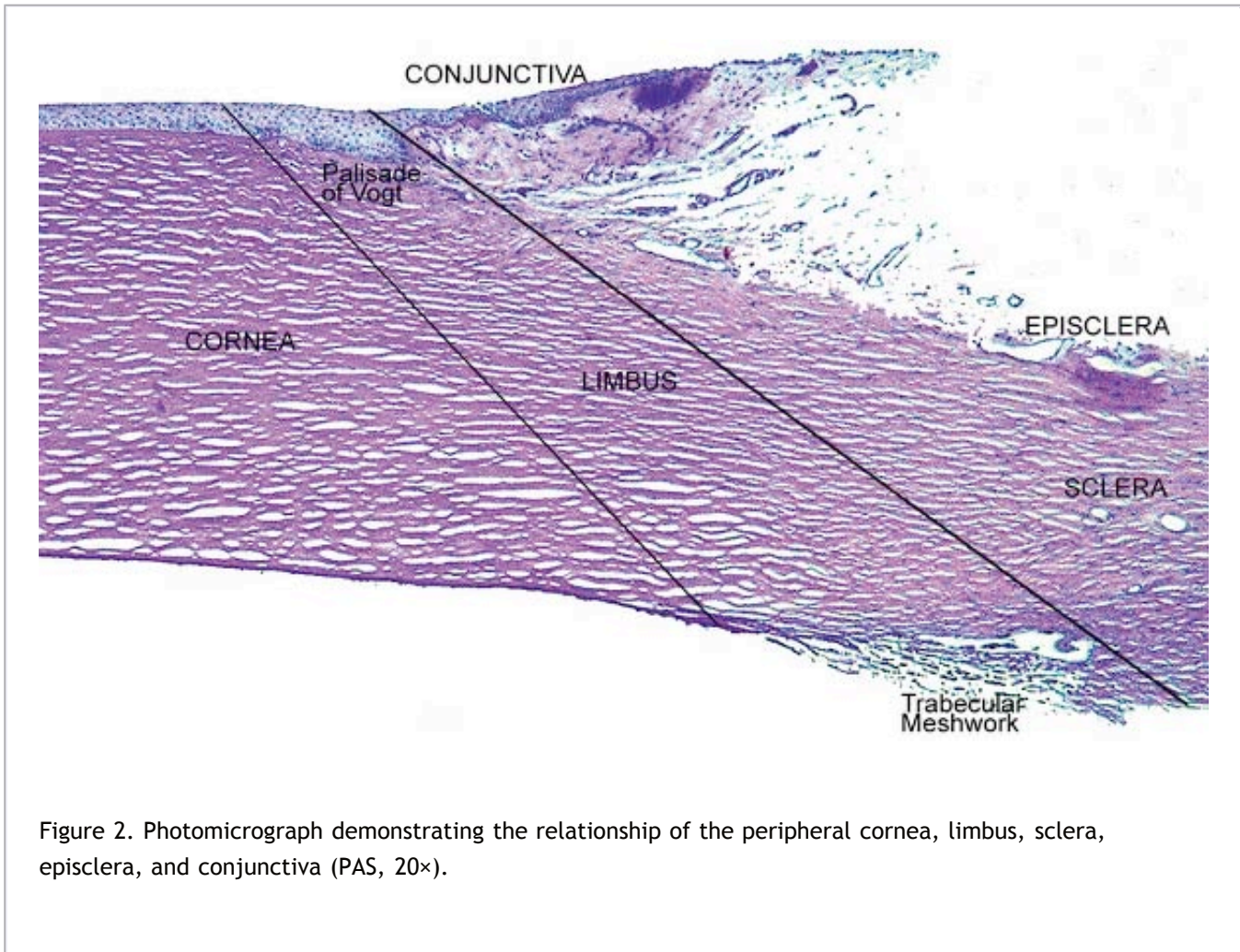


Figure 2. Photomicrograph demonstrating the relationship of the peripheral cornea, limbus, sclera, episclera, and conjunctiva (PAS, 20×).

The cornea is thinner in the center, measuring on average 520 μm and increases in thickness to approximately 700 μm as it reaches the limbus.^{1,2,3,4} The central 4 mm of the cornea overlying the pupil contains the optical center of central vision. It typically has a regular surface and structure, and commonly is near exact in spherical configuration. The more peripheral portions of the cornea are often slightly irregular and torical in configuration rather than spherical, giving the whole cornea a hyperbolic shape. If the central cornea is not exactly spherical, the condition of astigmatism (*stigma* meaning a point) usually results. With astigmatism, an optical image without a single point focus forms within the eye resulting in two line foci.

The average radius of curvature for the posterior corneal surface is shorter than the anterior corneal surface at 6.5 mm. In adult humans, the conjunctival surface area has been measured at 17.65 cm^2 , and the corneal surface area measures 1.38 cm^2 , giving a c/c ratio of 12.8.⁵ Because topical lipophilic drug delivery to the anterior chamber occurs primarily through the cornea with the conjunctiva supplying a minor secondary delivery route, surface area ratios of the cornea and conjunctiva are important because a large conjunctiva-to-corneas (c/c) surface area ratio results in less drug delivery to the anterior chamber. Therefore, surface area ratios need to be considered when comparing drug delivery studies.

MICROSCOPIC ANATOMY, ULTRASTRUCTURE, AND PHYSIOLOGY OF THE EPITHELIUM

The anterior surface of the human cornea is covered by a transparent, nonkeratinized, stratified (five- to seven-cell layer) squamous epithelium uniformly around 50 μm in thickness that is continuous with the epithelium of the limbus and conjunctiva (Figs. 1, 2, and 3). The basal corneal epithelial cells actively secrete extracellular material (type IV collagen, laminin, heparin, and small amounts of fibronectin and fibrin) that forms an underlying 75-nm thick basement membrane called the *basal lamina*. On electron microscopy, the morphology of basal lamina appears to be composed of two distinct layers: a 25-nm thick lamina lucida and a 50 nm thick lamina densa (Fig. 3).

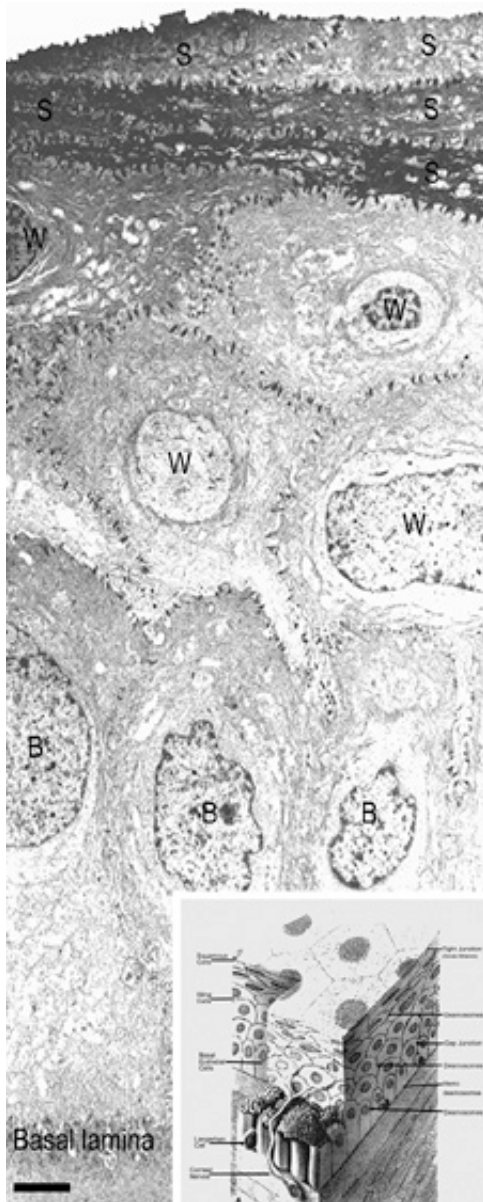


Figure 3. Transmission electron micrograph (3,500 \times) of the central corneal epithelium with a summary diagram (inset). Microvilli project from the anterior corneal surface into the tear film. S, squamous cells; W, wing cells; B, basal epithelial cells. Bar = 1 μm . (Inset modified from Hogan MJ, et al. *Histology of the human eye*. Philadelphia, WB Saunders, 1971.)

The cytoplasm of a corneal epithelial cell primarily contains cytoskeletal intermediate filaments and has sparse cytoplasmic organelles (i.e., mitochondria, endoplasmic reticulum, and golgi apparatus). The predominant cytoplasmic filament is keratin, whereas actin and microtubules are two other major types found in corneal epithelial cells. The epithelial cells are held together to one another by numerous anchoring junctions called *desmosomes*, whereas the basal surface of the epithelium adheres to the basal lamina and underlying Bowman's layer through an adhesion complex composed of hemidesmosomes, anchoring fibrils (type VII collagen), and anchoring plaques (Fig. 4). The function of the corneal epithelium is twofold: (a) to form a barrier from the environment to the corneal stroma of the cornea, and (b) to form a smooth refractive surface on the cornea through interaction with the tear film.

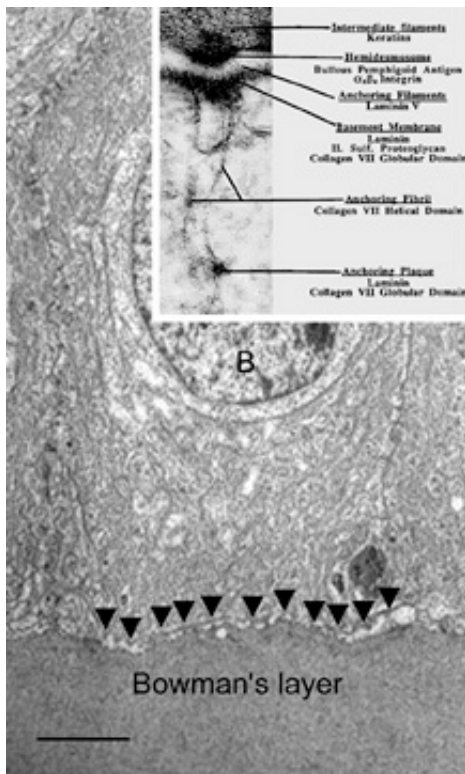


Figure 4. Transmission electron micrograph (10,000 \times) of a basal epithelial cell showing the adhesion complexes (arrowheads) that anchor it in place onto the Bowman's layer and summary inset. B, basal epithelial cell. Bar = 1 μm . (Inset from Albert and Jakobiec: Principles and practice of ophthalmology. Philadelphia, WB Saunders, 2000.)

The epithelial cells differentiate from the basal layer to form two to three cell layers of wing cells and finally to form two to three cell layers of squamous cells (Fig. 3). The squamous cells form a barrier junction because they are surrounded by a continuous encircling band of zonula occludens tight junctions, which serve as a semipermeable, high-resistance (12-16 $\text{k}\Omega \text{ cm}^2$) membrane^{6,7} by closing off the intercellular space. This barrier prevents the movement of fluid from the tears into the stroma and also protects the cornea and intraocular structures from infectious pathogens. The apical surface of the corneal epithelium is specialized to maintain the tear film as microplacae and microvilli on the surface of the most superficial epithelial cells is covered with a glycocalyx and membrane-spanning mucins (MUC 1 and possibly MUC 4); altogether these structures and substances form the 1.0 μm thick mucinous layer of the tear film (Fig. 5).^{8,9,10}

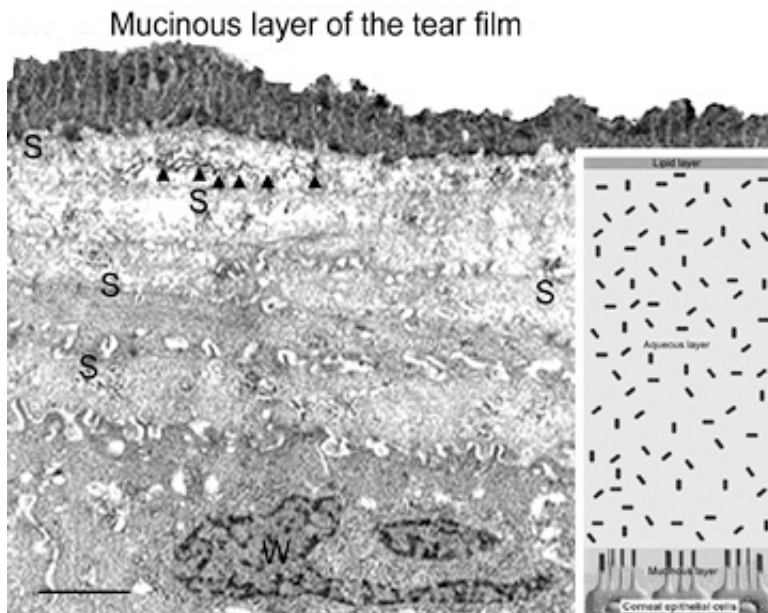


Figure 5 Transmission electron micrograph (10,000 \times) of surface epithelium from a specimen specially-preserved (glutaraldehyde + cetylpyridium chloride) and stained (tannic acid) to show the mucinous layer of the tear film (glycocalyx + membrane-bound mucins). Inset is a summary diagram showing how the tear film layers interact with the microvillae of the surface squamous epithelial cells. S, squamous cells; W, wing cells. Arrowheads = zonula occludens tight junctions. Arrowheads = zonula adherens tight junctions. Bar = 1 μ m.

The tear film typically measures 7 to 10 μ m in thickness and contains three layers (mucinous, aqueous, and lipid layers). Recently, the aqueous layer of the tear film has been found to contain gel-forming mucins (MUC 5AC and 2) along with lysosyme, immunoglobulin A, transferrin, defensin, and trefoil factor (Fig. 5, *inset*).¹⁰ Overall, the tear film functions in maintaining a healthy ocular surface by preventing ocular infections and forming a smooth optical surface required for clear vision. Deficiencies in the components that compose any of these layers potentially can cause ocular surface disease.

The corneal epithelium is in a state of constant healing as squamous cells are continuously

shed into the tear film (Fig. 6). It is estimated that all the cell layers of the corneal epithelium completely turn over every 7 to 10 days. The epithelial surface is maintained by basal epithelial cells, which can undergo mitosis resulting in two daughter cells that are found anterior to the basal cell layer, thus forming two wing cells and eventually squamous cells.^{11,12,13} This delicate balance of shedding followed by proliferation is critical in maintaining a smooth and uniform epithelial surface around 50 μ m in thickness. The shedding step is primarily induced by the friction that occurs from involuntary eyelid blinking, which happens on average every 7 seconds.

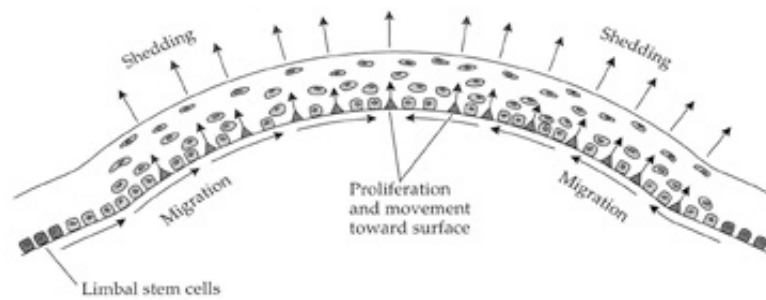


Figure 6. Diagram showing how the basal epithelial cells are continually replenished by a stem cell population that resides in the limbus. The basal epithelial cells migrate forward from the periphery to the center of the cornea. When they undergo mitosis, both daughter cells move into the anterior layers of the epithelium and continually move up in epithelium until eventually being shed. (From Thoft RA, et al. The X, Y, Z hypothesis of corneal epithelial maintenance. *Invest Ophthalmol Vis Sci* 24:1442, 1983.)

The signal for basal epithelial cell proliferation probably comes via the gap junctions, especially in the more basal layers, with connexin 43 being one of the common gap junction proteins present.^{7,14} Interestingly, gap junction communication between corneal epithelial cells is promoted by low concentrations of bicarbonate, which is abundant in the aqueous humor and tear film.¹⁵ The barrier function of the epithelium itself is due to zonula occludens tight junctions between the most superficial epithelial junction, which are made up of the tight junction proteins ZO-1, occludin, and claudin-1 as well as other claudin sub-types.¹⁶ Under normal conditions, this barrier is extremely tight, preventing the movement of ions between the superficial squamous cells. In some instances (*e.g.*, trauma, contact lens wear, infection), however, this barrier can be compromised. Activation of protein kinase C (PKC) by the mitogen-activated protein kinase (MAP kinase) signaling pathway, which in itself is activated by external stimuli such as growth factors and tyrosine kinases, appears to cause disruption of the epithelial barrier and perhaps is an initiating factor for basal cells to proliferate.¹⁷

In addition to basal epithelial cell mitosis, the corneal epithelium is maintained by migration of new basal epithelial cells into the cornea from the limbus. The cells migrate centripetally at about 120 $\mu\text{m}/\text{week}$ and originate from a subpopulation of limbal epithelial cells.^{18,19,20} Therefore, it appears that the corneal epithelium is maintained by a balance among the processes of limbal cell proliferation, basal corneal epithelial cell migration and proliferation, and shedding of superficial squamous corneal epithelial cells.^{21,22} This concept has been coined the X, Y, Z hypothesis by Thoft [X (basal corneal epithelial cell proliferation) + Y (limbal cell proliferation and basal corneal epithelial cell centripetal migration) = Z (epithelial cell loss from the surface)].²²

When this equilibrium is disturbed, corneal epithelial cell wound healing typically begins. Interestingly, after injury, these processes typically return back to equilibrium with a certain degree of adaptability. For instance, after epithelial and stromal injury, if a stromal deficit occurs (*e.g.*, corneal ulcers) then the epithelium can still maintain a smooth anterior surface either by developing elongated hypertrophic basal epithelial cells and/or by developing epithelial hyperplasia (> six cell layers).²³

As first described in the early 1960s by Maumenee, and expanded upon in the early 1970s by the work of

Davanger and Evensen and in the early 1980s by Shapiro, Friend and Thoft, the limbal epithelium contains cells that have the ability to resurface the cornea following loss of the corneal epithelium.^{24,25,26} This concept was applied clinically by Thoft in 1977, who described the use of autologous limbal epithelial transplants to treat unilateral chemical injury.²⁷ Subsequently, further study has determined that a portion of limbal basal epithelial cells are actually undifferentiated corneal epithelial cells, also known as corneal epithelial stem cells.^{28,29} These stem cells have the characteristics of being extremely long-lived, with very slow cell cycle times and a high proliferative potential. They anatomically are found within a well-defined, protective microenvironment called the *palisades of Vogt* (Fig. 7) and are controlled via delicate regulatory mechanisms.^{30,31,32} The progeny of stem cells are referred to as *transient amplifying (TA) cells*, which are cells that have more rapid cell cycles, yet have far less replicative potential than their parent stem cells. During terminal differentiation from the basalepithelial cell layer, the daughter cells migrate anteriorly in the epithelium becoming wing cells and, lastly, squamous cells.

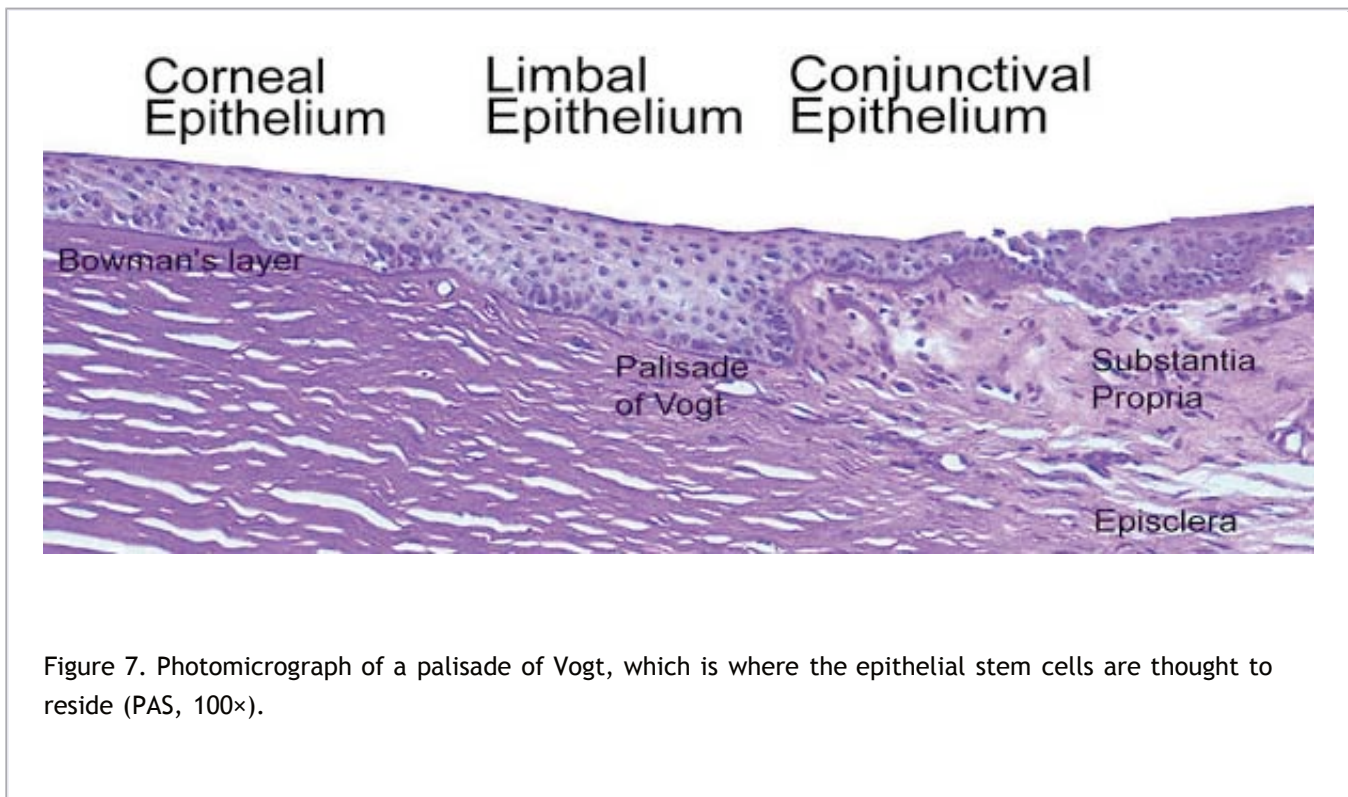


Figure 7. Photomicrograph of a palisade of Vogt, which is where the epithelial stem cells are thought to reside (PAS, 100×).

When the mammalian cornea is mounted in an Ussing chamber, it generates a transepithelial potential of 25 to 40 mV. This relatively high voltage is consistent with the low ionic conductance of the apical epithelial cell membranes and the high resistance of the tight junctions of the paracellular pathway, which normally is in the range of 12 to 16 $k\Omega\text{ cm}^2$.⁶ Almost 50% of the short-circuit current across the corneal epithelium is carried by chloride ions moving through apical membrane channels into the tears. This current is due to ionic gradients set up by epithelial transport of Na^+ and Cl^- ions. Na^+ ions are pumped from the epithelial cells toward the stroma by the Na^+/K^+ adenosine triphosphatase (ATPase) in the lateral membranes of the cells, which, as in other cells, maintains an inward Na^+ gradient. A Na^+ -chloride co-transporter, also located in the lateral membrane, facilitates the influx of Na^+ down its electrochemical gradient, carrying along chloride ions. The chloride ions then diffuse through channels in the apical membranes. This chloride secretion is blocked when the Na^+/K^+ ATPase is inhibited by ouabain, demonstrating the coupling of chloride secretion to Na^+ transport.^{33,34,35,36}

In addition to the transport mechanisms described, the corneal epithelial cells also contain a Na^+/H^+ exchanger and a lactate- H^+ co-transporter. These transport mechanisms serve to regulate intracellular pH by extrusion of

lactate and H⁺ ions.³⁷ The above discussion raises questions concerning the overall role of these transport mechanisms and second-messenger systems in corneal epithelial function. It has been demonstrated in vitro that ion transport can osmotically move water from the stroma to tears⁶; however, in vivo epithelial ion transport probably has a limited role, if any, in corneal deturgescence as compared to the endothelium.

Finally, it has been shown in both animal and human specimens that the corneal epithelium, although devoid of melanocytes, does contain immune cells. The basal epithelial cell layer of the peripheral cornea, along with the limbus and the conjunctiva, appears to have a subpopulation of cells intermixed that are bone-marrow-derived immune surveillance cells with high constitutive expression of major histocompatibility complex (MHC) type II antigen and co-stimulatory molecules.³⁸ This type of immune cell has previously been termed a *Langerhans cell*,³⁹ which functions as a “professional” antigen-presenting cell with an extraordinary capacity to initiate T-cell lymphocyte-dependent responses.⁴⁰ The functional steps of this cell type include the uptake and processing of antigens, the migration out of the cornea to lymph nodes where they stimulate naïve T-lymphocyte immune responses by presenting antigens and overexpressing co-stimulatory molecules. Recently, the central corneal epithelium also was found to have a similar subpopulation of immune cells that are apparently “immature” Langerhans cell types because their constitutive expression of MHC type II antigen and costimulatory molecules is low.⁴¹ Interestingly, these “immature” Langerhans cells under certain circumstances (*e.g.*, inflammation or trauma) may develop the requisite signals for T-cell priming.⁴¹

MICROSCOPIC ANATOMY, ULTRASTRUCTURE AND PHYSIOLOGY OF THE STROMA

The corneal stroma accounts for 90% of the corneal thickness. It is predominantly composed of water (78% hydrated or 3.5 g H₂O/g dry weight), which is stabilized by an organized structural network of insoluble and soluble cellular and extracellular proteins (Fig. 1).⁴² The dry weight of the adult human corneal stroma is made up of collagen (68%), keratocyte constituents (10%), proteoglycans (9%), and salts, glycoproteins, or other substances.⁴³

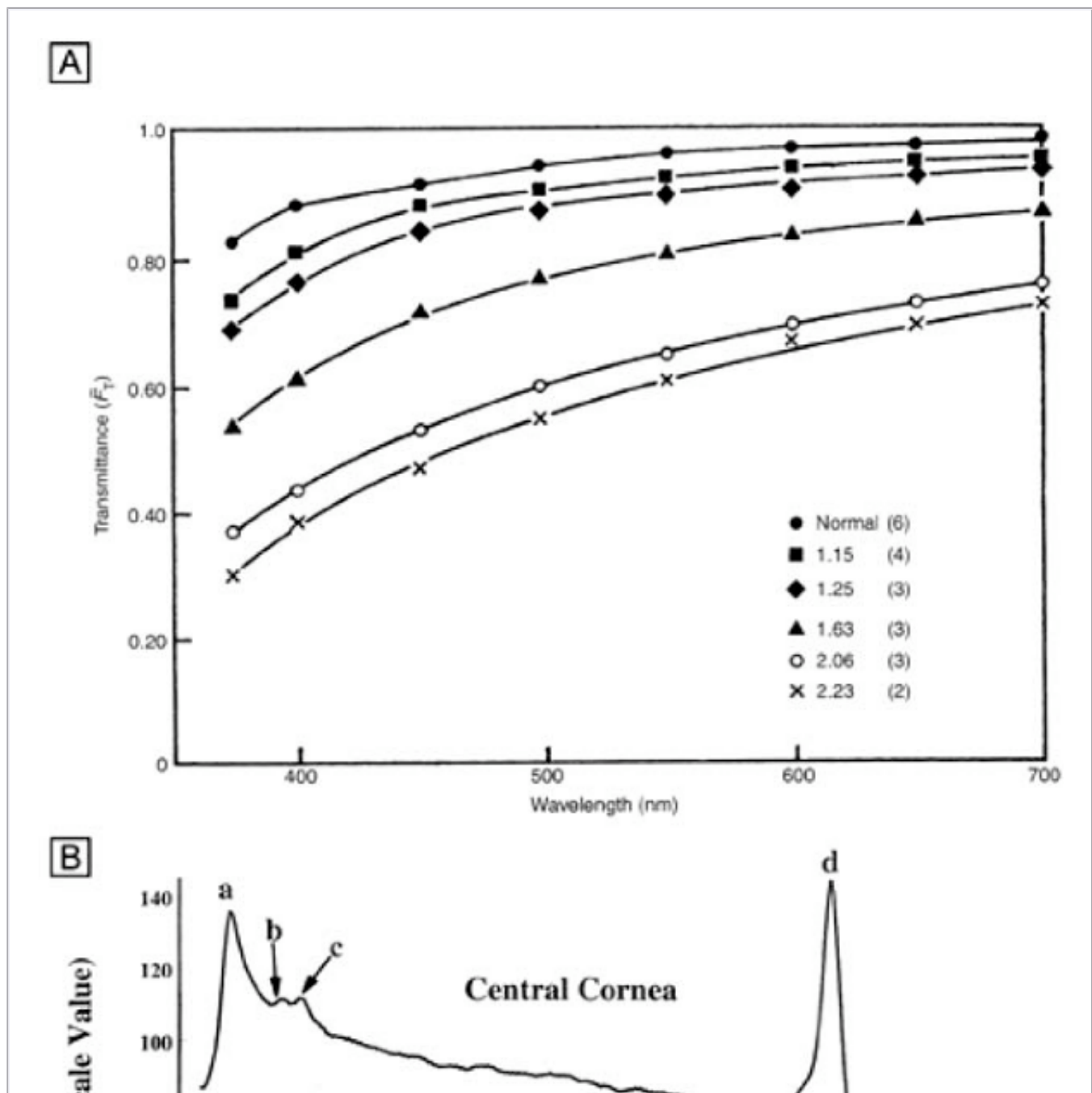
Collagen is a water-insoluble structural protein organized into an inextensible scaffold that forms the basic structural framework of connective tissues. In the human cornea, stromal collagens are poorly-ordered in the Bowman's layer (*i.e.*, the primary acellular stroma that is presumably ectodermally-derived), whereas they form a highly-ordered lattice-like structure in the secondary cellular stroma (neural crest-derived).⁴⁴ Overall, the corneal collagens are functionally important in establishing tissue transparency and in resisting tensile forces because collagen fibrils and filaments hold the cornea together (*i.e.*, cohesive strength), ultimately defining the size of the tissue.

Keratocyte components make up the second major component of the cornea's dry weight. Interspersed between collagen lamellae throughout the secondary cellular stroma, keratocytes form a closed, highly-organized syncytium. Keratocytes are neural crest-derived cells that enter the cornea during the second mesenchymal wave of corneal embryologic development. They function as modified fibroblasts during neonatal life, forming the extracellular matrix of the secondary cellular stroma. Subsequently, they typically remain in the cellular stroma throughout life as modified fibrocytes where they maintain the extracellular matrix of the corneal stroma, usually in an inconspicuous, or relatively transparent, fashion.

Proteoglycans, which are water-soluble glycoproteins, are the third major component of the cornea's dry weight. Each proteoglycan molecule consists of a protein core with a covalently attached anionic polysaccharide side chain called a glycosaminoglycan (GAG). The proteoglycans are three-dimensionally ordered in the corneal stroma because the protein core of the molecule is noncovalently attached to collagen fibrils evenly throughout the tissue, whereas the GAG sidechain extends into the interfibrillar space where it acts as a pressure-exerting polyelectrolyte gel.^{45,46,47} After Hedbys showed that the cornea collapses to around 20% of its volume if the

proteoglycans in the tissue are precipitated with cetylpyridinium,⁴⁸ it has become quite apparent that the primary function of proteoglycans is to provide tissue volume, maintain spatial order of collagen fibrils, and resist compressive forces. Water, collagens, proteoglycans, and keratocytes work together to maintain and establish a transparent cornea, while also creating a tough and resistant structure that keeps ocular integrity intact and maintains a stable shape.

Interestingly, although the cornea primarily absorbs light between 200 to 295 nm (ultraviolet)⁴⁹ and transmits variable amounts of light from around 300 nm in wavelength (ultraviolet) to 2,500 nm in wavelength (infrared)⁵⁰, peak transmission (95% to 99% of the incident light) occurs along wavelengths where light is visible to humans (visible spectrum of light = 400 to 700 nm). The remaining portion that is not directly transmitted (1% to 5%) is scattered in all directions by the cornea in a wavelength dependent fashion or absorbed by the tissue (Fig. 8).⁵¹ Clinical slit-lamp examination and in vivo confocal microscopy suggests that most of the scattered light (*i.e.*, reflected and scattered light) comes from cellular components in the cornea (endothelial cells > epithelial cells > nerve cells > keratocytes) as opposed to collagen fibrils (Figs. 1B and 8, bottom).^{52,53}



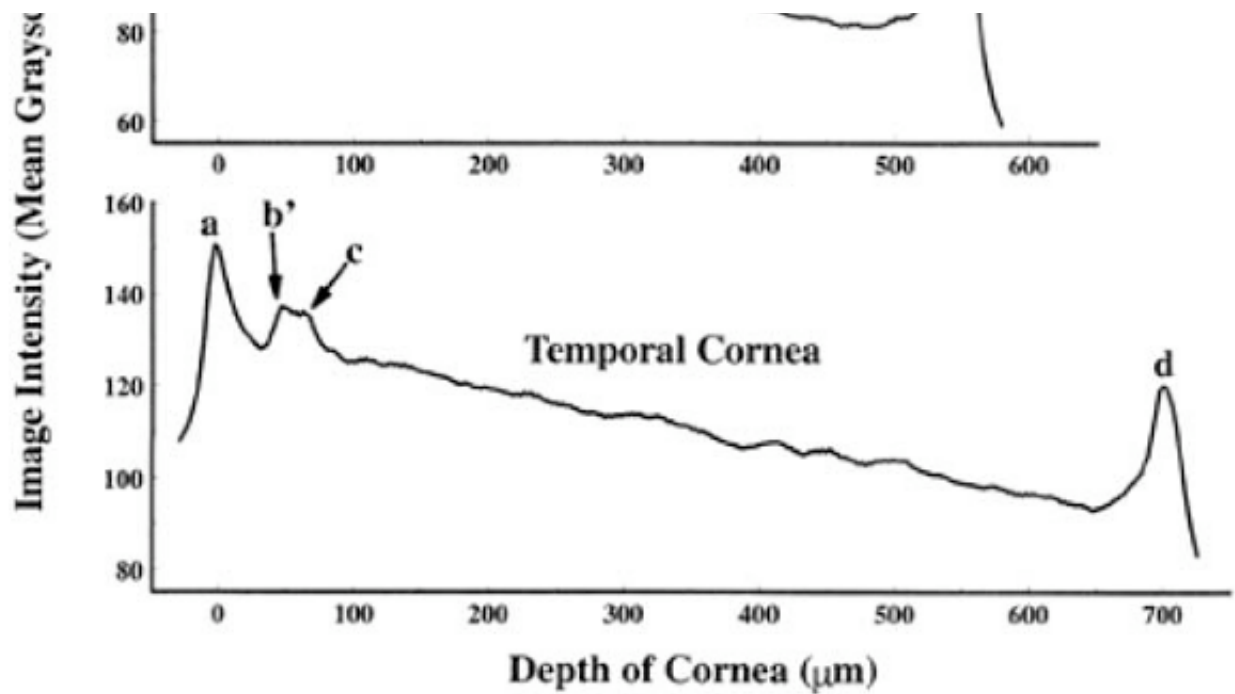


Figure 8. (A) Experimental values for the fraction of light transmitted through normal and edematous rabbit corneas as a function of wavelength. The ratio of the thickness of the edematous corneas to normal thickness values and the number of corneas used for each curve are given in the key. (From Farrell RA, et al. Wave-length dependencies of light scattering in normal and cold swollen rabbit corneas and their structural implications. *J Physiol* 233:589, 1973.) (B) In vivo confocal microscopy back-scattered light intensity profiles from the central and temporal portions of a 25-year-old human cornea. Intensity peaks correspond to the (a) epithelium, (b) subbasal nerve plexus, (c) most anterior keratocytes layer, and (d) endothelium. (From Patel SV, et al. Normal human keratocyte density and corneal thickness measurement by using confocal microscopy in vivo. *Invest Ophthalmol Vis Sci* 42:333, 2001.)

Collagen molecules measure 1.5 nm in width by 300 nm in length and are composed of a triple helix of three alpha chains (Fig. 9, top). There currently are 19 known collagen types as determined by the combination of alpha-chains that form the collagen molecule. The most common types usually aggregate into structural, banded (repeating pattern of polar amino acids seen on transmission electron microscopy [TEM]) fibrils by ordering themselves into a quarter-staggered parallel arrangement that is further stabilized in position by covalent intermolecular cross-links (Fig. 9, middle).

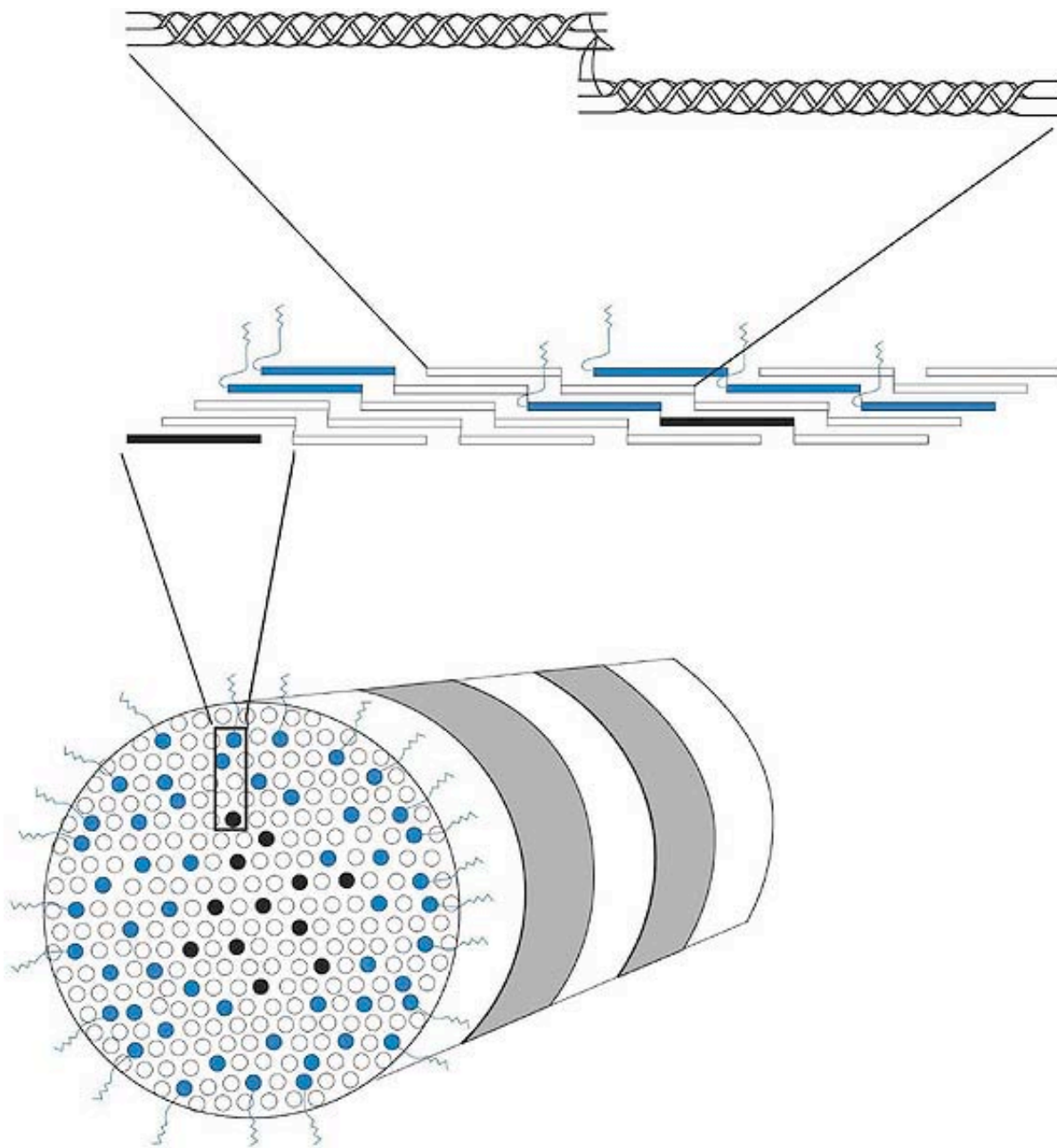


Figure 9. Cross-sectional oblique view of a 25-nm diameter, heterotypic, banded (periodicity = 68 nm) corneal stromal collagen fibril (bottom) composed of type I (white), III (black), and V (blue) collagen molecules. The amino-terminal domains on the type V collagen molecules appear to be important in regulating collagen fibril diameter as they project external to the fibril surface and presumably block further accretion of collagen molecules through steric and/or electrostatic hindrance effects. Notice that the collagen molecules on longitudinal view (middle) are aligned in a parallel, quarter-staggered (68 nm) arrangement with 40 nm gaps between molecules. Also, note that the longitudinal view (top) shows clearly that the ends of the alpha chains in each collagen molecules form intermolecular cross-links with adjacent collagen molecules.

Collagen fibrils are generally heterotypic (composed of two or more types of collagen molecules) and reach certain diameters based on their composition of collagen types. The fibrils in the corneal stroma are a co-polymerization of collagen types I, III, and V molecules that form uniform 22-nm diameter fibrils in the acellular Bowman's layer and uniform 25-nm diameter fibrils in the cellular corneal stroma with only slight variability

(Figs. 9, bottom and 10).^{54,55} Although the refractive index of collagen fibrils (1.47) is different from that of the extrafibrillar matrix (1.35), the highly uniform size (25 ± 2 SD nm) and interfibrillar spaces (40 ± 5 SD nm) along with the predominantly parallel directionality of these fibrils results in a highly-ordered lattice-like array of fibrils (*i.e.*, not a true crystalline lattice, but one with short-range order) that allows transparency of the cornea due to destructive interference effects (Fig. 10B, C).⁵⁶

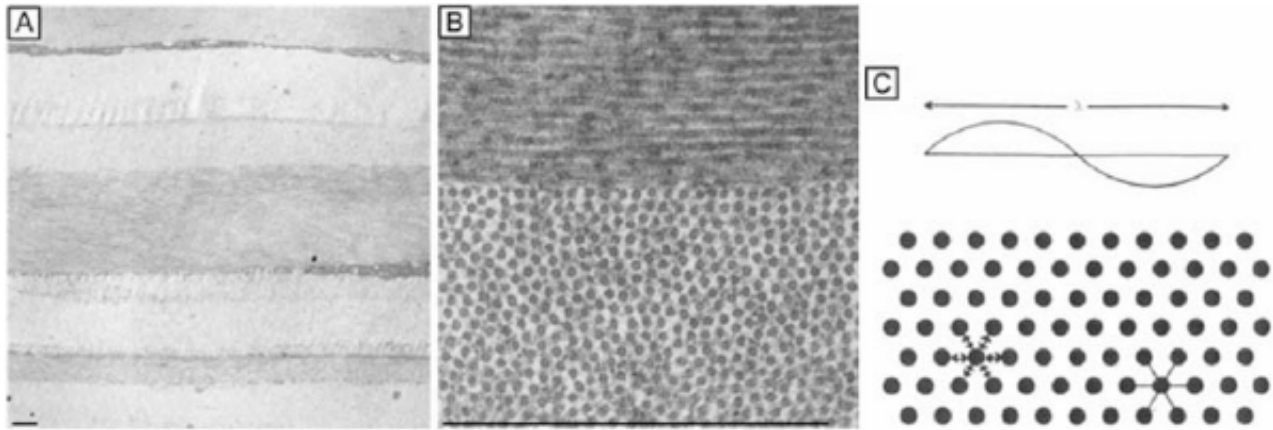


Figure 10. (A) Low magnification (4,750 \times) TEM of predominantly orthogonally stacked lamellae in the middle third of cellular corneal stroma. (B) Higher magnification (72,500 \times) TEM of two lamellae in the middle third of cellular corneal stroma. One lamellae is in longitudinal view (top) and other is in cross-sectional view (bottom). Notice the uniformly 25-nm diameter collagen fibrils and the 40-nm diameter interfibrillar spaces that demonstrate only a short-range order (*i.e.*, slight variability), but do not form a true crystalline lattice. (C) Cross-sectional diagram of collagen fibrils arranged in a true crystalline lattice arrangement. Size of a wavelength of light is shown above for comparison. Bars = 1 μ m. (From Maurice DM. The structure and transparency of the cornea. J Physiol 136:263, 1957.)

Collagen type VI is the third most common type of collagen in the corneal stroma, but is unique in that it is only able to aggregate into repeating tetramers of type VI molecules. Thus, it forms only 10 to 15 nm diameter, beaded (20×30 nm diameter ovals with a periodicity of 100 nm), nonbanded filaments (Fig. 11A). Functionally, it acts as a bridging filament that binds corneal lamellae together where they cross each other (Fig. 11B, C). Along with fibril-associated collagens with interrupted triple helices (FACIT collagens, type XII and XIV collagen molecules), it also bridges intralamellar fibrils together (Fig. 11D).^{57,58} Overall, this three-dimensional, supramolecular scaffold created by human corneal stromal collagens results in a one-dimensional ordered (~ 22 nm diameter collagen fibrils; ~ 40 nm interfibrillar spaces \times random directionality) 12- μ m thick acellular Bowman's layer (Figs. 12A and 13A) and a three-dimensionally-ordered (~ 25 nm diameter collagen fibrils; ~ 40 nm interfibrillar spaces \times parallel directionality) series of successive stacks of lamellae in the cellular stroma measuring in the center of cornea around 450 μ m in thickness.^{59,60,61}

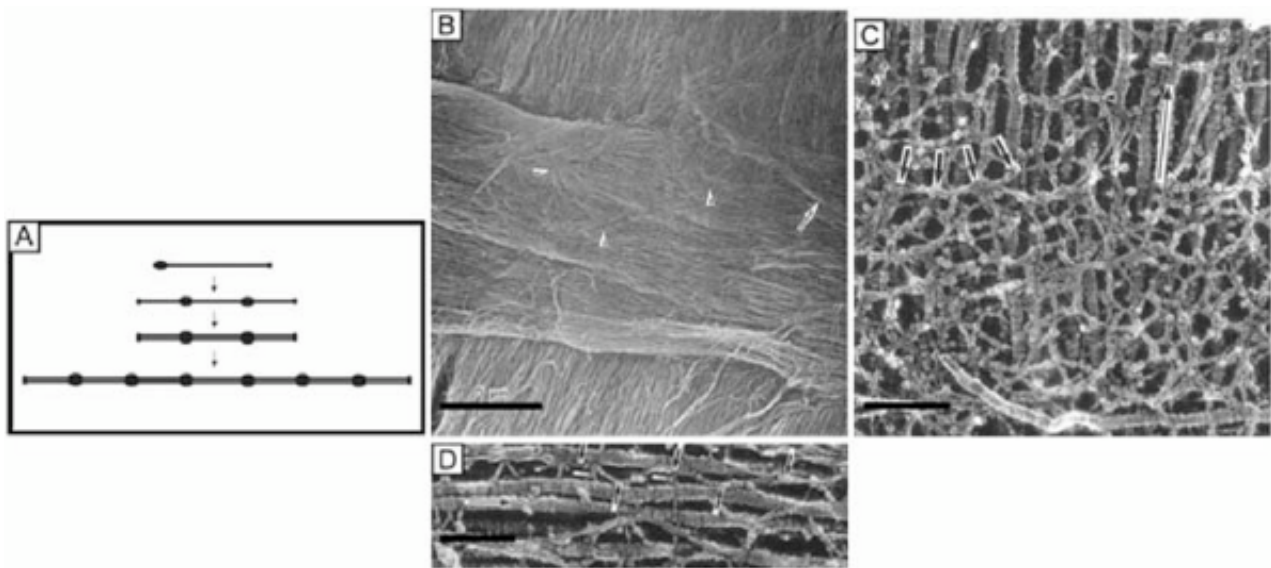


Figure 11. (A) Diagram of a type VI collagen molecule and how it assembles into filaments by aggregating into repeating tetramers of type VI molecules (periodicity of 100 nm). (B) Low magnification (6,200×) SEM showing bundles of collagen filaments extending between lamellae (arrow) and a loose meshwork of collagen filaments on the posterior surface of a corneal lamellae where an adjacent lamellae crosses it (arrowheads). Bar = 5 μm. (From Komai Y, et al. The three-dimensional organization of collagen fibrils in the human cornea and sclera. *Invest Ophthalmol Vis Sci* 32:2244, 1991.) (C) High magnification (115,000×) quick-freeze, deep-etched electron micrograph showing a loose meshwork of interlamellar beaded filaments with a periodicity of 100 nm (thick arrows) which appear to bind to collagen fibrils (long arrow) by their beads (arrowhead) and join fibrils from separate lamellae together. Bar = 0.2 μm. (D) Very high magnification (185,000×) quick-freeze, deep-etched electron micrograph of intralamellar collagen fibrils (long arrows) with beaded filaments (thick arrows) crisscrossing between fibrils and projecting three finger-like structures, which both appear to function in joining neighboring fibrils together. Bar = 0.1 μm. (C and D are from Hirsch M, et al. Three-dimensional supramolecular organization of the extracellular matrix in human and rabbit corneal stroma, as revealed by ultrarapid-freezing and deep-etching methods. *Exp Eye Res* 72:123, 2001.)

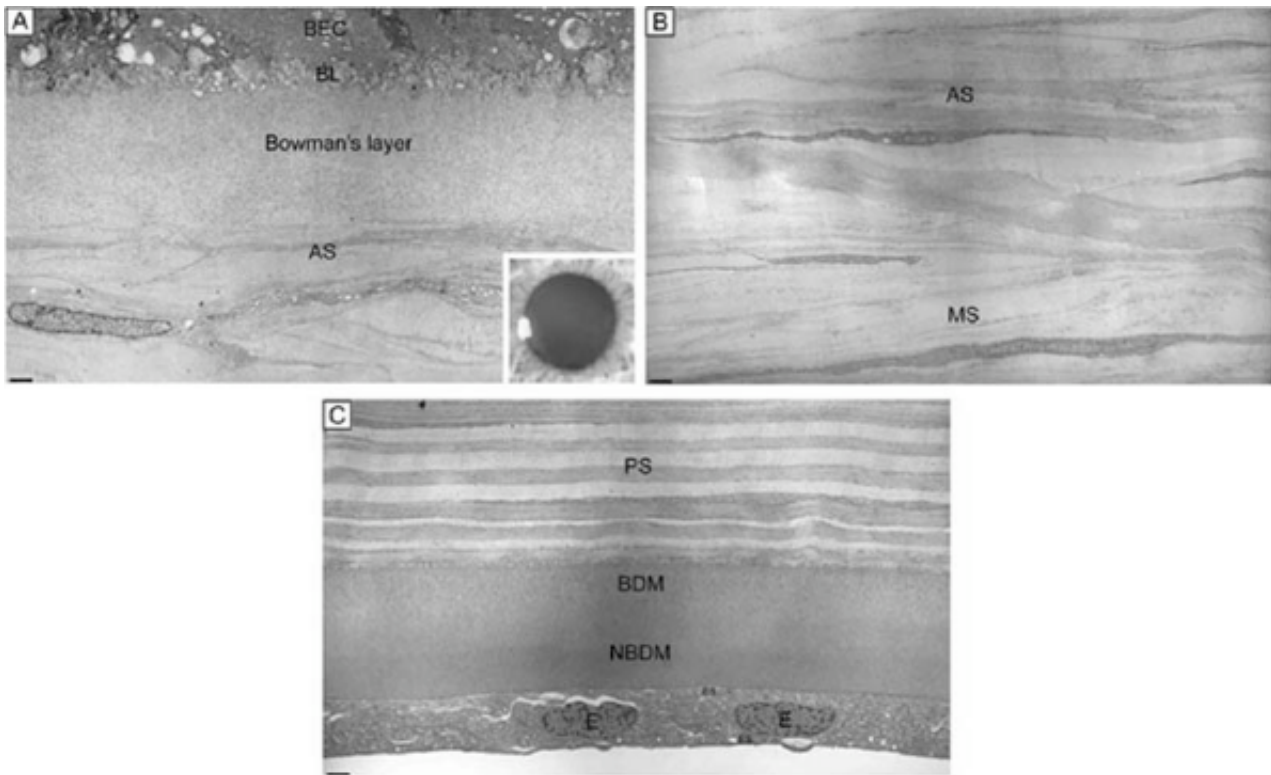


Figure 12. (A) The acellular Bowman's layer and anterior-most portion of the cellular corneal stroma. Notice that the interweaving lamellae of cellular stroma branch and insert into the posterior surface of the Bowman's layer forming an anterior corneal mosaic pattern after applying digital pressure on the corneal surface through the eyelid and fluorescein is instilled (inset). (B) The anterior third of the cellular corneal stroma showing the predominantly oblique lamellar orientation and the extensive vertical lamellar branches and interweaving. (C) The posterior third of the cellular corneal stroma, Descemet's membrane and endothelium. Notice the parallel oriented and predominantly orthogonal arrangement of lamellae in this portion of corneal stroma. Although some collagen fibrils randomly insert into Descemet's membrane, no specific pattern can be induced in this region of the cornea. BEC, basal epithelial cells; BL, basal lamina; AS, anterior stroma; MS, midstroma; PS, posterior stroma; BDM, banded portion of Descemet's membrane; NBDM, non-banded portion of Descemet's membrane; E, endothelial cells; ES, extracellular space. Bars = 1 μm . (TEM 4,750 \times .)

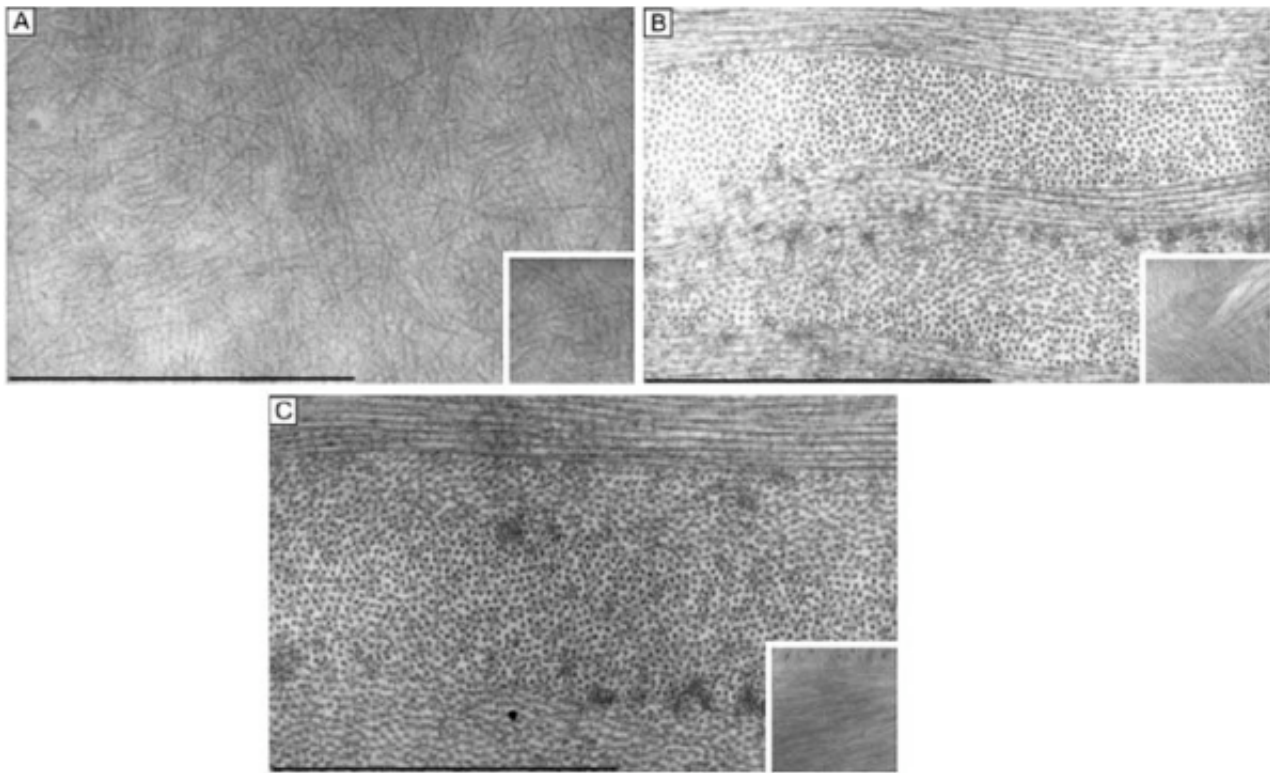


Figure 13. (A) The acellular Bowman's layer in cross-section and frontal section (inset). Notice the random directionality of the 22-nm diameter collagen fibrils in this portion of the stroma. (B) The anterior third of the cellular corneal stroma in cross-section and frontal section (inset). Notice the thin and more obliquely oriented lamellae in this region of the corneal stroma and its lattice-like arrangement of 25-nm diameter collagen fibrils. (C) The posterior third of the cellular corneal stroma in cross-section and frontal section (inset). Notice the thick and parallel oriented lamellae in this region of the cornea stroma and its lattice-like arrangement of 25-nm diameter collagen fibrils. Also, note the orthogonal nature of lamellae (inset) compared to that in the inset from (B). Bars = 1 μm . (TEM 72,500 \times .)

Although difficult to count exactly, the central cornea has been found to have approximately 300 corneal lamellae, whereas the peripheral cornea has approximately 500.⁶¹ Although these lamellae are generally described as running parallel to the corneal surface in orthogonal directions to one another, regional differences exist in their size, directionality, and amount of interweaving. The anterior third of the cellular corneal stroma has thinner (0.2- to 1.2- μm thick), narrower (0.5- to 30- μm wide), and mostly obliquely oriented lamellae with extensive vertical and horizontal interweaving (Figs. 12B and 13B), whereas the posterior two-thirds has thicker (1- to 2.5- μm thick), wider (100- to 200- μm wide), and mostly parallel oriented lamellae with only slight horizontal interweaving (Figs. 12C and 13C).⁶⁰

Additionally, only lamellae in the posterior two-thirds of the cellular corneal stroma run in the classic orthogonal directions, whereas all of the lamellae of the anterior third and a minority of lamellae in the posterior two-thirds run in nonorthogonal directions. Because the lamellae in the anterior-most layers of cellular stroma branch so extensively, it is not surprising that they also interweave with (*i.e.*, are attached to) the Bowman's layer in a polygonal fashion, creating a mosaic appearance that can be seen on the anterior corneal surface under certain circumstances (Fig. 12A, inset). Finally, all corneal lamellae appear to stretch across the cornea from limbus to limbus where they turn and form an annulus approximately 1.5- to 2.0-mm wide around the cornea. This maintains the curvature of the cornea, while blending with limbal collagen fibrils.^{61,62,63}

Corneal proteoglycans previously were referred to as extrafibrillar amorphous ground substance because their water soluble state made them difficult to fully delineate with light and electron microscopy (Fig. 14A). It was not until an electron-dense, cationic dye called cupromeronic blue and a critical-electrolyte-concentration of 0.1 M $MgCl_2$ were used in combination to stain specifically for the sulfate-ester groups on corneal stromal proteoglycans that the shape, size, arrangement, and location of this material was observed with light and electron microscopy (Fig. 14B).⁶⁴ Since that time, it has become quite apparent that corneal proteoglycans are not amorphous, but rather are tadpole-shaped structural molecules composed of a globular core protein (10 to 15 nm in diameter) with a covalently attached GAG sidechain or tail (7 nm wide \times 45 to 70 nm in length). They are arranged in the cornea stroma orthogonal to collagen fibrils with a constant separation around 65 nm between each other along the fibrils. Their core proteins noncovalently bind to collagen fibrils in specific gap zones along the peripheral portions of the collagen fibril (core proteins with dermatan sulfate sidechains bind to d and e gap zones and those with keratan sulfate side chains bind to a and c gap zones).⁶⁵ GAGs are highly negatively-charged, stiff polymers that extend into the interfibrillar space and form antiparallel duplexes with adjacent GAG sidechains, thereby crosslinking different collagen fibrils together by forming dumbbell-like structures (Fig. 14C).

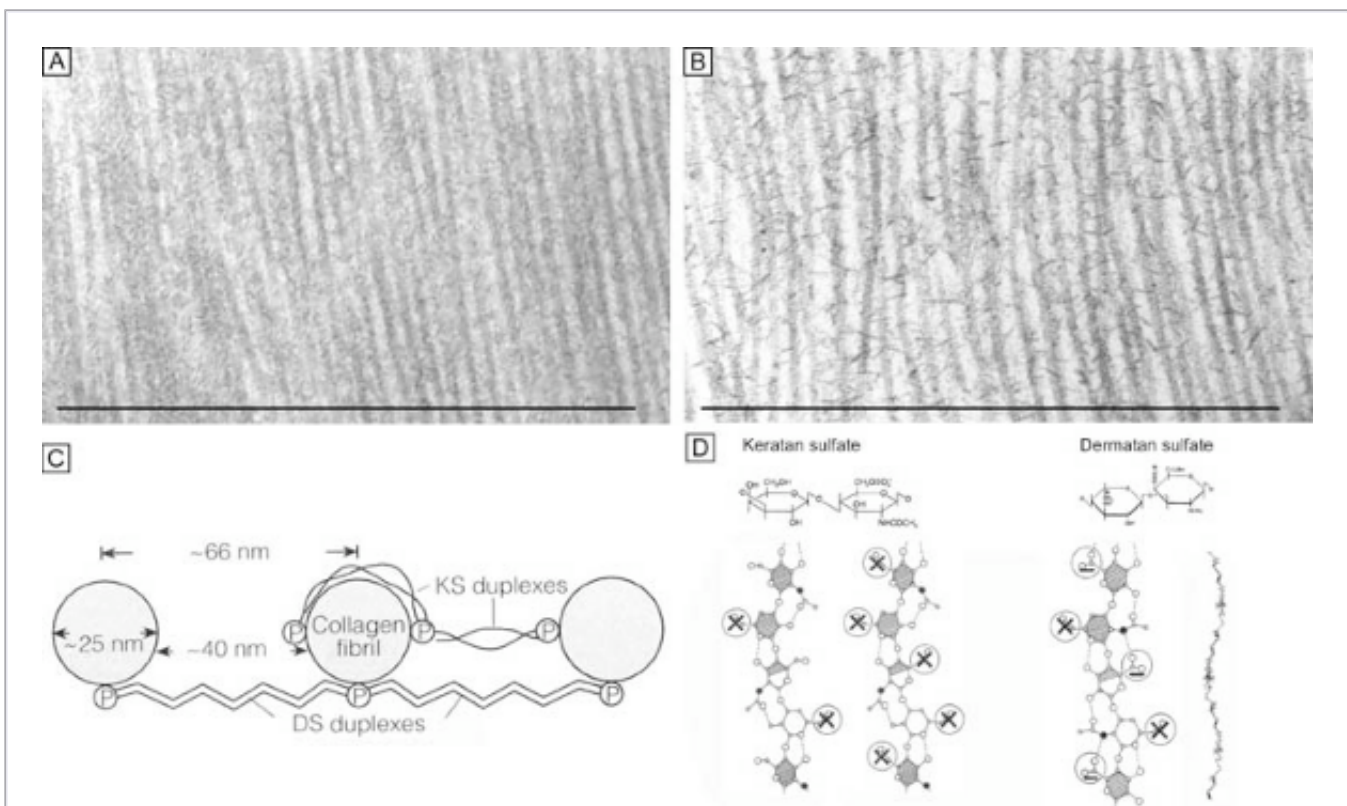


Figure 14. Frontal section TEMs (90,000 \times) of longitudinally running corneal stromal collagen fibrils in a lamellae without (A) and with (B) Cupromeronic blue staining. Notice the scattered “amorphous ground substance” in the interfibrillar spaces in (A), whereas in (B) duplexes of proteoglycans are clearly seen bridging collagen fibrils. Bars = 1 μ m. (C) Diagram of how proteoglycans attach along the periphery of collagen fibrils via their core proteins (P) and how the GAGs duplex in an anti-parallel fashion in the interfibrillar space. (D) Diagram of the polymer backbones of keratan sulfate and dermatan sulfate. The top portion shows the primary structure of the repeating disaccharide units of keratan sulfate (top left) and dermatan sulfate (top right). The bottom portion of the diagram shows the secondary structures of each proteoglycan. Notice that in the human cornea ~50% of keratan sulfate is in the normal-sulfated state (bottom, farthest left), whereas the other ~50% is in the oversulfated state (bottom, center left). Also, notice that all three displayed proteoglycan polymers have similar backbones and therefore form similar

secondary structures of a twofold helix (bottom, farthest right). Anionic charges = sulfate esters (X) and carboxylic acid (-). Bars = 1 μm . (C and D are modified from Scott JE. Proteoglycan: collagen interactions and corneal ultrastructure. *Biochem Soc Trans* 19:877, 1991.)

Because the genes that produce the core proteins have now been cloned, four types of corneal proteoglycan core proteins have been identified: decorin, lumican, keratocan, and mimecan.⁶⁶ Subsequently, decorin was found to contain a single dermatan sulfate GAG sidechain, whereas lumican and mimecan had single keratan sulfate GAG sidechains and keratocan had three keratan sulfate GAG sidechains. Thus, there are four known types of proteoglycan core proteins and only two types of GAGs: keratan sulfate (60%) and dermatan sulfate (40%), found in the human cornea stroma. The GAGs are polymers of repeating disaccharide units of galactose and N-acetylglucosamine or iduronic acid and N-acetylgalactosamine, respectively (Fig. 14D).⁶⁵ Because GAG sidechains are posttranslationally added to the core protein portions in the golgi apparatus, there seems to be some flexibility in how long or how sulfated they can become depending of the type and functional needs of the connective tissue producing them. The human cornea is unique in that the GAGs are fibril-associated, small in length (keratan sulfate [congruent]45 nm and dermatan sulfate [congruent]70 nm), and with a higher proportion are oversulfated.

Interestingly, a comparative study of corneas from 12 mammalian species suggests that dermatan sulfate is the preferred proteoglycan in oxygen-rich environments such as thin corneas (*e.g.*, mice) or in the anterior portion of thicker corneas (*e.g.*, humans or rabbits), whereas keratin sulfate is a functional substitute produced through an alternate metabolic pathway in thicker corneas, especially in the posterior portion where oxygen levels may be dramatically reduced (Fig. 15, inset).^{48,66} Functionally, this duality is quite useful because dermatan sulfate appears to be more efficient at holding water as it absorbs less total amounts of water, but most in a tightly-bound state (*i.e.*, in a nonfreezable state) than does keratin sulfate.^{47,67} These explanations are consistent with the fact that dermatan sulfate is highest in amount in the anterior portion of the corneal stroma in humans (region of highest oxygen tension and most affected by evaporation), whereas keratin sulfate is highest in amount in the posterior portion of the corneal stroma (region with the lowest oxygen tension, least affected by evaporation, and area where the need for loosely-bound water is required for transport across the endothelium through the endothelial cell metabolic pump) (Fig. 15).

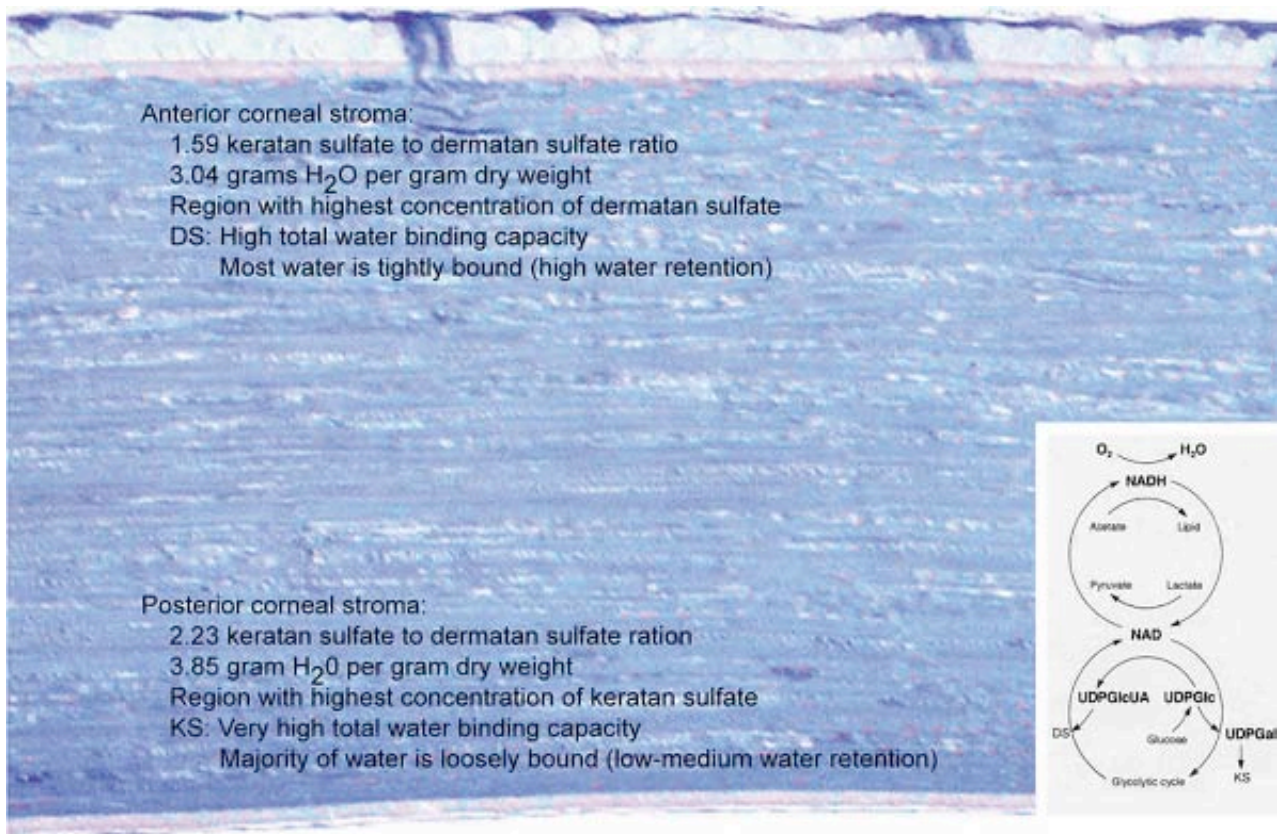


Figure 15. Diagram demonstrating the regional differences in the corneal stroma for the proportion of the two types of corneal proteoglycans and the water absorbing properties in these regions. (Inset) Diagram of the metabolic pathways for dermatan sulfate and keratan sulfate production. Notice that the supply of oxygen is the initial factor whether dermatan sulfate is made through an aerobic pathway or whether keratan sulfate is made through an anaerobic alternative pathway. (Modified from Scott JE. Oxygen and the connective tissues. TIBS 17:340, 1992.)

The corneal stroma is maintained by a closed, highly-organized syncytium of keratocytes communicating with each other through gap junctions present on their long dendritic processes.⁶⁸ Keratocytes occupy 10% to 40% of the stromal volume (decreases from 40% in infancy to 10% in adulthood) that on two-dimensional, cross-sectional views appear as flattened (cell body = 20 μ m in length \times 1 μ m in height), quiescent (*i.e.*, scant intracytoplasmic organelles) cells lying between corneal lamella (Fig. 16A, B). In actuality, keratocytes are three-dimensional, stellate-shaped cells composed of a cell body ([congruent]1 \times 15 \times 20 μ m) with numerous dendritic-processes that extend up to 50 μ m in length from the cell body. Two-dimensional tangential sections of the normal cornea suggest that these cells are more highly metabolically active in the resting state than initially presumed; in tangential sections (cell body view = 15 μ m width \times 20 μ m), an abundance of cytoplasmic organelles is commonly seen (Fig. 16C, D).⁶⁹

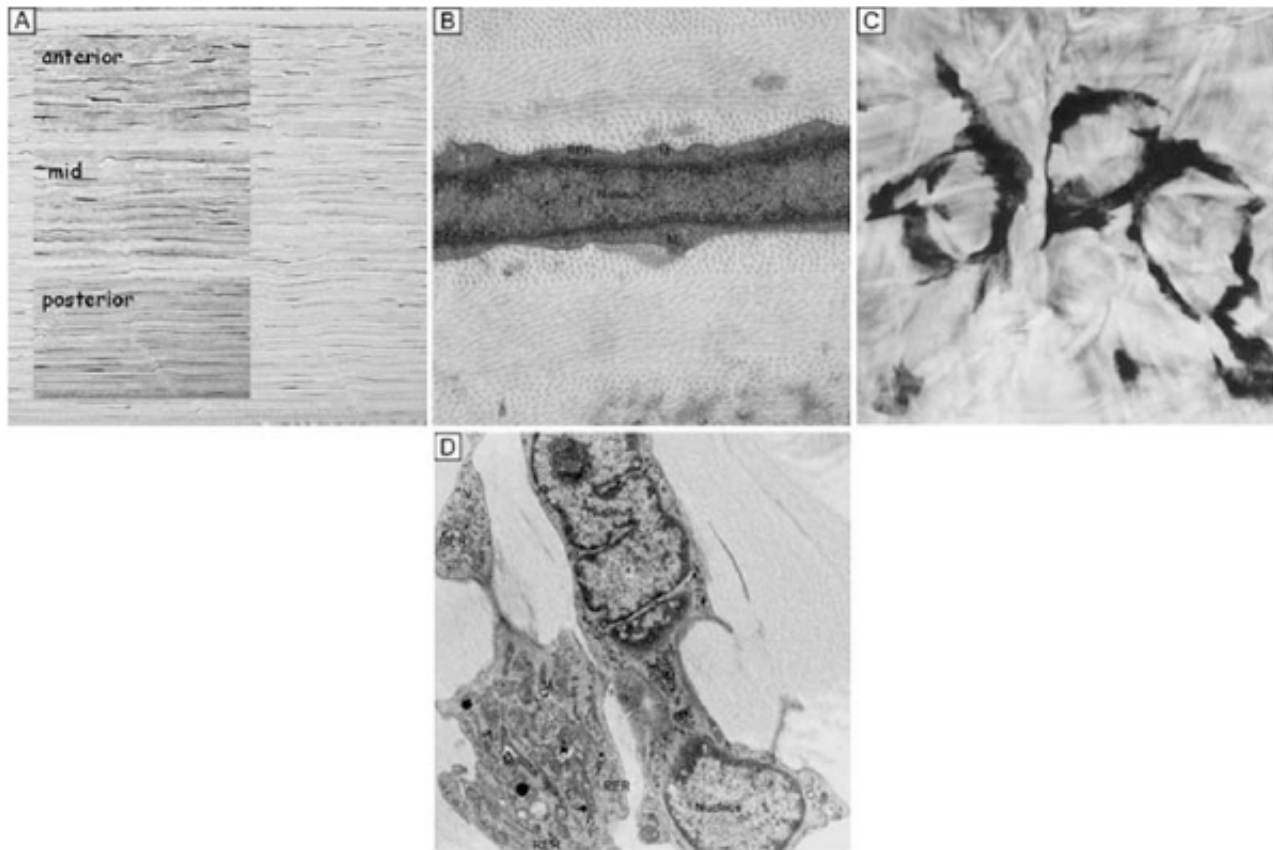


Figure 16. Light and TEM micrographs shown in cross and frontal-sectional views of the cellular corneal stroma demonstrating differences in the appearance of keratocytes depending on the cut, or perspective, of the section. (A) Cross-sectional light microscopy shows that keratocytes are primarily obliquely aligned to corneal surface in the anterior one-third of cellular corneal stroma and are aligned parallel to the corneal surface in the posterior two-thirds. (B) Cross-sectional TEM additionally shows that keratocyte nuclei occupy most of the area of the keratocyte seen in this perspective with only a thin rim of surrounding cytoplasm that contains only small numbers of cytoplasmic organelles. (C) From a tangential perspective, frontal-section light microscopy shows that keratocytes are arranged in a circular fashion. (D) Frontal-section TEM additionally shows that supposedly quiescent keratocytes may be more active in the baseline state than initially thought as an extensive amount of cytoplasmic organelles can be seen in this view. M, mitochondria; RER, rough endoplasmic reticulum; V, vacuoles. *Main portion of nucleus that contains nucleolus. (Modified from Muller LJ, et al. Novel aspects of the ultrastructural organization of human corneal keratocytes. Invest Ophthalmol Vis Sci 36:2557, 1995.)

Tangential sections also have shown more clearly that the anterior stromal keratocytes contain twice the number of mitochondria than the posterior two-thirds of the stroma, which correlates with the oxygen tension levels in the cornea. It also has demonstrated that a higher density or volume of cells reside in the anterior stroma than in the mid or posterior stroma (Fig. 17). Moreover, these views make it easy to appreciate that, in all levels, the keratocytes are highly spatially-ordered as they turn in a clockwise direction like a corkscrew.

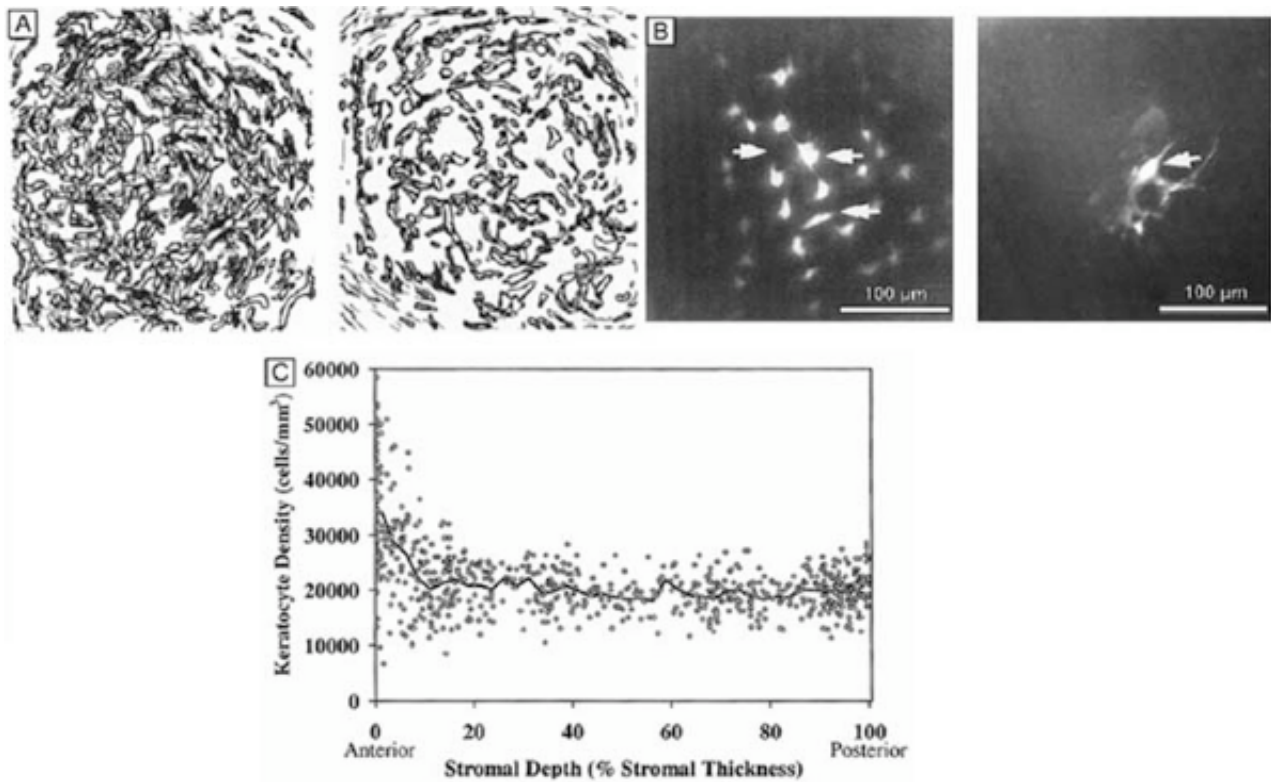
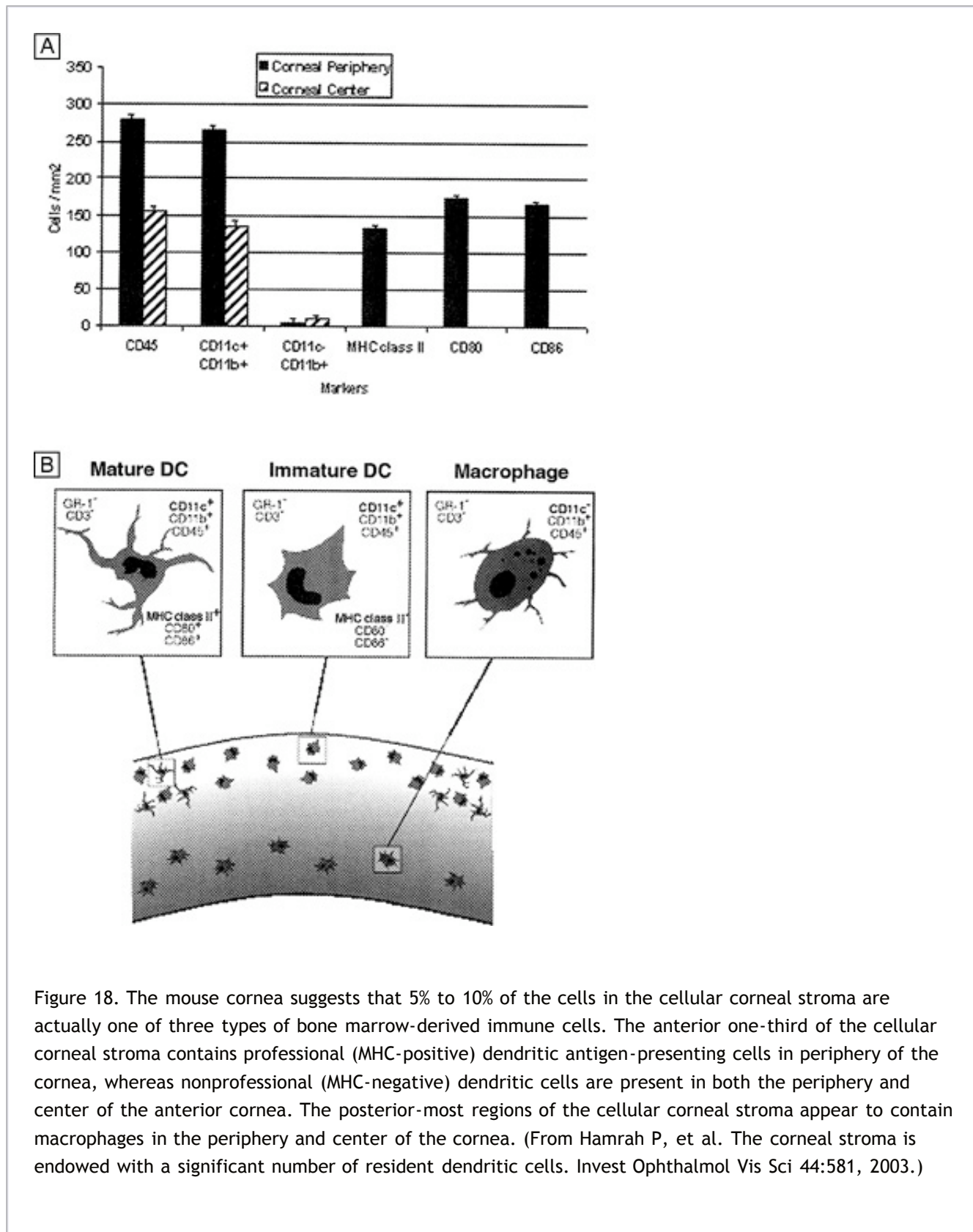


Figure 17. (A) Reconstruction of keratocyte outlines seen in frontal-section in the anterior and posterior thirds of the cellular corneal stroma. (Modified from Muller LJ, et al. Novel aspects of the ultrastructural organization of human corneal keratocytes. *Invest Ophthalmol Vis Sci* 36:2557, 1995.) (B) Fluorescent-dye spreading between many adjacent keratocytes in rabbit (center left) and human corneas (center right), which demonstrates the intimate importance of gap junctions in how keratocytes communicate with one another. (From Watsky MA. Keratocyte gap junctional dye spread in normal and wounded rabbit corneas and human corneas. *Invest Ophthalmol Vis Sci* 36:522, 1995.) (C) Mean keratocyte density along the depth of central cellular corneal stroma. Notice the zone of increased density the closer one gets to the epithelial-stromal junction. Perhaps this is due to baseline, normal epithelial-stromal interactions. (From Patel SV, et al. Normal human keratocyte density and corneal thickness measurement by using confocal microscopy in vivo. *Invest Ophthalmol Vis Sci* 42:333, 2001.)

In vivo confocal microscopy of normal human corneas has shown keratocyte densities average around 20,000 keratocytes/mm³ (or an area of 328 cells/mm²). The focal zone of increased cell density directly under the epithelial surface averages 35,000 keratocytes/mm³ in the anterior-most 9-μm layer and gradually tapers to 20,000 keratocytes/mm³ over the initial 60 μm in depth (Fig. 17C).⁷⁰ Confocal microscopy also concurs with previous studies as it shows that stromal cellular density decreases with age at approximately 0.45% per year of life. Interestingly, studies using immunohistochemistry on animal corneas^{71,72} and ultrastructural studies on human corneas^{69,72} suggest that not all the cells in the corneal stroma are keratocytes (*i.e.*, fibrocytes), but some are one of three types of bone marrow-derived immune cells (“professional” dendritic cells, “nonprofessional” dendritic cells, and histiocytes) (Fig. 18). Thus, although the majority of cells in the stroma are keratocytes, which maintain the corneal stroma by synthesizing and secreting collagen type I, III, V, VI, XII, XIV, keratan sulfate, dermatan sulfate, and matrix metalloproteinases, a minority of cells in the stroma are also “professional” stromal dendritic cells, “nonprofessional” stromal dendritic cells, or stromal histiocytes. They appear to play a pivotal role in the induction of immune tolerance versus immune initiation into cell-mediated immune pathways. Additionally, the stromal histiocytes play a role in innate immunity as phagocytic effectors

cells.



Two ion channels similar to those found in excitable cells have been characterized in keratocytes isolated from corneal stroma.⁷³ These channels include a delayed rectifier K⁺ channel and a tetrodotoxin-sensitive Na⁺ channel. The physiologic function of these channels has not been determined, but they may function in maintaining the ionic balance of the cells in their inactive state. In addition, because these channels allow the

keratocytes to elicit action potentials when injected with a clamping current, it is possible they may act as intercellular signalers via the gap junctions between cells. This could be a route for information exchange between cells in different regions of the cornea.

Corneal Edema

The *Donnan effect* states that the swelling pressure in a charged gel, like the corneal stroma, results from ionic imbalances. The fixed negative charges on corneal proteoglycan GAG sidechains (one carboxylic acid and one sulfate ester sidechain per disaccharide repeat on a dermatan sulfate GAG polymer, and one or two sulfate ester sidechains per disaccharide repeat on a keratan sulfate GAG polymer) have a central role in this effect as the antiparallel GAG duplexes (tertiary structure) produce long-range electrostatic repulsive forces that induce an expansive force termed swelling pressure (SP). Because the corneal stroma also has a cohesive tensile strength that resists this expansion, the normal SP of the nonedematous corneal stroma is around 55 mm Hg.^{74,75} If the stroma is further compressed (e.g., increasing intraocular pressure [IOP] or mechanical appplanation) or expanded (e.g., corneal edema), the SP will correspondingly increase or decrease, respectively.

Conversely, the negatively-charged GAG sidechains also form a twofold helix in aqueous solution (secondary structure) that attracts and binds Na^+ counterions, which results in an osmotic effect leading to the diffusion and subsequent absorption of water to proteoglycans via the Na^+ cations. Thus, the central corneal thickness is maintained around its average value of 520 μm because the fixed negatively-charged proteoglycans induce a swelling pressure through anionic repulsive forces. Additionally, the hydration level of corneal stroma is maintained around 78% water because these proteoglycans also imbibe water through cationic attractive forces.⁴⁵

Under normal circumstances, the negative pressure drawing fluid into the cornea, called the *imbibition pressure* (IP) of the corneal stroma, is around -40 mm Hg.⁷⁶ This implies that the negative charges on corneal proteoglycans are only about one-quarter ([congruent]27 %) saturated, or bound, with water with the remaining unbound proportion wanting to bind more Na^+ and absorb more water if given the opportunity. Fortunately, the highly impermeable epithelium and mildly impermeable endothelium keep the diffusion of electrolytes and fluid flow in the stroma to such a low level [resistance to diffusion of electrolytes and fluid flow = epithelium (2000) >> endothelium (10) > stroma (1)] that the continuously working endothelial cell metabolic pump can maintain stromal hydration in the normal range. Although $\text{IP} = \text{SP}$ when corneas are in the *ex vivo* state, IP actually is lower than SP in the *in vivo* state because the hydrostatic pressure induced by the IOP must now be accounted for. This is best represented by the equation $\text{IP} = \text{IOP} - \text{SP}$ ⁷⁶ and explains why the hydration level of patient's cornea is not only dependent on having normal barrier functions, but also on having a normal IOP. Therefore, a loss of corneal barrier function, an $\text{IOP} \geq 55$ mm Hg, or a combination of the two results in corneal edema (Fig. 19).⁷⁷

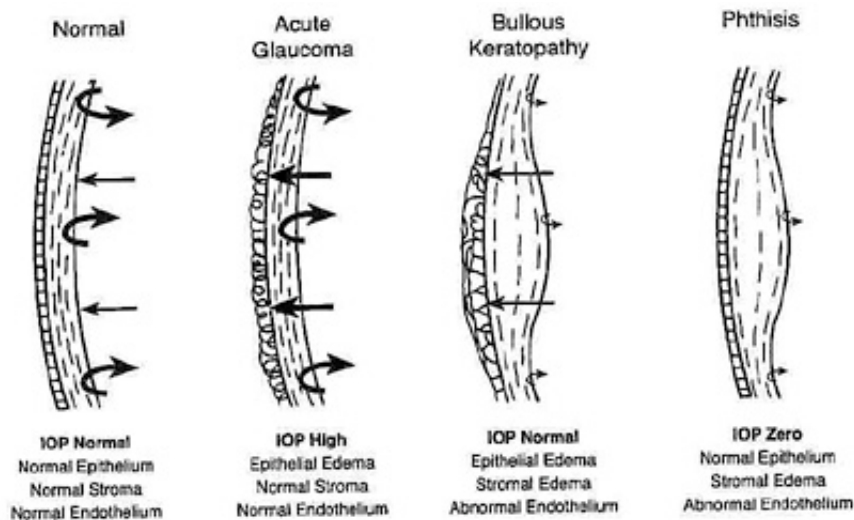


Figure 19. Diagram demonstrating the delicate balance between stromal swelling pressure, endothelial pump function, and intraocular pressure. Usually if endothelial cell pump function fails and IOP remains normal, slightly decreases, or increases, both stromal and epithelial edema occurs (center right). Only when IOP increases above the swelling pressure of the stroma and the endothelium functions normal do we see epithelial cell edema alone (center left) and only when IOP is zero and the endothelium functions abnormally do we see stromal edema alone (far right). (From Hatton MP, et al. Corneal edema in ocular hypotony. *Exp Eye Res* 78:549, 2004.)

Corneal edema is a term often used loosely and nonspecifically by clinicians, but literally refers to a cornea that is more hydrated than normal (*i.e.*, >78% water). The topic of corneal edema is important for clinicians to understand because it affects the architecture and function of the epithelium and the stroma. Epithelial edema clinically causes a hazy microcystic appearance to occur in the epithelium in mild to moderate cases, significantly decreasing vision and increasing glare. It also can cause the development of large, painful, subepithelial bullae in severe cases. These changes correlate histopathologically with hydropic basal epithelial cell degenerative changes and the development of extraepithelial cellular fluid filled spaces (*e.g.*, cysts and bullae). Interestingly, if bullae are chronically present, a fibrocollagenous degenerative pannus often times will grow into the subepithelial space, decreasing vision further while reducing the pain.

Stromal edema clinically appears as a painless, hazy thickening of the corneal stroma resulting in a mild to moderate reduction in visual acuity and an increase in glare. At the same time, Descemet's membrane folds commonly appear on the posterior surface of the cornea. Histopathologically, these changes correlate with the light microscopic findings of thickening of the corneal stroma in the posterior cross-sectional direction with loss of artifactual stromal clefting.⁷⁸ Ultrastructural and biochemical studies have further shown that stromal edema causes an increase in the distance and disruption of spatial order between collagen fibrils,⁷⁸ a decrease in the refractive index of the extracellular matrix,⁷⁹ hydropic degenerative changes or cell lysis in the resident keratocyte population,⁸⁰ and a loss of proteoglycans.⁸¹

Although different proportions of the two types of negatively-charged proteoglycan may account for the higher hydration levels in the posterior stroma compared to the anterior stroma,^{46,82} it appears that the directional orientation of the collagen fibrils probably has the greatest influence on how much each region thickens, or swells, as a result of increased hydration levels. Because the collagenous architecture of the stroma (*i.e.*, limbus-to-limbus directional orientation of collagen fibrils) highly resists circumferential expansion, only anterior-posterior expansion occurs in the human cornea, mostly in the posterior direction. This latter fact

occurs because extensive lamellar interweaving occurs in the anterior portions of the corneal stroma, whereas weak bridging filaments (*i.e.*, type VI and FACIT collagens) occur diffusely throughout the entire corneal stroma. Furthermore, this lamellar interweaving also explains why the anterior third of the cornea mildly swells and actually maintains its anterior corneal curvature even when the remaining stroma swells to up three times its normal thickness.⁸⁰ Because fibrotic corneal scars have random directionally-oriented interweaving collagen fibrils, they also have been found to resist swelling under edematous conditions.⁸³

Therefore, although it is commonly stated that corneal thickness and interfibrillar spacing increase in a linear fashion to the hydration level of the corneal stroma,^{75,78} one needs to be aware that this relationship mainly applies to the mid and posterior stromal regions.

Finally, although both epithelial and stromal edema commonly co-exist together, there are two notable exceptions that are important to understand. Because the epithelium lacks fixed negatively-charged proteoglycans and has a different set of cohesive mechanical strengths than the stroma (*e.g.*, intercellular desmosomal junctions), its state of hydration is mainly dictated by IOP levels.⁸⁴ Conversely, because collagen fibrils in corneal stroma are anchored at the limbus for 360 degrees, they exert increasing cohesive tensile mechanical forces on the corneal stroma (*i.e.*, compression of stromal tissue) as the IOP elevates above normal. This results in the transmission of edema to the epithelial surface in cases of high IOP. Therefore, if IOP is ≥ 55 mm Hg with normal endothelial barrier and pump function, epithelial edema usually occurs by itself. In contrast, if endothelial cell dysfunction and hypotony (IOP -0 mm Hg) occur together, then stromal edema occurs alone (see Fig. 19).

MICROSCOPIC ANATOMY, ULTRASTRUCTURE, AND PHYSIOLOGY OF THE ENDOTHELIUM

The endothelium of the infant cornea is composed of a single layer of approximately 500,000 neural crest-derived cells, each measuring around 5 μm in thickness by 20 μm in diameter and cover a surface area of 250 μm^2 .^{58,85} The cells lie on the posterior surface of the cornea and form an irregular polygonal mosaic. The tangential appearance of each corneal endothelial cell is uniquely irregular, usually uniform in size to one another, and typically six-sided (*i.e.*, hexagons). They abut one another in an interdigitating fashion with 20 nm wide intercellular space between each other. The intercellular space is known to contain discontinuous apical tight junctions (macula occludens) and lateral gap junctions, thereby forming an incomplete barrier to diffusion of small molecules. As corneal endothelial cells have numerous cytoplasmic organelles, particularly mitochondrial organelles, they have been inferred to have the second highest aerobic metabolic rate of cells in the eye next to retinal photoreceptors.⁵⁸

At birth, the central endothelial cell density of the cornea is around 5,000 cells/ mm^2 .⁸⁵ Because the corneal endothelium has very limited regenerative capabilities, there is a well-documented decline in central endothelial cell density with age that typical involves two phases: a rapid and a slow component.^{85,86} Due to corneal growth and age-related, or developmental, selective cell death, during the fast component, the central endothelial cell density decreases exponentially to about 3,500 cells/ mm^2 by age 5 years and 3,000 cells/ mm^2 by age 20 years.⁸⁶ Thereafter, a slow component occurs where central endothelial cell density decreases to a linear steady rate of 0.6% per year, resulting in cell counts around 2,500 cell/ mm^2 in senescence (Fig. 20).^{85,86} Because endothelium maintains its continuity by migration and expansion of surviving cells, it is not surprising that the percentage of hexagonal cells decreases (pleomorphism) and the coefficient of variation of cell area increases (polymegathism) with age.⁸⁶

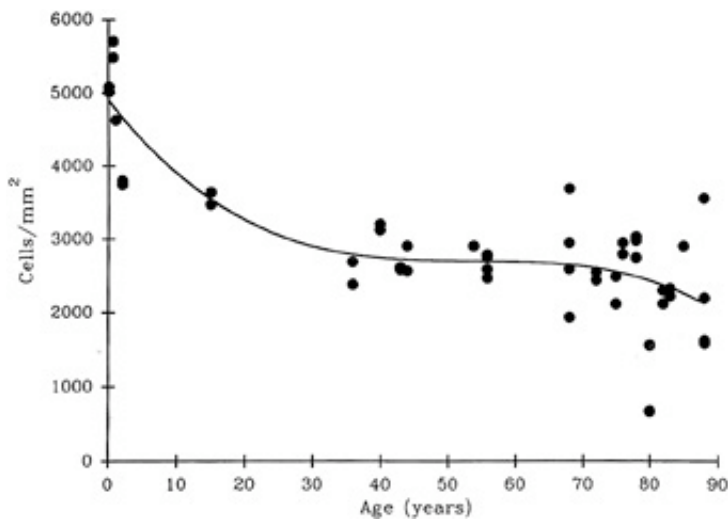


Figure 20. Scatterplot with best fit curve showing the average central corneal endothelial cell density for normal, healthy eyes of different ages. (From Williams KK, et al. Correlation of histologic corneal endothelial cells counts with specular microscopic cell density. Arch Ophthalmol 110:1146, 1992.)

It is important when reviewing this information to realize that these are average central corneal endothelial cell measurements from predominantly Caucasian U.S. populations, as racial and geographic differences can exist. Also, understand that this data applies only to central corneal endothelial measurements because recent work has shown that higher cell densities can typically be found in more peripheral aspects of the cornea (Fig. 21).⁸⁷ Therefore, based on these studies, it appears that central corneal endothelial cell numbers decrease on average about 50% from birth to death in normal subjects. Because corneal decompensation typically does not occur until central values reach around 500 cells/mm², there appears to be plenty of cellular reserve potential remaining after an average human life span.⁸⁶ Estimates suggest that healthy, normal human corneal endothelium could maintain corneal clarity up to a minimum of 215 years of life, if humans lived that long.⁸⁵

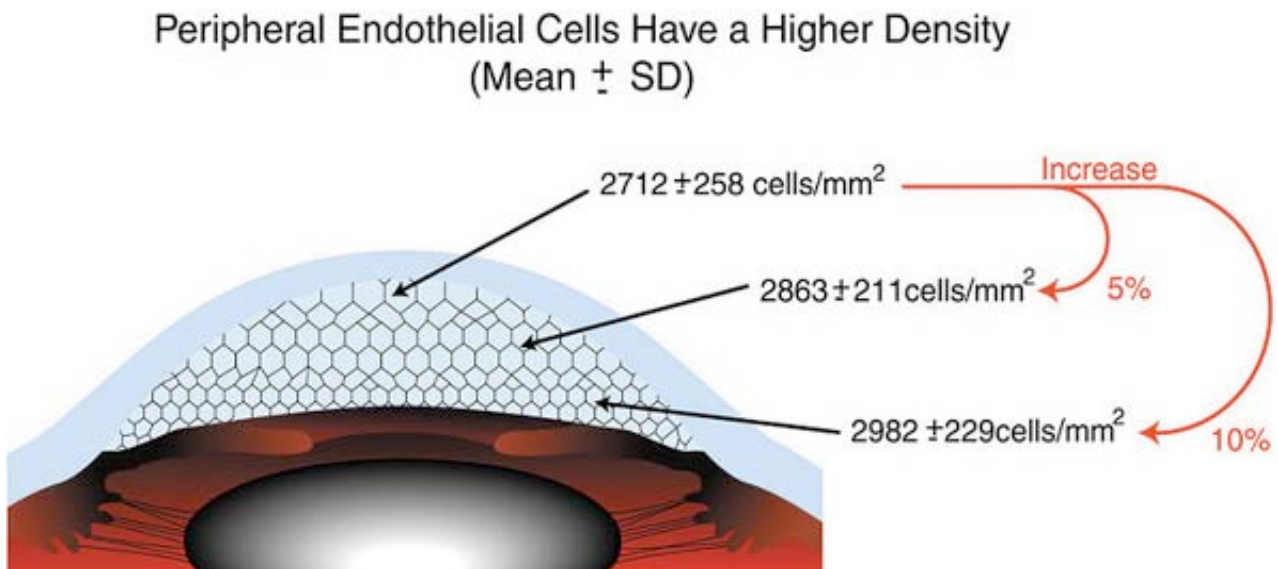


Figure 21. Diagram illustrating the central, paracentral, and peripheral corneal endothelial cell densities in

healthy, normal subjects (From Amann J, et al. Increased endothelial cell density in the paracentral and peripheral regions of the human cornea. *Am J Ophthalmol* 135:584, 2003.)

The primary function of the corneal endothelium is to maintain the health, deturgescence, and clarity of the cornea through a pump-leak mechanism first described by David Maurice (Fig. 22).⁸⁸ Secondly, it is also known to secrete an anteriorly-located basement membrane called Descemet's membrane and a posteriorly-located glycocalyx.⁵⁸

LOCATION OF CORNEAL ENDOTHELIAL METABOLIC PUMP AND BARRIER

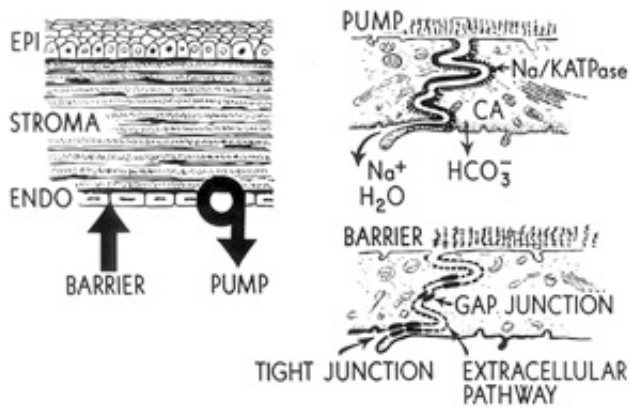


Figure 22. Diagram illustrating the opposing forces of the corneal endothelial barrier and metabolic pump. When the leak rate equals the metabolic pump rate, the corneal stroma is 78% hydrated and the corneal thickness is maintained. (From Waring GO, et al: The corneal endothelium. Normal and pathologic structure and function. *Ophthalmology* 89:531, 1982.)

Having a sufficient number of endothelial cells to cover the posterior surface of the cornea along with having integrity of their cell junctions (tight and gap junctions), which are present in the intercellular spaces between endothelial cells, establishes the barrier function of endothelium (Figs. 12 and 22,23,24). Clinically, the barrier function of the cornea can be assessed in vivo by the use of specular microscopy or confocal microscopy (endothelial cell density) or fluorophotometry (permeability). In healthy human eyes, this barrier prevents the bulk flow of fluid from the aqueous humor to the corneal stroma, but does allow moderate diffusion of nutrients, water, and other metabolites to cross into the stroma through the 20 nm wide intercellular space. This leaky endothelial barrier may initially seem inefficient, but when one considers that most nutrients for all layers of the cornea come from the aqueous humor, the situation is reasonable.

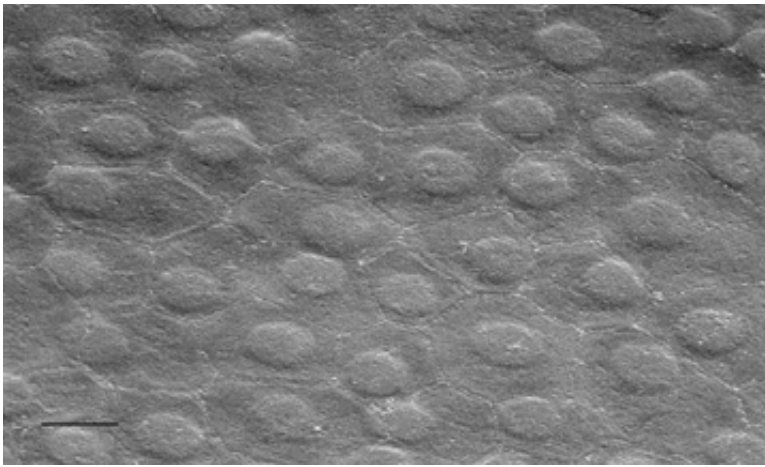


Figure 23. Scanning electron micrograph (1,000×) on the posterior surface of the corneal endothelium from a 65-year-old patient with healthy eyes. Note how the hexagonal endothelial cells form a uniform monolayer. Bar = 10 μm .

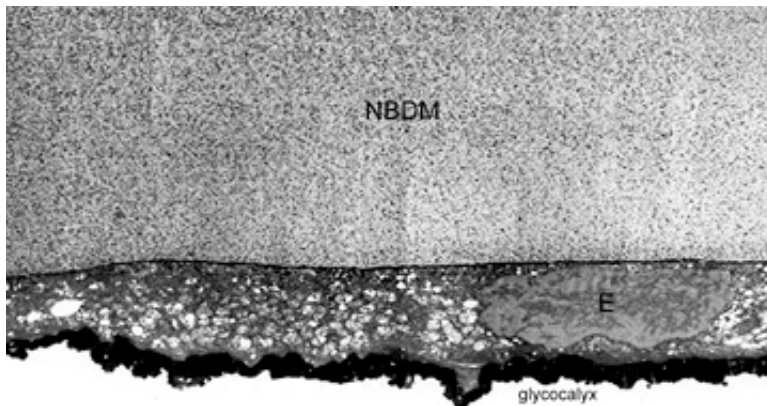


Figure 24. Transmission electron micrograph (15,000×) of corneal endothelium from a specimen specially-preserved (glutaraldehyde + cetylpyridium chloride) and stained (tannic acid) to show the glycocalyx of the endothelium. NBDM, nonbanded Descemet's membrane; E, endothelial cells. Bar = 1 μm .

Additionally, despite the normal loss of endothelial cells that occurs with age, there appears to be no increase in the permeability of normal, healthy-aged corneas. Only when the endothelium is severely reduced in density, acutely damaged, and/or has disrupted cell junctions can the permeability, as measured with carboxyfluorescein increase up to sixfold (12.85×10^{-4} cm/min) from normal (2.26×10^{-4} cm/min).⁸⁹ Recent studies have inferred that during the fifth month of gestation the tight junctions completely form and decrease endothelial permeability.⁹⁰

A number of factors have been known to acutely affect the barrier function of the endothelium, including the following: reversible disruption of cell junctions (calcium-free solutions or glutathione-restricted solutions [Fig. 25]), mechanical damage (e.g., trauma, intraocular lens [IOL] insertion, surgical instruments), or chemical injury (e.g., noncomplete toxic intraocular solutions, preservatives). Fortunately, if enough of the remaining viable cells are able to migrate, recover the posterior corneal surface by spreading out over a larger surface area, and reestablish the intercellular cell junctions, the barrier function of the corneal endothelium is restored.

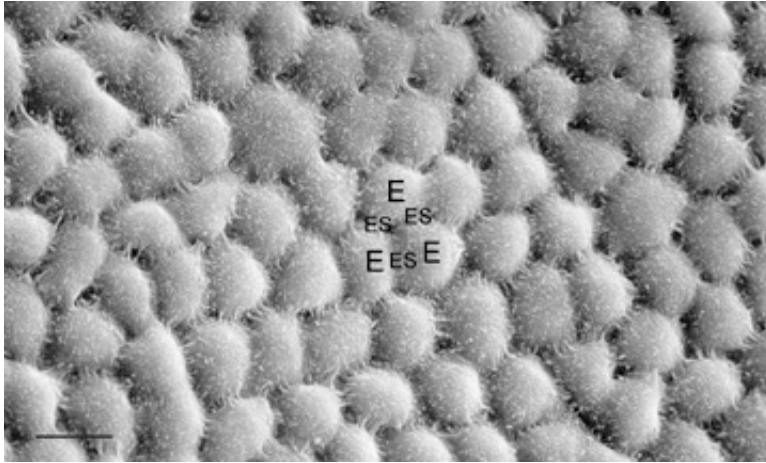


Figure 25. Scanning electron micrograph (1,000 \times) of the endothelium after perfusion with calcium free irrigating solutions after 30 minutes. Without calcium, endothelial cells round up into small mounds as the intercellular junctions become disrupted, resulting in exposure of large areas of Descemet's membrane, loss of barrier function, and corneal swelling. E, endothelial cells; ES, extracellular space. Bar = 10 μm .

The first evidence to suggest that corneal endothelial cells have metabolic pumps was the observation that stromal edema (*i.e.*, corneal clarity) is temperature-dependent.⁹¹ Lowering the temperature arrested the endothelial metabolic pump causing corneal stromal edema, whereas restoring it back to physiologic levels resolved the edema. Subsequently, it was determined that the lateral plasma membrane of endothelial cells contains ATP-dependent transport proteins that catalyze the movements of ions from the stroma to the aqueous humor, creating an osmotic gradient that draws water from the stroma.⁹² It is important to note that this osmotic gradient occurs only if the endothelial cell barrier is not breached. The primary transport proteins creating this effect were later determined as Na^+/K^+ -ATPases (Fig. 22).^{93,94} Subsequently, the number and density of Na^+/K^+ -ATPases sites has also been quantified using [³H]-ouabain, which calculated that approximately 3 million Na^+/K^+ -ATPases sites are present around the lateral membrane of a single endothelial cell (average density of pump sites along lateral plasma membrane wall = 4.4 trillion sites/ mm^2).⁹⁵ Recent studies have inferred that only by 5 to 7 months of gestation does the density of Na^+/K^+ -ATPases increase to adult levels so that the cornea becomes dehydrated and transparent.⁹⁶ Clinically, the metabolic pump of the corneal endothelium can be assessed *in vivo* by measuring the how quickly the corneal thickness (pachymetry) recovers after being purposefully swollen by wearing oxygen-impermeable contact lens.

A number of factors are known to alter endothelial pump function: pharmacologic inhibition of Na/K -ATPase (e.g., ouabain), decreased temperature, lack of bicarbonate or carbonic anhydrase inhibitors, and chronic

reduction in endothelial cell numbers from mechanical injury, chemical injury, or disease states. Fortunately, physiologic compensatory mechanisms prevent corneal edema from occurring to a certain degree (central endothelial cell densities between 2,000 to 750 cells/mm³) by increasing the activity of pump sites already present (requiring more ATP production by the cell) and/or by increasing the total number and density of pump sites on the lateral membranes of endothelial cells (Figs. 26 and 27).⁹⁵ A similar phenomenon occurs in the cells of the kidney's proximal tubule to adjust for an increased salt load. For example, with Fuchs' endothelial dystrophy, the cornea has been known to remain clear and of normal thickness, despite having very low endothelial cell counts and increased endothelial fluorescein permeability (2.89×10^{-3} to 5.30×10^{-3} mm/min).⁹⁵ Apparently, this occurs because the density of the Na⁺/K⁺ pump sites increases (mean of 10.2×10^9 sites/mm²) to compensate for increased permeability.⁹⁷ The point at which compensatory mechanisms appear to ultimately fail is when central endothelial cell density reaches levels around 500 cells/mm³ (range of 250 to 750 cells/mm³) (Figs. 26 and 27).^{85,98} At this low cell number, the permeability has greatly increased to such a point that the endothelial cells, which are spread so thin, do not have enough room on their lateral cell membranes for more metabolic pump sites and all the current pumps are maximally active. Therefore, the metabolic pump fails to balance the leak and corneal edema results.

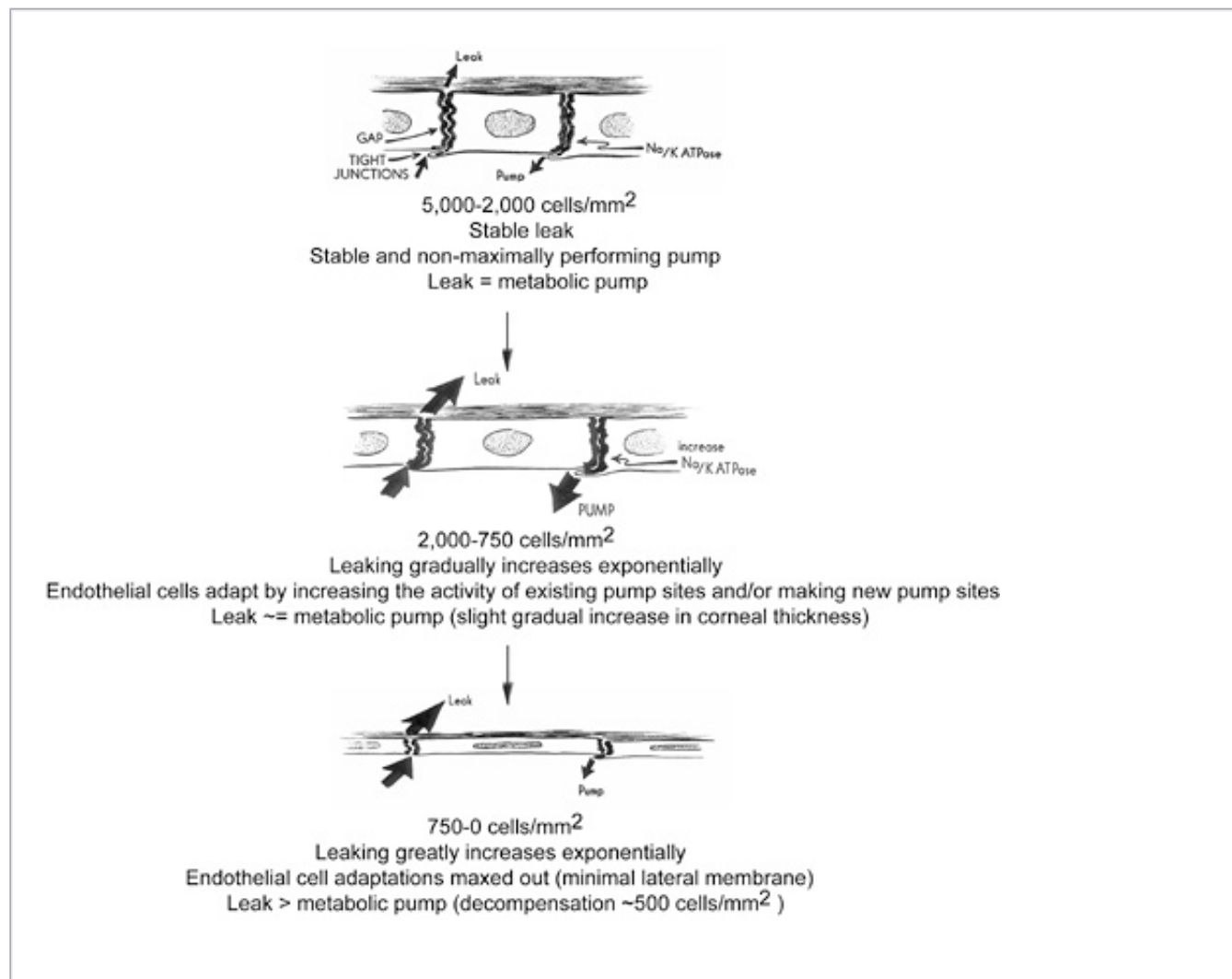


Figure 26. Diagram illustrating the relationship between central endothelial cell density, barrier function, and pump sites. Note that the number pump sites are not all maximally used in the normal states (5,000 to 2,000 cells/mm²). With increased leaking (2,000 to 750 cells/mm²), there is an adaptive phase in which the endothelial cells can form more pump sites to offset the leak up to a point. When the surface area of the lateral membranes of endothelial cells progressively becomes too small (750 to 0 cells/mm²),

these adaptations max out and eventually decline. The point where endothelial cell pump-site adaptations cross permeability (500 cells/mm^2) is typically when corneal decompensation occurs.

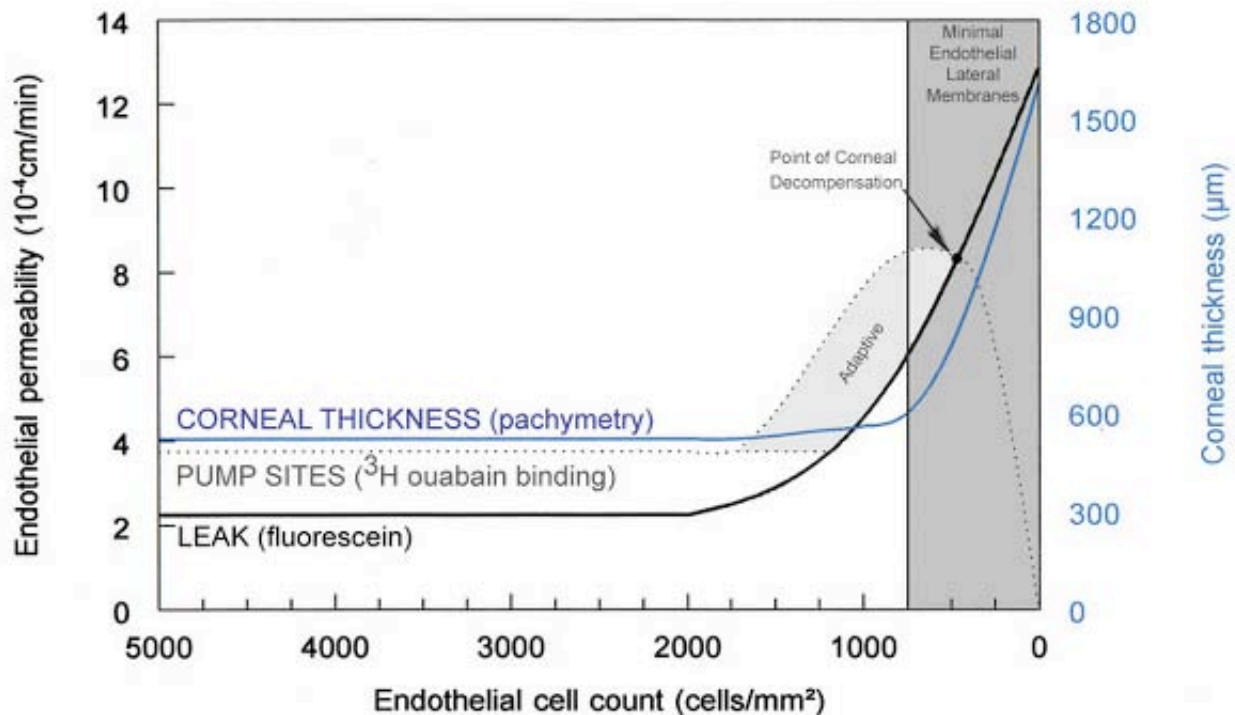


Figure 27. Summary graph illustrating the relationship between central endothelial cell density, barrier function, pump sites, and pachymetry.

A diagram summarizing the current understanding of the endothelial cell transport system is shown in Figure 28. This subject was most recently reviewed in detail by Bonanno.⁹⁹ When the corneal endothelial barrier and metabolic pump are functioning, the corneal stroma has a total Na^+ concentration of 179 mEq/L (134.4 mEq/L free and 44.6 mEq/L bound to stromal PGs), whereas the aqueous humor has a total Na^+ concentration of 142.9 mEq/L (all free).¹⁰⁰ Therefore, after accounting for the chloride activity and stromal imbibition pressure, an osmotic gradient of 30.4 mm Hg exists, causing water to diffuse from the stroma to the aqueous humor (Fig. 29). Additionally, the corneal endothelial cells contain high concentrations of carbonic anhydrase, which forms HCO_3^- (bicarbonate) from metabolic CO_2^- . The HCO_3^- diffuses down its concentration gradient into the extracellular space or across the membrane via the $\text{Cl}^-/\text{HCO}_3^-$ exchanger¹⁰¹ or through Cl^- (anion) channels.^{102,103} Bicarbonate can also enter the cells via a $\text{Na}^+/\text{HCO}_3^-$ co-transporter,¹⁰⁵ and the intracellular pH can be regulated, at least in part, by a basal Na^+/H^+ exchanger.¹⁰⁴ Endothelial Cl^- transport occurs through both transporters and channels, with Cl^- entering the cell from the stroma via a basal $\text{Na}^+/\text{K}^+/\text{2Cl}^-$ transporter and the $\text{HCO}_3^-/\text{Cl}^-$ exchanger, and exiting into the aqueous humor via apical anion channels.^{105,106}

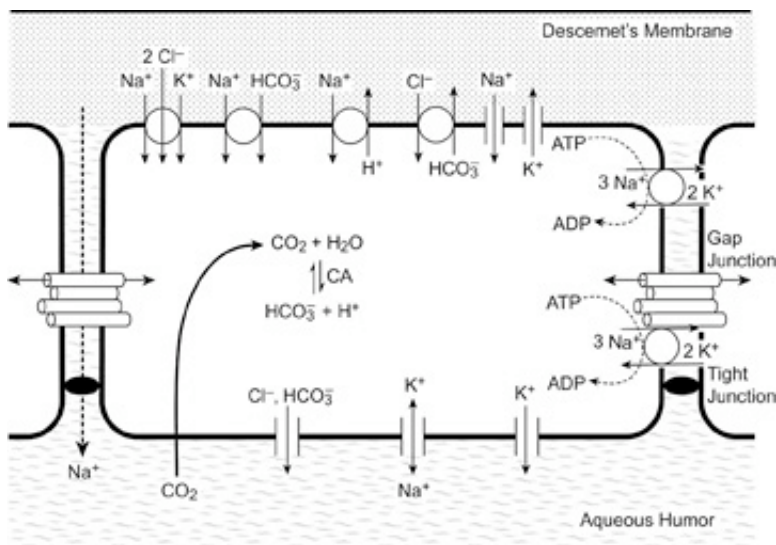


Figure 28. Transporters and channels identified in corneal endothelial cells. Cells are connected by apicolateral macula occludens type tight junctions and by lateral gap junctions that allow for intercellular communication within the monolayer. A Na^+ concentration gradient and negative intercellular potential is set up by the basolateral Na^+/K^+ ATPase, which allows Na^+ to enter the cell via a Na^+/H^+ exchanger, $\text{Na}^+/\text{HCO}_3^-$ and $\text{Na}^+/\text{K}^+ / 2\text{Cl}^-$ co-transporters, and Na^+ permeable channels. K^+ leaves the cell via the Na^+/K^+ ATPase, down its concentration gradient through at least two different K^+ channels and through the nonselective cation channel. CO_2 diffuses across the membrane from the aqueous humor, where it combines with H_2O in the presence of carbonic anhydrase (CA) to form HCO_3^- and H^+ . The H^+ leaves the cell through the Na^+/H^+ exchanger, and HCO_3^- exits via an exchanger and anion channels. The Cl^- can then exit down its electrical gradient via anion channels on the apical membrane.

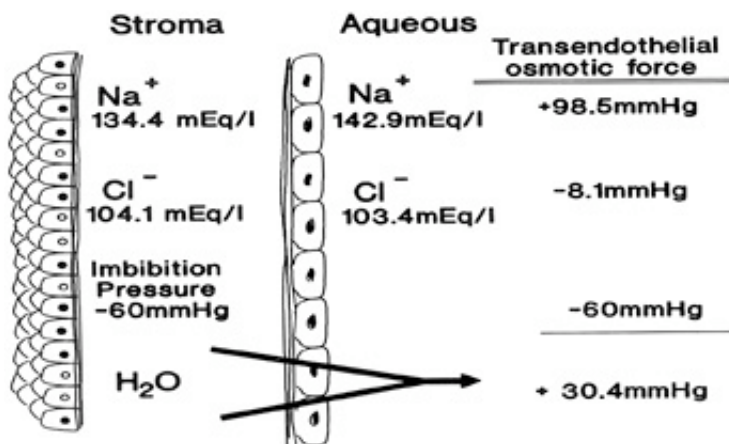


Figure 29. Diagram illustrating the total transendothelial osmotic force due to Na^+ activity, Cl^- activity, and imbibition pressure. Although the Na^+ activity within the aqueous humor is greater than that within

the stroma (142.9 vs. 134.4 mEq/L, $P < 0.05$.), using a reflection coefficient of 0.6, the calculated osmotic force due to Na^+ is 98.5 mm Hg. Similar calculations for Cl^- and imbibition pressure result in osmotic forces of -8.1 and -60 mm Hg, respectively. The sum of these forces results in a total osmotic force of +30.4 mm Hg, which ultimately results in deturgescence of the cornea. (From Stiemke MM, et al. Na^+ activity in the aqueous humor and corneal stroma of the rabbit. *J Exp Eye Res* 55:425, 1992.)

In addition to the transporting proteins, several types of ion channels have been characterized in the endothelial cells. These include two K^+ channels, a nonselective cation channel, a large conductance anion channel the CFTR channel, a Ca^{++} -activated Cl^- channel (also permeable to HCO_3^- , and a tetrodotoxin-blockable Na^+ channel).^{107,108,109} It is believed that these channels act as pathways to help maintain ionic balance within the cells. It has been shown that at least one of the K^+ channels is important in maintaining the resting voltage of the endothelium, whereas the Cl^- channels may also assist in HCO_3^- transport.^{107,108,109}

As with the other cell types of the cornea, endothelial cells have intercellular connections via gap junctions. These junctions have been visualized by transmission electron microscopy¹¹⁰ and freeze fracture microscopy,⁷ and their permeability and gating characteristics have been measured by dye spread and patch clamp techniques.^{111,112,113} Connexin-43 is one of the major gap junction proteins present in human gap junction complexes.¹¹⁴ As in the corneal epithelium, endothelial gap junctions have increased connectivity in the presence of bicarbonate.¹⁵

Although this review is primarily concerned with healthy, normal corneal endothelium, there are many exogenous stresses that could potentially damage the corneal endothelium. Perhaps the most common interventions that affect the cornea/endothelium include contact lens wear, excimer laser refractive surgery (LASIK, PRK), and intraocular surgery (cataract surgery, refractive IOL surgery, corneal transplantation). Contact lens wear does not appear to cause loss of endothelial cell density, but can acutely induce reversible corneal edema and/or can cause chronic signs of endothelial cell stress (increased polymegathism and decreased pleomorphism).^{58,114} Contact lens-induced endothelial cell changes are thought to occur because of hypoxia, as they are not observed with more oxygen permeable lenses.¹¹⁴ Excimer-based refractive surgery has only been found to induce acute, transient endothelial cell stress (increased polymegathism and decreased pleomorphism) and loss of barrier function if performed on a cornea with a residual corneal thickness $\leq 200 \mu\text{m}$, presumably because of the shockwave produced by the laser ablation.⁸⁵ Otherwise, no long-term effects have been linked to laser refractive surgery.⁸⁵

By comparison, all intraocular surgeries have been found to cause varying degrees of both acute and, more importantly, long-term chronic damage to endothelium. Modern small incision cataract surgery (Kelman phacoemulsification [KPE] + foldable IOLs) has been shown to cause an exponential reduction in the central endothelial cell density; at 1 year after surgery, endothelial cell density loss averages 10.5%.¹¹⁵ Additionally, no significant change in polymegathism or pleomorphism has been found.¹¹⁵ This fast component period of cell loss is similar to extracapsular cataract extraction (ECCE), another common way of performing cataract surgery, which results in a 9.1% reduction in endothelial cell density at 1 year after surgery.¹¹⁵ Capsule rupture with vitreous loss, hard cataracts, and age at the time of surgery are factors that have been shown to significantly increase endothelial cell loss rates in KPE cases compared to ECCE cases.¹¹⁵ Longer-term slow component cell loss data is currently unknown on KPE, whereas ECCE data shows that a 2.5% linear rate of cell loss occurs from 1 to 10 years after surgery.¹¹⁴ Early data from refractive IOL procedures seem to show even less damage to the cornea/endothelium than cataract surgery.

Finally, corneal transplants have been found to have the greatest long-term decreases in central endothelial cell densities of all the intraocular anterior segment procedures, perhaps because of the peripheral loss of adult stem-like cells that are located on or near Schwabe's line.¹¹⁶ Long-term longitudinal studies out to 20 years postoperatively show that endothelial cell loss after corneal transplantation occurs in two phases: a fast and a slow component. During the fast component, the central endothelial cell density decreases exponentially with 36.7% cell loss at 1 year and 8.4% cell loss at 5 years after surgery.¹¹⁷ Thereafter, a slow component occurs where central endothelial cell density decreases at a linear steady rate of 4.2% per year.¹¹⁷ Concurrently, polymegathism gradually increased and pleomorphism gradually decreased throughout the longitudinal follow-up period.

A secondary function of endothelium is its ability to secrete an extracellular matrix. The secreted and deposited extracellular matrix along the basal surface of the endothelium is known as *Descemet's membrane* (Fig. 12) and is essentially a lifelong accumulated basement membrane of the endothelial cells, similar to that of a tree trunk with accumulating tree rings. Although some collagen fibrils from the posterior stroma are embedded in the Descemet's membrane, it has no junctional or adhesional complexes. Descemet's membrane is highly elastic and strong as it is primarily composed of collagen (type IV and VIII) and glycoproteins (fibronectin, laminin, thrombospondin). At birth, it is 4- μm thick. On electron microscopy, this fetal Descemet's membrane is composed of many wide-spaced, 110-nm banded collagens.¹¹⁸ After birth, collagen is gradually added to this initial fetal layer throughout life, being notably different from the fetal layer as it is nonbanded and contains small diameter collagen fibrils that arrange into a lattice matrix.¹¹⁸ Typically, the Descemet's membrane at senescence in normal adults free of eye disease measures 10- to 15- μm thick (4- μm thick banded layer and a 6- to 11- μm thick non-banded layer). With disease (*e.g.*, Fuchs' endothelial dystrophy, bullous keratopathy), the Descemet's membrane may become focally or diffusely thicker than normal from abnormal collagen deposition. This newly deposited abnormal collagen is called the posterior collagenous layer of the Descemet's membrane and is classified as one of three types: banded, fibrillar, and fibrocellular.¹¹⁹ Presumably, this posterior collagenous layer is deposited because endothelial cells become stressed from damage or disease.

Finally, the endothelium is also known to secrete a 0.5- μm thick glycocalyx layer on its apical surface (Fig. 24).⁸⁵ Functionally, it appears to protect endothelium, particularly in regard to anterior segment surgery.

CORNEAL METABOLISM

Epithelium

Because of the cornea's exposure to the external environment, metabolism is carried out under a broad range of temperatures. The average temperature of the human cornea has been estimated to be 34.8°C but will vary with the extremes of the environmental temperature.¹²⁰

The corneal epithelium primarily uses glucose and glycogen for energy production. Glucose reaches the cells by diffusion from the aqueous humor, and the corneal epithelial cells store high levels of glycogen. Epithelial glycogen is rapidly depleted under stress, such as hard contact lens wear or trauma.^{121,122,123,124} Glucose is metabolized in the corneal epithelium primarily by anaerobic glycolysis (Embden-Meyerhof pathway); however, up to 35% of glucose enters the hexose monophosphate (HMP) shunt. The HMP shunt converts hexoses to pentoses required for nucleic acid synthesis and produces the reduced form of nicotinamide-adenine dinucleotide phosphate (NADPH), a high-energy reducing agent required for fatty-acid synthesis and membrane repair. NADPH and pentoses are both required for a tissue with a high mitotic index, like the corneal epithelium. Glucose in the cornea may also enter the sorbitol pathway, which produces sorbitol and fructose. In the presence of excess glucose, sorbitol may accumulate in the cornea as it does in the lens and peripheral nerves, causing osmotic cell damage. However, the role of sorbitol in corneal epithelial damage in diabetes is not clear.^{125,126}

The corneal epithelium receives its oxygen from the atmosphere under open-eye conditions where it is exposed to a partial oxygen pressure of 155 mm Hg in the tears. When the eyelids are closed, the oxygen pressure drops to 55 mm Hg, which is apparently adequate to maintain the epithelium, although a degree of epithelial edema does occur during sleep.¹²⁷ Corneal thickness is increased in the morning following overnight eyelid closure.

The cornea consumes approximately 3.5 μL of oxygen/ cm^2 /hour.^{128,129} Under aerobic conditions, pyruvate from glycolysis can enter the tricarboxylic acid cycle (Krebs cycle), although the activity of the pathway is low in the epithelium because of the paucity of mitochondria.^{123,128,130} Under hypoxic conditions (e.g., during contact lens wear), pyruvate is converted to lactate which, as described earlier, is transported from the cells to maintain intracellular pH at between 7.3 to 7.4. Lactate cannot diffuse across the apical barrier and builds up in the stroma.¹³¹ Associated with this lactic acid is anoxia of the epithelial cells, leading to epithelial edema that clinically can cause halo formation, glare, and reduced contrast sensitivity. The acidification of the extracellular fluid may interfere with cellular metabolism and mitosis, leading to epithelial thinning and erosion.^{132,133}

The cytochrome P450 system is also functional in the corneal epithelium. Under conditions of hypoxia or inflammation, arachidonic acid is metabolized through this pathway with the production of two eicosanoids, 12(R)-hydroxyeicosa-tetraenoic acid (12(R)HETE) and 12(R)-hydroxyeicosatrienoic acid (12(R)HETrE).^{134,135} Both of these eicosanoids have pathophysiologic importance. 12(R)HETE has the potential to diffuse from the epithelium to the endothelium and inhibit Na^+/K^+ ATPase and the endothelial metabolic pump, ultimately causing corneal swelling.¹³⁶ 12(R)HETrE can serve as a chemoattractant and induce stromal neovascularization.¹³⁷ Contact lenses that do not fit well or have low oxygen permeability can lead to inflammation and hypoxia from 12(R)HETE or lactate, which can have an adverse effect on the structure and function of the corneal endothelium.¹³⁸

Stroma

Very little is currently known about the metabolism of corneal stroma besides traditional cross-sectional ultrastructural analysis of stromal keratocytes that show these cells as metabolically quiescent cell types.⁶⁹ Only recently has tangential ultrastructural analysis been performed, which suggests that the resting metabolic state of the stromal keratocyte is probably much higher than initially thought as these cell must produce and maintain the extracellular matrix of the corneal stroma.⁶⁹

Endothelium

The endothelium utilizes the same carbohydrate metabolism pathways as the epithelium. The transport function of the cells in the endothelial monolayer requires oxidative activity that is five to six times that of the cells in the epithelium.¹³⁹ Atmospheric oxygen is the primary source of oxygen to the endothelium. Interruption of this oxygen supply by low-oxygen transmissibility contact lenses or a low-oxygen environment will result in a shift to anaerobic metabolism, a concurrent increase in stromal lactic acid and CO_2 , and a drop in stromal pH.¹³¹ In addition, this hypoxia can stimulate epithelial production of 12(R)HETE, a potent inhibitor of the endothelial Na^+/K^+ ATPase.^{136,140} Acute reversible clinical changes seen with hypoxia include stromal swelling, endothelial dysfunction, and endothelial blebbing. Chronic hypoxia can lead to irreversible endothelial polymegathism and pleomorphism. Pulse et al have shown chronic hypoxia in humans alters the endothelium's ability to reverse induced swelling.¹⁴¹

It has been estimated that glycolysis accounts for 93% of the conversion of glucose-6-phosphate to pyruvate in the endothelium. The aerobic tricarboxylic acid cycle converts 30% of the pyruvate to ATP, whereas the remaining 70% is converted to lactic acid by the anaerobic pathway of lactate dehydrogenase.¹³⁹ Geroski and

colleagues¹⁴² found that 37% of the glucose in the rabbit corneal endothelium is metabolized by the pentose phosphate shunt pathway. Adenosine has been found to stimulate this pathway in bovine endothelial cells.¹⁴³

The endothelium also has the ability to extract and metabolize dehydro-L-ascorbic acid from the aqueous humor. Bode et al found that bovine endothelial cells can take up dehydro-L-ascorbic acid, the oxidized form of ascorbic acid, and reduce it to ascorbic acid.¹⁴⁴ Ascorbic acid is a free-radical scavenger that may act to protect the cells from radiation-induced free-radical damage.

WOUND HEALING

Epithelium

Following injury, the epithelium heals through three distinct steps: cell migration, cell proliferation, and cell adhesion. Before entering these steps, a 4- to 6-hour latent phase occurs where the epithelium responds by desquamating damaged cells, polymerizing actin filaments, synthesizing structural proteins, and releasing all hemidesmosomal attachments to the basal lamina extending 50 to 70 μm from the wound edge and significantly reducing those up to 200 μm from the wound edge.¹⁴⁵ This is followed by a linear cell migration phase where a flattened monolayer of epithelial cells slide over the abraded areas and re-establish a barrier.¹⁴⁶ Cell sliding, or migration, occurs at a constant rate of 60 to 80 $\mu\text{m}/\text{hour}$ until the wound closure.^{145,146,147,148} The normal number of cell layers is subsequently re-established by limbal stem cell proliferation, basal epithelial cell centripetal migration, and vertical basal epithelial cell proliferation.¹¹⁵ As discussed earlier, the epithelium usually heals to normal thickness around 50 μm approximately 1 to 4 weeks after injury, but alternatively, it may thin over elevations or thicken over defects in the underlying stroma. Finally, adhesion complexes are usually regenerated by 1 to 2 months after injury, thereby permanently anchoring the healed epithelium firmly to the underlying stroma.¹⁴⁹

The migratory step is a process that is independent of cell proliferation and is an energy-consuming step as glycogen is depleted from epithelial cells at the wound edge during healing.^{146,149} Both basal and suprabasal cells participate in the migratory process as epithelial cells appear to prefer to migrate centripetally as one continuous coherent sheet.^{149,150} The formation of lamellipodia and filopodia mark the beginning of cell migration. These areas of the cells as well as at the leading edge of the migrating epithelial cells seem to contain dense networks of contractile actin filaments that are important in the mechanics of epithelial cell motility.¹⁵¹ Experimentally, blocking polymerization of actin has resulted in loss of cell migration.¹⁵² Lamellipodial and filopodial activity continues until wound closure is complete with at least a continuous monolayer of epithelial cells recovering the defect. Commonly, individual or small groups of epithelial cells migrate independently from the coherent sheet and form predominantly clockwise whorls on the surface of the healing cornea.¹⁴⁹ This unique pattern of healing has been termed *hurricane keratopathy*. It is postulated to occur because the migrating epithelial cells respond in this fashion to electromagnetic field generated by the electrical potential of the eye.¹⁵³ Despite acting independently, cell proliferation appears to complement cell migration as epithelial cells away from the wound increase their rate of cell proliferation.¹⁵⁰ Therefore, a wave of cells moves from the periphery to the wound, while the epithelial cells in the wound cease proliferating until a continuous monolayer of cells is re-established.

Although epithelial cell migration occurs without hemidesmosomal adhesion complexes, adhesion is still maintained via transient macromolecular focal contacts that are constantly formed and released during cell migration.¹⁴⁹ After epithelial wounding, fibronectin, fibrin, laminin, tenascin, and dimeric glycoproteins accumulate on the denuded corneal stroma surface if the basal lamina is not left intact after injury.¹⁵⁴ Migratory epithelial cells form focal temporary cell-to-substrate macromolecular contacts known as *adhesion plaques*. Intracellular actin mediates such attachments by aggregating into stress fibers oriented in the direction

of migration and with the help of several cell surface adhesion molecules (*i.e.*, vinculin, talin, integrin, fimbrin, and α -actin) that are synthesized by the epithelium during wound healing and bind to the extracellular substrates. Vinculin, a 110-kD cytoplasmic protein that links actin to talin, is concentrated in focal adhesion plaques on the plasma membrane at the wound edge where talin in turn is linked to integrin.^{155,156,157} It appears that the increase in vinculin synthesis during migration promotes the interaction of contractile protein (actin) with adhesion proteins (talin and integrin) so that the migrating cells can adhere to extracellular substrates in the absence of hemidesmosomes. The temporary focal contacts enable the cells to slide forward, then the epithelial cells release plasminogen activator at these focal contact areas. This in turn converts plasminogen to plasmin, which lyses previously used as adhesion plaques, allowing the cell to advance and form new adhesion plaques. The actual strength of these adhesion plaques is apparently relatively weak because regenerating epithelium can be easily peeled off as a sheet.¹⁵⁸ Temporary adhesion plaques cease forming after wound closure from epithelial cell contact inhibition, at which time permanent hemidesmosomal adhesion complexes start being produced. The rapidity with which these permanent adhesion complexes form depends on whether the epithelial basal lamina remains intact. In rabbits, permanent adhesion complexes have been found to be regenerated within 1 week of wound closure if the basal lamina was left intact after injury, whereas it takes 6 weeks to occur if the basal lamina had to be resynthesized.¹⁵⁸ Besides requiring energy, epithelial healing also appears to require calcium since cell migration is inhibited by calmodulin inhibitors.¹⁵⁹ Additionally, corneal nerves also have an effect on epithelial wound healing, as is evident from denervated corneal epithelial tissue which shows a markedly reduced proliferation rate.¹⁵³

Usually, an epithelial injury heals rapidly and uneventfully. Occasionally, however, persistent epithelial defects or recurrent corneal erosions develop, which is either due to deficiencies in the migratory or proliferation steps, or to the cell adhesion step, respectively. This has led to a search for therapeutic agents that promote or enhance wound healing. Various agents known to be involved in epithelial growth, adhesion, and differentiation have been studied experimentally and in clinical trials. These include topically applied epidermal growth factor, fibronectin, vitamin A, and many other agents.^{149,160,161,162,163,164} Although promising experimental results have been obtained, no agent has been identified to date that can consistently stimulate epithelial repair. In particular, there is no uniform confirmation of the utility of these agents in human disease.

As described earlier, limbal corneal epithelial stem cells produce the progenitor cells that are responsible for corneal epithelial cell regeneration. The stem cells are normally slow-cycling, long-lived cells that can be stimulated to replicate to a higher degree after wounding to produce many rapidly-dividing transient amplifying cells (TA) that help in healing corneal surface injuries. Because it has been known for some time that corneal injuries can be replaced by vascular conjunctival epithelium, it is also understood that under normal circumstances the limbal epithelium acts as an inhibitory barrier to the migration of conjunctival epithelium onto the cornea.¹⁶⁵ However, when corneal epithelial injury also includes the limbus, this barrier can be permanently destroyed. This often is followed by permanent vascular conjunctival epithelial migration onto the corneal surface.¹⁶⁶ Although conjunctival epithelium can theoretically undergo a slow transformation back to normal corneal epithelium called *conjunctival transdifferentiation*,¹⁶⁷ animal models suggest that the transdifferentiated conjunctival epithelium is still far from normal and at best represents squamous metaplasia with loss of goblet cells.^{168,169,170} The main problem with this type of conjunctival epithelium is that it is thinner than normal, stains with fluorescein, attracts new blood vessels, and is prone to recurrent corneal erosions. Therefore, it significantly affects the optical qualities of the cornea and can be quite irritating to the patient.

The knowledge gained from the basic science discoveries of a limbal corneal epithelial stem cell population and the problems encountered by limbal stem cell deficiency has led to the development of limbal stem cell transplantation. As described earlier, the concept of using autologous conjunctival epithelial transplants to treat unilateral chemical injury was first described by Thoft in 1977.¹¹⁵ This concept was first put into clinical

practice in 1989 by Kenyon and Tseng.¹⁷¹ Currently, limbal stem cell transplantation uses both autograft or allografts with amniotic membrane as a carrier for the cells.^{172,173} Because autografts are limited mainly to unilateral disease and allografts require significant and sometimes unsuccessful immunosuppression, cultured autologous limbal, corneal, and even oral mucosa epithelial sheets are being experimented with for corneal epithelial transplantation.^{174,175} The amniotic membrane, through its host of growth factors and matrix proteins, appears to facilitate epithelialization and to reduce inflammation, vascularization, and scarring, and can be used alone (with no corneal or limbal epithelial cells) to treat corneal epithelial disorders such as those associated with symptomatic bullous keratopathy or corneal burns.^{176,177}

Stroma

The first published report specifically addressing the cellular reactions in the cornea stroma after injury occurred in 1958.¹⁷⁸ It described the morphologic changes of stromal cells after different types of trauma and found that stromal cells lose their interconnecting, dendritic processes immediately after injury with many cells subsequently developing signs of degeneration. That report also described the appearance of morphologically-unique spindle-shaped corneal fibroblastic cells invading into the wound region during later stages of stromal healing. Since that time, many excellent animal corneal wound healing studies have further addressed the changes in the extracellular matrix^{179,180,181,182} and the stromal cells^{183,184,185} after stromal injury. They suggest that corneal stromal injury is immediately followed by a zone of keratocyte apoptosis around the site of stromal injury (Fig. 30A) with a subsequent influx of transient mixed acute and chronic inflammatory cell infiltration, proliferation and migration of surviving keratocytes (Fig. 30B), and finally differentiation of the keratocytes into a transiently metabolically activated cell type called an activated keratocyte. This latter cell type is functionally important because it synthesizes and deposits the extracellular matrix of the stromal scar, while also degrading and remodeling the cellular and extracellular tissues around the wound. Interestingly, epithelial injury alone can also cause transient cellular injury to the underlying stroma (*i.e.*, apoptosis, proliferation, migration, and possibly activation of keratocytes) along with causing stromal edema, presumably from factors in the tears.^{184,186}

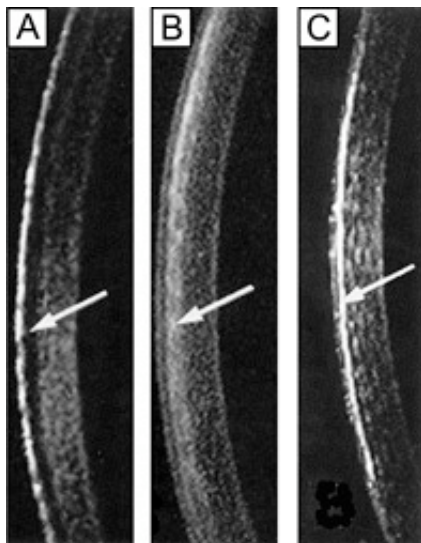


Figure 30. Slit lamp biomicroscopy of rabbit corneas 4 days (A) and 3 weeks (B) after manual epithelial debridement and 1 month after PRK (C). (A) demonstrates a 100 μm zone of keratocyte apoptosis and (B) demonstrates the repopulation of the acellular zone with migratory and activated keratocytes. Note that the epithelial debrided corneas completely returned to normal transparency by 8 weeks after injury. (C)

demonstrates increased light scattering caused by myofibroblasts that are found in a hypercellular fibrotic scar. Note in the PRK corneas that the haze improved over the first year after surgery, but has not returned to normal levels. Arrows = area of interest. (Modified from Moller-Pedersen T. Keratocyte reflectivity and corneal haze. *Exp Eye Res* 78:553, 2004.)

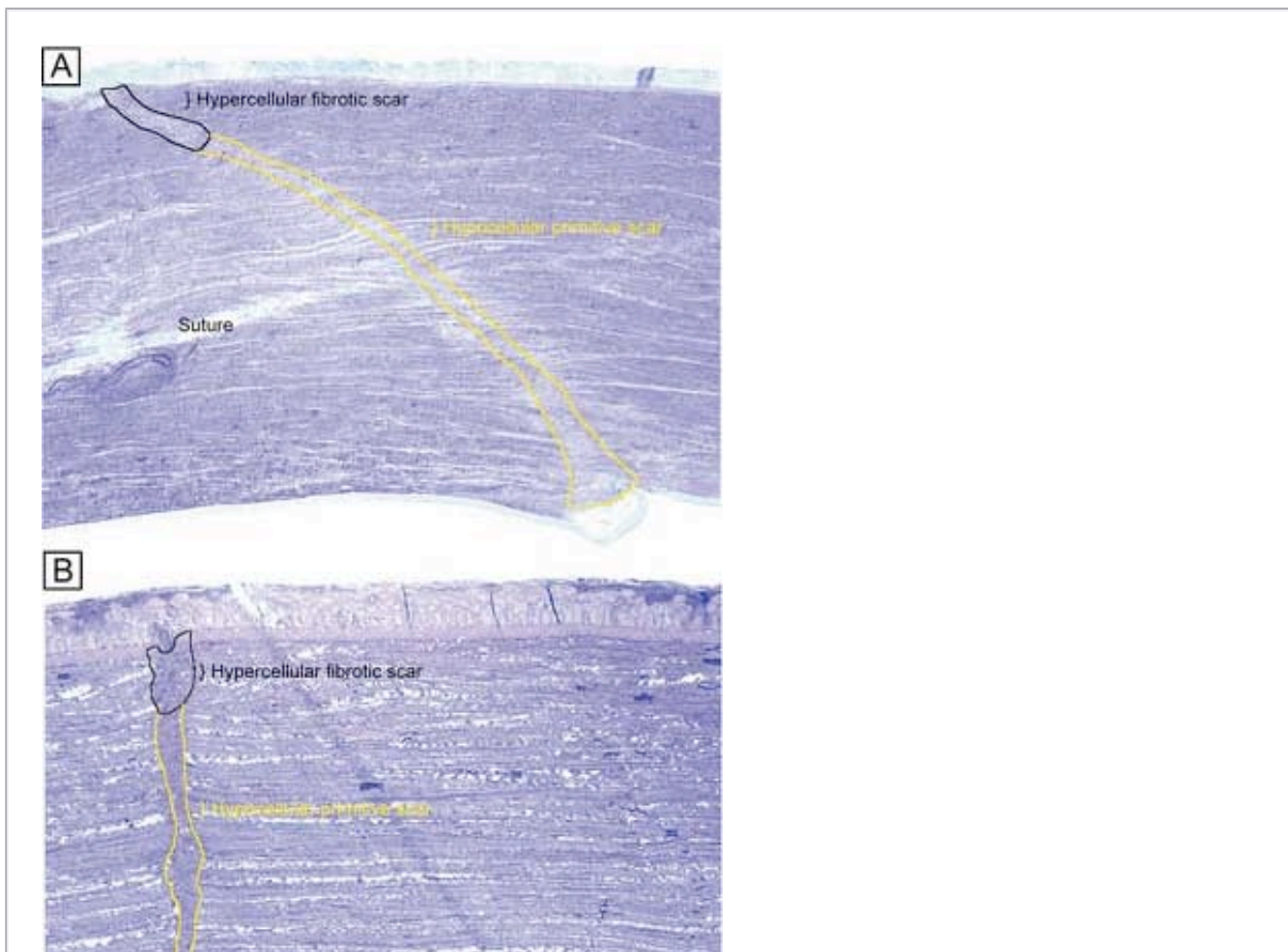
Electrophysiologic studies evaluating corneal keratocytes have examined the migration of keratocytes in an electric field.¹⁸⁷ These studies found a positive galvanic response in keratocytes. Studies in other wounded tissues have found similar electrical fields generated in the area of the wound. Such electrical fields may act to attract keratocytes to the wound site. It is possible that ion channels have a role in the activation of and/or responses of keratocytes in the wounded corneal stroma. Interestingly, keratocytes isolated from wounded corneas (myofibroblasts) lose their major ionic conductances (Na^+ and K^+) and gain a Cl^- channel that is not found in quiescent keratocytes. This Cl^- channel can be activated via a receptor-mediated response by lysophosphatidic acid (LPA) and other members of the lipid growth factor (PLGF) family, including sphingosine-1-phosphate (S1P).^{188,189,190,191,192} Rabbit studies have also shown that many of these PLGFs become elevated in the aqueous humor and in tear following corneal injury.¹⁹³

Epithelial-stromal interactions appear to be important to the process of stromal wound healing as it causes an increase in the number of proliferating and migrating keratocytes within the wound, some of which differentiate beyond the activated keratocyte stage into myofibroblastic cell types (Figure 30C).¹⁹⁴ Many studies have focused on initiation of keratocyte activation and the substances secreted by these activated cells. Several substances associated with the corneal wound healing process have been shown to activate keratocytes. These activating factors include epithelial growth factor (previously called mesodermal growth factor),^{195,196} fibroblast growth factor (FGF),¹⁹⁷ interleukin-1, transforming growth factor- β ,¹⁹⁸ insulin,¹⁹⁹ retinoic acid,^{200,201} and LPA.¹⁹⁰ Transforming growth factor- β is currently the major epithelial growth factor of this group that is also known to stimulate myofibroblast transformation and enhance the normal repair process.^{184,194,198} Once activated, keratocytes exhibit a wide range of cellular responses, including increased tritiated thymidine uptake (indicating increased cell proliferation),^{199,201} initiation of protease and collagenase activity,^{202,203} phagocytosis,^{204,205} interferon, prostaglandin and complement factor I production,^{206,207,208} as well as fibronectin, collagen, and proteoglycan secretion.^{209,210,211,212,213,214,215} Epithelial-stromal interactions appear to augment the wound healing process by causing the production of a thicker and stronger extracellular scar matrix than that found in deeper stromal wound regions that receive no epithelial cell factors.²¹⁶

When reviewing the literature, it is important to realize that human studies^{217,218,219,220} concur with animal studies on most issues with the following notable differences: adult human corneas heal less aggressively, more slowly, and not as completely as animal corneas. However, both animal and human studies show that corneal stromal wounds heal in two distinct phases: (a) an active phase that results in the production of a stromal scar (over the first 6 months after injury in humans), and (b) a remodeling phase that improves corneal transparency and increases wound strength (occurs up to 3.5 years after injury in humans). Overall, the long-term result in human corneas is the production of a hypercellular fibrotic stromal scar type in wound regions where epithelial-stromal interactions occur and a hypocellular primitive stromal scar type in wound regions where keratocyte injury pathways work alone. These two histologic wound types have functional significance as the hypercellular fibrotic stromal scar is strong, but can look clinically hazy because of myofibroblastic cells populating this scar type.²²¹ In contrast, the hypocellular primitive stromal scar is transparent, but is very weak in tensile strength and serves as a potential space for fluid, inflammatory cells, and microbes. An additional variable to consider in this simplified scheme is the fact that more precisely realigned wounds (*i.e.*, sutured wounds or unsutured wounds with minimal gapping and no epithelial cell plugging) heal better than poorly-aligned wounds (*i.e.*,

wounds with wide wound gaping, epithelial plugging, or incarceration of adjacent corneal tissue).

The location and the variable amounts of scar types along with the variable degrees of wound realignment in the human cornea is best exemplified when one reviews published human histopathologic studies that describe findings in corneas that have had common ophthalmic procedures such as cataract extraction (CE), penetrating keratoplasty (PKP), radial keratotomy (RK), AK, PRK, or LASIK. Sutured and unsutured clear corneal cataract wounds are corneal stromal incisions constructed at oblique angles to corneal surface so that they self-seal. They usually heal with well-aligned external wound margins and wound edges, which results in a small, 50 to 75 μm in depth, subepithelial zone of hypercellular fibrotic scarring and a remaining deeper zone of hypocellular primitive scarring (Fig. 31A). Occasional small epithelial plugs are found in the external wound of unsutured clear corneal cataract wounds and commonly Descemet's membrane is found partially detached or poorly realigned along the internal wound margin so that some stromal ingrowth occurs. In marked contrast, limbal and scleral tunnel cataract incisions heal because fibrovascular granulation tissue from the episclera completely grows into the wound by 15 days after surgery and finishes remodeling by 2.5 years after surgery.^{222,223,224} PKP wounds heal similar to sutured clear corneal cataract wounds with the notable exceptions of having significant wound compression because of the 0.25- to 0.5-mm oversized nature of the donor button and wound edge mismatch caused by the irregular, asymmetric nature found between donor and host wound edges. Additionally, a high percentage of PKP cases have overriding external or internal wound edges with Bowman's layer or Descemet's membrane incarceration.²²⁵ Although partial thickness (70% to 95% depth) and constructed perpendicular to the corneal surface, RK and AK wounds heal similarly to that of unsutured clear corneal cataract wounds.^{226,227,228,229,230} The most notable difference from unsutured cataract wounds is the more commonly present and more widely variable degree of external wound gaping found in these corneas (Fig. 31B). Additionally, when wound gaping occurred, epithelial cells almost universally migrated into these areas and formed epithelial plugs that rarely resolved (~90% of cases).



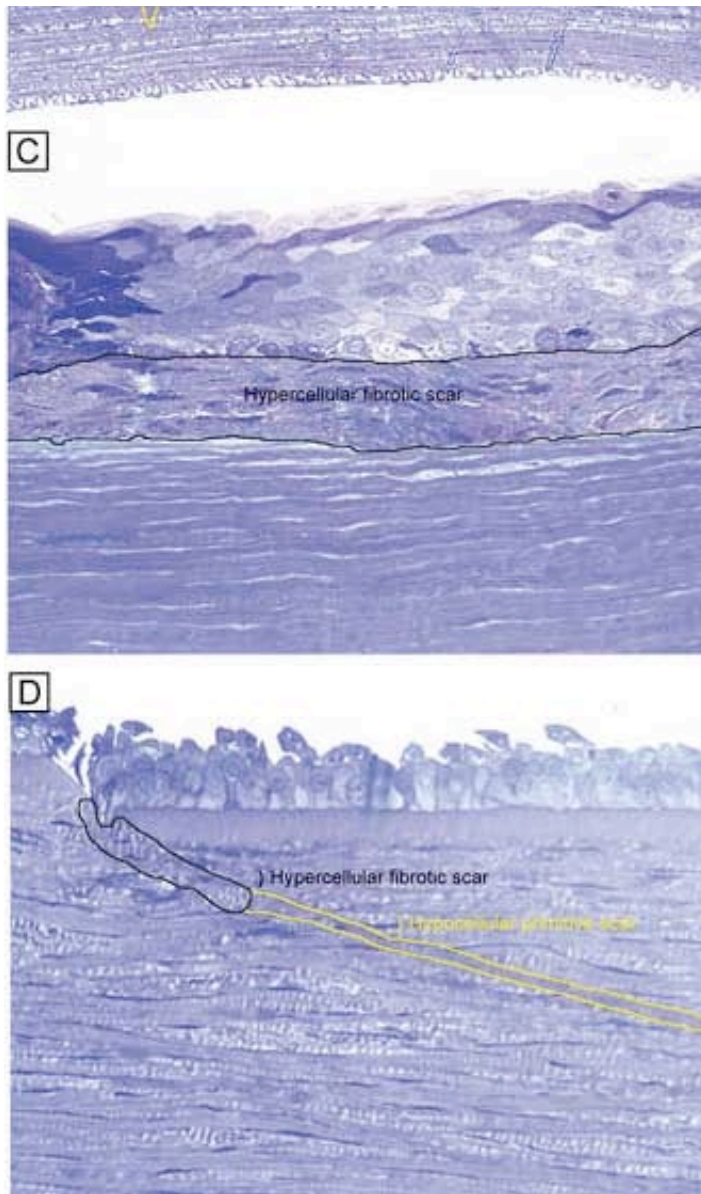


Figure 31. Light photomicrographs of corneas that haze undergone sutured, temporal, clear-corneal cataract surgery (A), astigmatic keratotomy (B), photorefractive keratotomy (C), and laser-assisted in situ keratomileusis (D). Note that the corneas demonstrate the long-term results of surgery as all corneas are greater than 4 years after surgery. (coluidene blue 15× for A, 25× for B and 100× for C and D).

PRK consists of submicron accurate anterior keratectomy using the excimer laser resulting in a surface wound that heals entirely under the influence epithelial-stroma interactions. Therefore, a disc-shaped hypercellular fibrotic stroma scar is produced, which usually is 15% to 25% in thickness of the amount initially ablated (Fig. 31C).^{231,232} As LASIK involves a partial-thickness lamellar incision (mechanical or laser created) followed by excimer laser guided intrastromal excision of tissue, it heals most similar to that of unsutured clear corneal cataract incisions. A subepithelial zone of hypercellular fibrotic scarring occurs at the flap wound margin and the remainder heals by producing a hypocellular primitive stromal scar usually with a thickness around 3% to 10% of that amount ablated by the excimer laser (Fig. 31D).^{233,234,235} Around 50% of the LASIK cases were found have at least some microscopic epithelial ingrowth present.

Endothelium

The corneal endothelium is the primary regulator of corneal hydration and, in turn, its transparency. Therefore, any injury to the endothelium must be compensated for in order to maintain a clear cornea.

Following injury to the central endothelium, both the central and peripheral cell densities (cells/mm²) and percent hexagonal cells are reduced, whereas the coefficient of variation of cell size (an indicator of polymegathism) is increased.^{236,237,238} In the rabbit, where wound healing is accompanied by both endothelial migration and extensive endothelial cell proliferation, these parameters shift toward preoperative values during the time course of wound healing. In cat corneas, where minimal cell division occurs following endothelial wounding, cell density remains depressed; a similar situation occurs in the human cornea.

Several studies have examined endothelial function following wound healing via corneal thickness measurements. Yee examined the permeability characteristics of the endothelium over the time course of wound healing while incorporating an ouabain-binding analysis to quantitate endothelial Na⁺/K⁺ ATPase pump-site densities.²³⁸ From this study, it was concluded that the endothelium of the rabbit following a transcorneal freeze heals in three stages. Stage 1 (0 to 3 days) is characterized by an initial coverage of the wound by pleomorphic spindle-shaped cells that form a functional but incomplete barrier and have minimal pump site density. In stage 2 (4 to 7 days), the cells assume a flattened configuration, have an irregular polygonal shape, and establish normal pump-site density and barrier function. Stage 3 (8 to 30 days) is characterized by a continuation of the remodeling of the monolayer. During the final stages of wound healing, cell rearrangement occurs (exchange of neighbors among cells by sliding past one another).

Endothelial wound healing in the cat cornea is slower and less complete in terms of returning to preoperative values. Ling and co-workers found that removal of the central 6 mm of endothelium in the cat cornea results in stromal swelling that returns to preoperative values 35 days after wounding.²³⁹ Central endothelial cell density is decreased by 25% at 4 weeks after wounding, and the coefficient of variation increases by 60%. In a separate study, it was found that stromal swelling occurred in the cat when cell density was reduced to below 40% to 45% of control values.²⁴⁰ Humans appear to tolerate more cell loss before stromal swelling occurs. Human corneal decompensation occurs when the cell density drops below 500 cells/mm².

IN-VITRO HUMAN CORNEAL MODEL

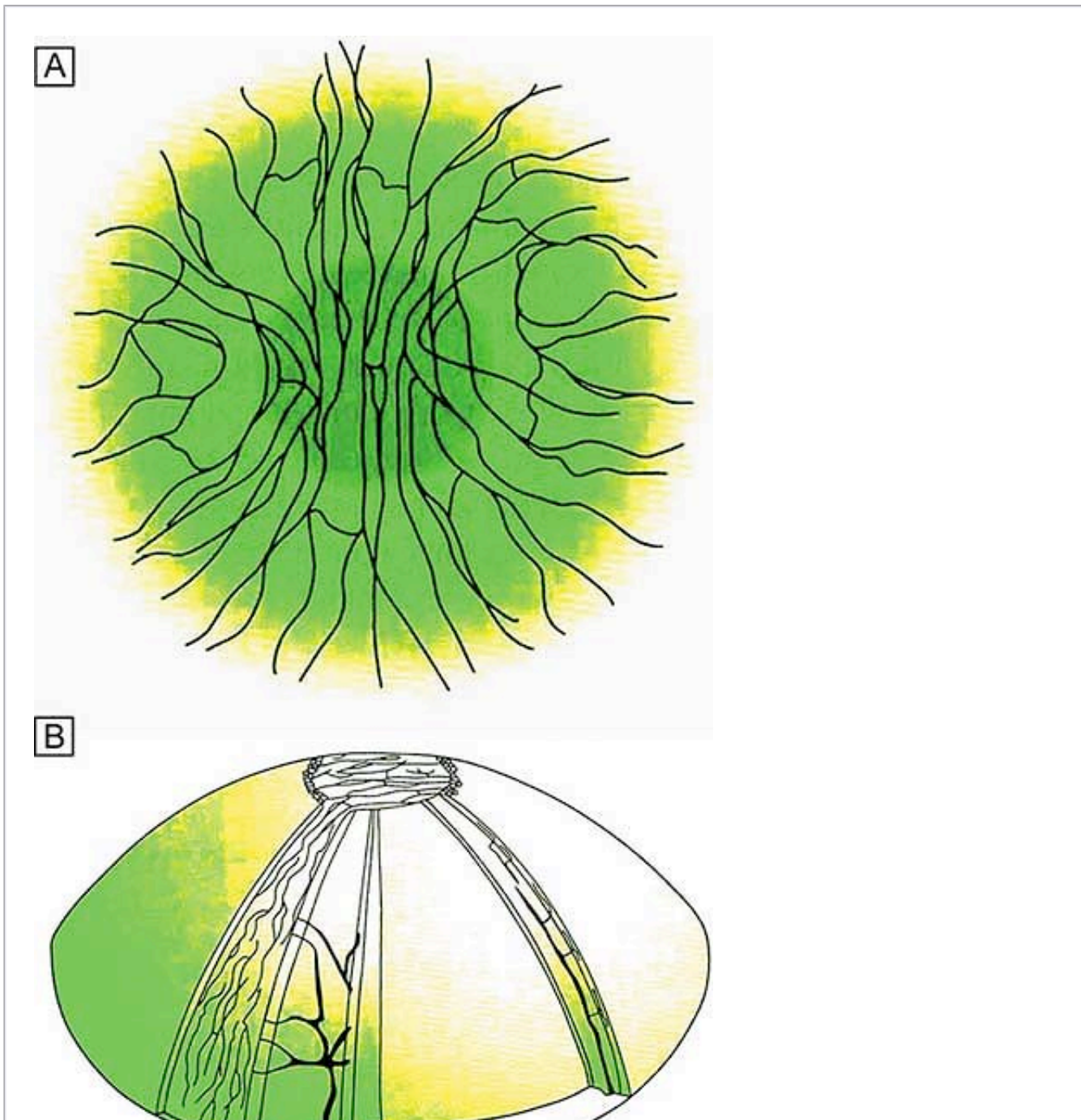
It is now possible to study human corneal wound healing and other physiological and pathophysiological corneal functions using a bioengineered human cornea developed by Griffith, Doillon, and Watsky.^{241,242} The stroma of this bioengineered cornea is comprised of type I collagen and chondroitin sulfate, whereas the cells are all cell lines derived from human corneal epithelium, keratocytes, and endothelium. It has a vascularized sclera surrounding it, and most recently has been functionally innervated.²⁴³ Functional studies demonstrate that it can volume-regulate and its wounds heal in a manner similar to that of human corneas *in vivo*. As such, it is also being used as a substitute for animal cornea studies in industrial toxicology applications. Future modifications of this bioengineered tissue could lead to a substitute for human donor corneas for penetrating keratoplasty procedures.

CORNEAL INNERVATION AND SENSITIVITY

The epithelium of the cornea is the most densely innervated surface epithelium of the body, with about 2,500 nerve terminals/mm² (300 to 600 times more dense than skin).²⁴⁴ As the surface area of the adult cornea is approximately 138 mm², it is estimated that each cornea contains around 315,000 to 630,000 nerve endings. Most of the nerve fibers in the cornea are sensory in origin and are derived from the ophthalmic branch of the trigeminal nerve (cranial nerve [CN] III₁), which supplies the eye mainly through two long ciliary nerves.²⁴⁵ Although all mammalian species have been found to receive variable proportions of nerve fibers in the cornea

from the sympathetic and parasympathetic autonomic nervous system, humans corneas appear to be on extreme end of this spectrum, as these corneas have a very small proportion of their nerve fibers derived from the autonomic nervous system.²⁴⁵

Innervation of the cornea (corneal epithelium and the anterior third of the corneal stroma) arises from the long ciliary nerves that penetrate the sclera around the scleral canal and begin to branch in the outermost layers of the choroid, or epichoroidal space, as they pass beneath the ora serrata. The main nerve trunks are myelinated and provide branching networks that supply the sclera, episclera, and conjunctiva. The remaining branches form a circumcorneal network around the limbus called the annular plexus where 60 to 80 radial nerve trunks enter the peripheral cornea at or above the midpoint of the corneal stroma (Fig. 32A). Within 1 mm of the limbus, these stromal nerve trunks lose their myelin sheaths and perineurium but retain their Schwann cell sheaths. These radial nerve trunks then branch extensively in the anterior third of stroma interconnecting among themselves in the subepithelial plexus. Few if any of the nerves pass posteriorly to innervate the area of the deeper stroma and none pass through Descemet's membrane to supply the endothelial cells.



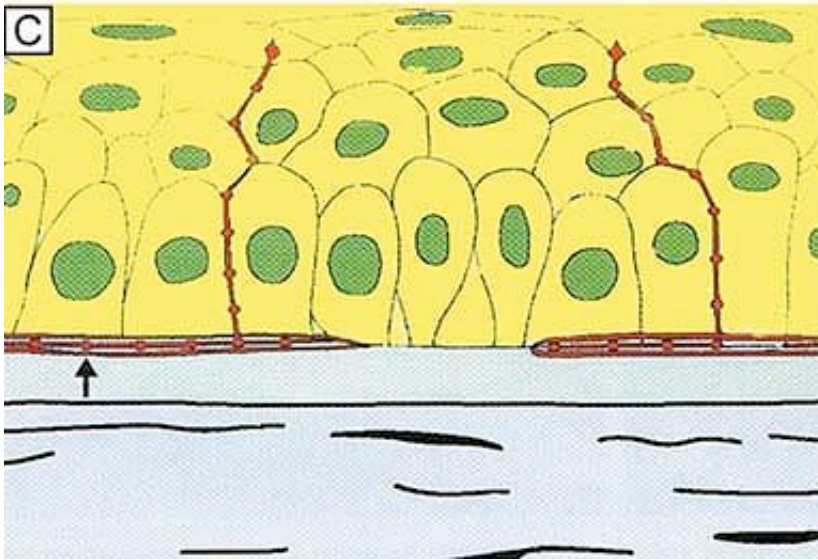


Figure 32. Schematic diagram of the distribution of nerves in the corneal stroma and subbasal nerve plexus in human corneas in (A) and (B). (C) A schematic diagram of the architecture of the nerve bundles in the subbasal plexuses (arrow) containing straight and beaded fibers. Note that only the beaded fibers branch and turn upwards to extend into the epithelium. (Modified from Muller LJ, et al. Corneal nerves: structure, contents, and function. *Exp Eye Res* 76:521, 2003.)

Although only a few nerve fibers in subepithelial plexus terminate in anterior third of the corneal stroma, parts of the stromal nerves in the subepithelial plexus that have gaps in the Schwann cell sheaths also act as receptor elements. When the nerves bundles abruptly turn 90 degrees to penetrate the Bowman's layer throughout the peripheral and central cornea, they lose their Schwann cell sheaths. They then turn 90 degrees again to continue parallel to the corneal surface forming the subbasal nerve plexus that is composed of nerve bundles that contain straight and beaded nerve fibers (Fig. 32B, C). Only the beaded fibers branch from the subbasal nerve plexus and form epithelial nerves, which course between superficial epithelial cells before finally terminating into 10 to 20 unspecialized free nerve endings (Fig. 32C). The terminals generally extend up to the most superficial epithelial cell layers. Since different types of epithelial nerve fibers can be distinguished on the basis of their ultrastructure, it appears that epithelial nerves are primarily A-delta and C fibers (touch and pain sensations). The free nerve endings in the cornea are able to generate action potentials from nonspecific stimuli. For example, generator potentials may be created from the inward diffusion of Na^+ , the outward diffusion of K^+ , or an osmotic change. The nerve ending may also be altered by pH, which can affect the ionic diffusion necessary to elicit generator potentials. It should be noted that nerve fibers from the conjunctiva and episclera also may enter the peripheral cornea and ramify, usually 2 to 3 mm past the limbus. This explains why areas of cold sensitivity can be found in the cornea.

Because the corneal nerve fibers ultimately terminate in the brainstem, it appears that interneurons, or intermediate pathways must relay the information to the sensation areas of cerebrum. Additionally, there must also be intermediate relays to efferent systems that trigger the reflex pathways of involuntary blinking (orbicularis motor innervation of CN VII) and reflex tearing (parasympathetic innervation of lacrimal gland). The intricate details of these pathways are currently unknown.

Corneal nerves appear to be very important in maintaining the health of the corneal epithelium and the ocular

surface via trophic influences and/or other factors.²⁴⁵ Since the earliest experimental studies by Magendie,²⁴⁶ it has been shown that dysfunction of corneal innervation produces a degenerative condition to the corneal epithelium called *neurotrophic keratitis*. Although many disorders can cause neurotrophic keratitis such as trigeminal nerve damage or herpes keratitis, keratorefractive surgery has gained the most attention lately for transiently causing this condition, particularly LASIK.²⁴⁷ This usually results in symptoms of dry eye after the surgery which is more common, more severe, and longer in duration following LASIK than PRK. This is because the total surface area and depth of corneal nerve injury are less after PRK than LASIK, so reinnervation takes less time with PRK than LASIK.²⁴⁸ In general, PRK is immediately followed by a loss of corneal sensation and corneal nerves in the ablated region of the cornea. Subsequently, regrowth of the subbasal nerve plexus and epithelial nerves starts around the first month after the PRK with corneal sensation recovering to normal levels by 3 months postoperatively.^{245,248} In contrast, LASIK is immediately followed by loss of corneal sensation over the flap and gradual disappearance of most of the corneal nerves in the flap over the first 2 days after surgery. Regrowth of the subbasal nerve plexus starts between 3 to 6 months after the procedure with corneal sensation recovering to normal levels by 6 to 12 months postoperatively.^{245,248} Interestingly, the total length and morphologies of the corneal nerve fibers and corneal sensation only reaches maximum levels 1 to 2 years after both of these surgeries and never completely returns to normal preoperative levels in both cases.

Corneal sensitivity is usually tested clinically in a semiquantitative fashion with a Cochet and Bonnet esthesiometer, which is a thin, flexible, nylon filament of variable length. When the filament is long, it applies very little pressure to the cornea surface because it bends easily, whereas when short it applies a proportionally higher pressure. If one maps corneal sensitivity, it is found that the cornea is most sensitive in the central 5 mm of the cornea as compared to periphery. Additionally, it is more sensitive along the horizontal meridian and least sensitive in the vertical meridian, and more sensitive in the morning than in the evening. Corneal sensitivity may be evaluated subjectively by asking the patients when they feel touch upon the cornea or objectively when a blink response is triggered. The subjective and objective thresholds are quite similar in normal corneas with the subjective threshold being slightly lower. In the center of the normal cornea, the average subjective threshold is usually 15 mg. Near the limbus this increases to approximately 31 mg for the subjective threshold and 34 mg for the objective touch threshold.²⁴⁹

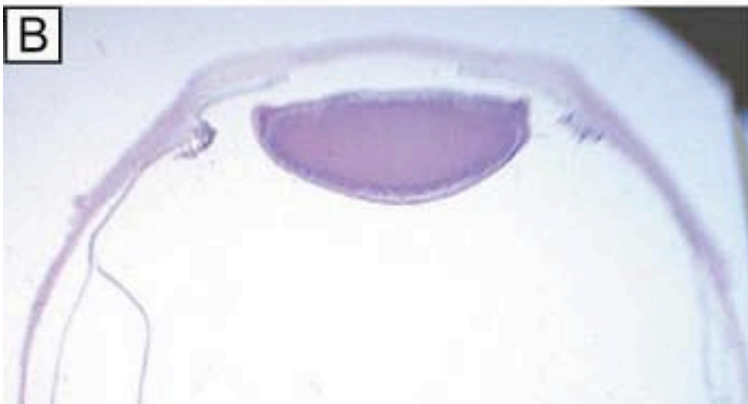
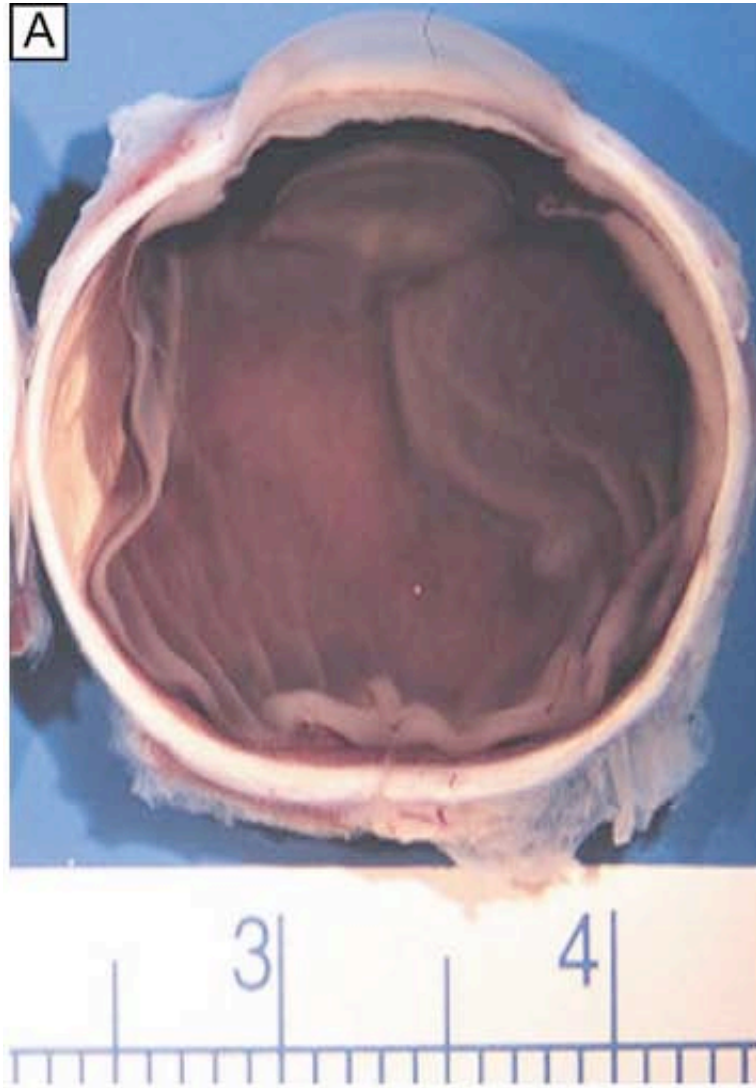
Corneal sensitivity has been found to decrease with age as the threshold of corneal stimulation normally from childhood to age 50 is around 10 to 15 mg, and gradually increases from age 50 to reach a value of 40 to 50 mg over the age of 60.²⁵⁰ It also is variably decreased following full recovery of surgical procedures on the anterior segment of the eye. As nerve regeneration occurs at the rate of approximately 1 mm per month, it may take 6 to 12 months or longer for corneal reinnervation to completely occur and corneal sensation to recover. After complete recovery, the sensitivity in the portion of the cornea involved by the procedure often is variably less than that which was present prior to surgery. For example, after complete recovery of corneal sensation from LASIK or PRK surgeries, the subjective threshold increases back to about 95% of that measured preoperatively.²⁵¹ The remarkable neural recovery abilities of cornea is perhaps most uniquely demonstrated following penetrating keratoplasty (donor tissue) as corneal sensation increases in the graft over the first couple postsurgical years. It appears that host corneal nerves can innervate the donor tissue by penetrating the full thickness scar and reinnervating the graft stroma and epithelium.

The mechanisms by which corneal nerves maintain the ocular surface and promote healing after eye injuries is currently under active research in several laboratories. The most recent, detailed review on this subject was published in 2003.²⁴⁵

SCLERA

The sclera is a relatively avascular and metabolically inert, white, rigid, dense connective tissue that covers the globe posterior to the cornea (Fig. 33A).^{252,253,254,255} It is composed of three layers: the episclera, scleral

stroma proper, and the lamina fusca.²⁵⁵ In comparison to the cornea, the sclera is significantly more opaque and more rigid, is regionally vascular, and does not have an epithelial or endothelial surface (Fig. 33B). It also is notable for containing a moderately rich nerve supply, predominantly around episcleral blood vessels, and for having no lymphatic channels. The principal function of the sclera is to provide a strong, tough external framework and coating to protect and maintain the shape of the globe so that the inner eye is undisturbed. Secondly, it serves as an expansile-resistant structure maintaining the forces generated by the intraocular pressure and provides attachments sites for the extraocular muscles to rotate the globe.



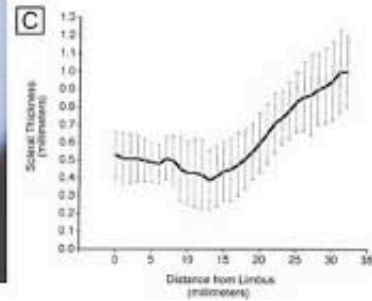
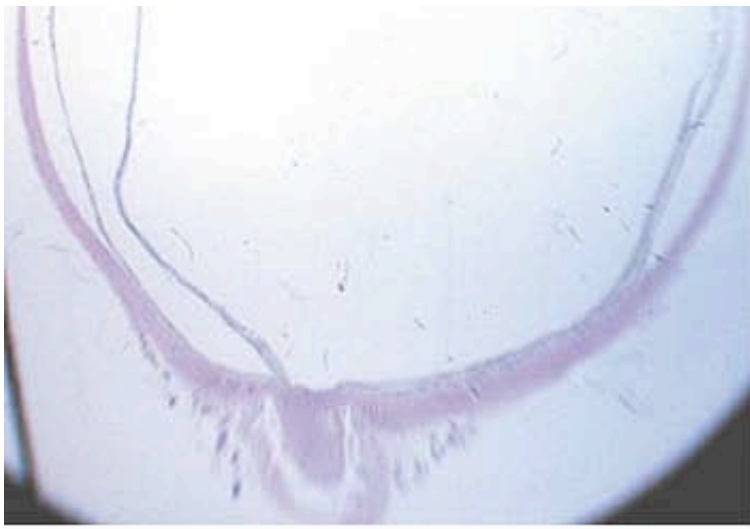


Figure 33. (A) Gross photo of the superior section of a horizontally bisected normal globe demonstrating the cross-sectional appearance of the sclera, limbus, and cornea. (B) Photomicrograph of a normal globe showing the cross-sectional appearance of the sclera, limbus, and cornea (PAS, 2X). (C) Line graph summarizing the average scleral thickness (\pm SD) vs. distance from the limbus in normal eyes (n = 550). ([C] is from Olsen TW, et al. Human sclera: thickness and surface area. *Am J Ophthalmol* 125:237, 1998.)

EMBRYOLOGY AND DEVELOPMENT

The sclera is predominantly neural crest-derived, except for a small temporal portion that comes from the mesoderm.²⁵⁵ The development of the sclera begins during the seventh week of gestation as the anterior periocular mesenchyme, which is derived from neural crest cells, condenses anteriorly on the optic cup. It subsequently differentiates into an inner vascular layer forming the uvea (iris, ciliary body, choroid) and an outer fibrous layer forming the sclera. By the third month of gestation, a well-formed sclera completely envelopes the eye. It gradually increases in thickness and denseness during the remaining months of gestation.

At birth, the sclera is relatively thin, highly distensible, and translucent. This latter feature explains why the blue color from the underlying uvea oftentimes shows through the infant sclera. During the first 3 years of life, it grows in size, remains thin, and remains relatively-translucent, but gradually loses its high distensibility. This latter fact explains why the sclera can expand from increased intraocular pressure resulting in a buphthalmic eye (“ox eye”) only from birth to around the age of 3 years old. Thereafter, the sclera distends only slightly from increased intraocular pressure with the notable exception being that of highly myopic eyes. After age 3, in addition to gradually thickening and becoming more opaque, it continues to grow throughout childhood, reaching adult size at 14 to 18 years of age. Thereafter, the sclera continues to become even less distensible and more rigid with advancing age.

GROSS ANATOMY

The sclera is an incomplete sphere that surrounds the posterior five-sixths of the globe.²⁵⁵ It has a total outer surface area of 16.3 to 17 cm² and an outer diameter of 24 mm.²⁵⁵ It is thickest posteriorly near the optic nerve (1.0 mm), decreasing gradually as it approaches the equator of the globe (0.4 mm) before becoming thinnest typically near the rectus muscle insertion sites (0.3 mm).²⁵⁶ It then gradually increases in thickness up to the limbus (0.8 mm) (Fig. 33C).²⁵⁶

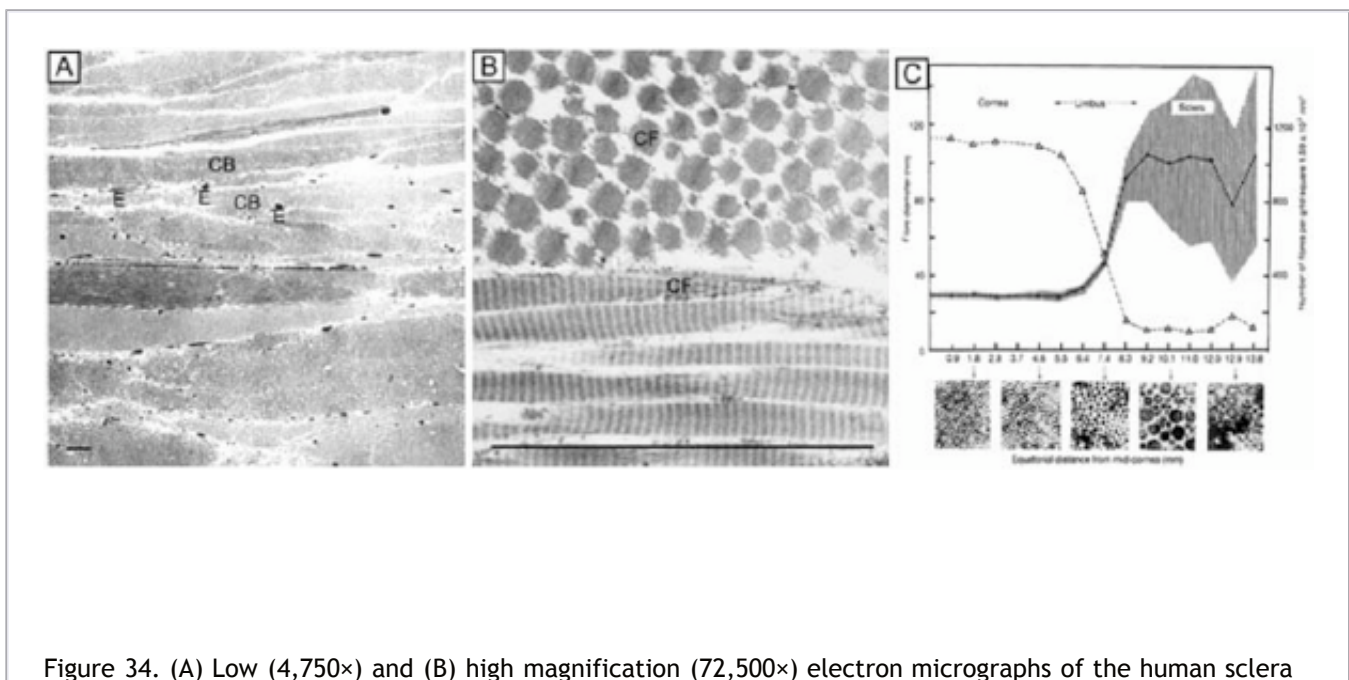
There are two major openings in the sclera: the anterior scleral foramen (13.7 mm diameter; circumscribes the area of the cornea and limbus) and the posterior-nasally located, fenestrated posterior scleral foramen, or scleral canal (2.0- to 3.0- mm diameter; circumscribes the area of the optic nerve). The scleral canal is very important clinically because the inner third of sclera forms a fenestrated scaffold in this canal termed the lamina cribosa that supports the optic nerve axons. Because the lamina cribosa is the weakest point of globe to expansile forces, diseases that cause high intraocular pressure, like glaucoma, preferentially cause lamina cribosa ectasia and damage to the optic nerve fibers. There are also numerous minor openings in the sclera, including the 30 to 40 emissary channels (ciliary arteries, veins, or nerves) and the 4 to 7 vortex vein channels.

The outer surface of the sclera is smooth, except where the tendons of the extraocular muscles insert (spiral of Tillaux and oblique muscle insertion sites) and where Tenon's capsule adheres (within 1 mm of limbus, over rectus muscle insertion sites, and around the optic nerve). The superficial layer of the sclera, called the episclera, is a thin, highly-vascularized, dense connective tissue. It is around 15- to 20- μm thick near the limbus, progressively thinning as it extends into the posterior aspect of the eye. The scleral stroma proper is a white, relatively avascular, dense connective tissue accounting for $\geq 95\%$ of total scleral thickness. Finally, the inner surface of the sclera is a brown, avascular, very thin (5 μm) layer called the lamina fusca.

MICROSCOPIC ANATOMY, ULTRASTRUCTURE, AND PHYSIOLOGY OF THE SCLERA

The sclera is predominantly composed of water (68% hydrated) that is stabilized in a severely disorganized structural network of insoluble and soluble extracellular proteins with few fibrocytes.²⁵² The dry weight of the adult human sclera is due to collagen (75%), proteoglycans (2%), fibrocyte constituents (2%), elastin (2%), blood vessels constituents, and salts, glycoproteins, or other substances.²⁵³

The majority of the sclera consists of the scleral stroma proper, which is somewhat similar in structure and composition to the corneal stroma.²⁵⁵ Collagen is the major water insoluble extracellular protein of the scleral stroma proper (80% type I, 5% type III, and minor amounts of type V and VI collagen), whereas elastin is a minor component.²⁵² In contrast to the cornea, the collagen fibrils (collagen type I, III, V) that make up the sclera are wider (averages 100 nm in diameter), more nonuniform in diameter (range 25 to 300 nm in diameter), more irregularly spaced, and are arranged in variously sized (0.5- to 6- μm thick by 10- to 50- μm wide), highly interweaving, irregularly-directed bundles (Fig. 34).^{253,255,257}



in the region of the scleral stroma proper. Compare these to Figures 10A and B to see how much more irregular the collagen bundles are in the sclera and how much more variable the collagen fibril diameters and spaces are. CB, collagen bundle; E, elastin fibers; CF, collagen fibril. (C) Summary diagram comparing the collagen fibril diameters and densities in the cornea, limbus, and sclera. ([C] is from Borcherding MS, et al. Proteoglycans and collagen fibre organization in human corneoscleral tissue. Exp Eye Res 21:59, 1975.)

Similarly, proteoglycans that make up the scleral stroma proper (36% dermatan sulfate, 35% chondroitin sulfate, 23% hyaluronic acid, and 6% heparin sulfate) differ significantly from the corneal stroma.^{252,253} However, like the corneal stroma, the scleral stroma proper does contain a syncytium of fibrocytes, albeit at a much lower level of cellularity or cellular density. Although the scleral stroma proper is traversed by ciliary blood vessels and nerves, it has no direct blood supply and does not contain a capillary plexus.²⁵² It derives its nutrition by diffusion from the episcleral and choroidal vascular networks. The episclera is different from the scleral stroma proper in that its collagen bundles are more loosely arranged. It contains melanocytes and a few residential histocytes, unmyelinated and myelinated free nerve endings, and, most obviously, a very rich direct blood supply.²⁵⁵

The blood supply of the episclera is particularly prominent along the 4 mm of episclera anterior to the rectus muscle insertion sites (Fig. 35). This area is called the *episcleral arterial circle*, which is fed by the seven anterior ciliary arteries of the eye, whereas the more posterior regions of episclera are significantly less vascular.²⁵² This episcleral arterial circle has both superficial and deep branches that directly nourish the episclera through superficial and deep episcleral capillary plexi, or branches into conjunctival or limbal arteries that have their own capillary plexi. The vessels of the capillary plexi of the episclera, limbus, and conjunctiva are notable for having a continuous nonfenestrated endothelium, being connected to each other by a thin interendothelial cleft that has no tight junctions. Therefore, it is not surprising that these vessels are permeable to small molecules, but resist bulk fluid flow.²⁵⁸ Interestingly, because the precapillary arterioles of the anterior segment (superficial episcleral, deep episcleral, and limbal) do not have a smooth muscle wall, they tend to be thrown into tortuous folds resulting in turbulent blood flow.

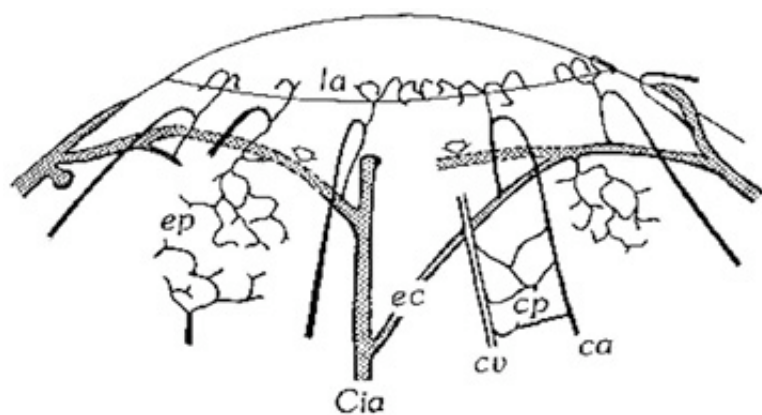


Figure 35. Schematic diagram of the arterial circulation of the episclera and conjunctival. Cia, anterior ciliary artery; Ec, episcleral arterial circle (deep component is represented by dashed lines and labeled

with open arrows); ca, conjunctival artery; ep, episcleral capillary plexus; cp, conjunctival capillary plexus; la, limbal arcades; cv, conjunctival vein. (From Meyer PAR, et al. Low dose fluorescein angiography of the conjunctiva and episclera. BJO 71:2, 1987.)

Additionally, because regions between the rectus muscles have a substantially lower arterial pressure, being further away from the feeding anterior ciliary arteries, blood flow appears to oscillate or stagnate in these tortuous regions.²⁵² Therefore, systemic immune complexes from autoimmune diseases, like systemic lupus erythematosus or Wegner's granulomatosis, seem to preferentially deposit in these tissue regions causing inflammatory microangiopathy (e.g., peripheral ulcerative keratitis, episcleritis, scleritis).²⁵² Moreover, since most of these regions (e.g., sclera and peripheral cornea) are devoid of lymphatics and considerably far away from neighboring lymphatics, the normal mechanisms for removing these antigens are severely limited leading often times to chronic disease.²⁵² Finally, the lamina fusca appears to merely serve as a transition zone from the sclera to the choroid as it contains more fibrocytes, more loosely arranged collagen fibrils, numerous melanocytes and more elastin fibers.²⁵⁵

Although the sclera is constantly under stress by the intraocular pressure, analogous to the systemic muscular arteries in the body, it typically displays only a limited ability to stretch, termed *scleral distensibility* (except for the first 3 years of life). Like most other viscoelastic systems, the sclera's distension abilities are proportionately greater with higher acute elevations in intraocular pressure; however, as it distends over time, the resistance to further distension increases. This resistance to distension is termed *scleral rigidity*, which can be subtyped into immediate ocular rigidity and time-dependent ocular rigidity. Therefore, the amount of distension or rigidity of the sclera are not fixed, but determined by how high and how long the pressure changes have acted on the sclera.²⁵⁹ A good example of this is when measuring intraocular pressure by indentation methods. The pressure measurements recorded by indentation methods initially increase the intraocular pressure of the eye by indenting inward the cornea, but by the time you read it, it typically is back to normal levels. In some individuals (e.g., high myopes, scleral malacia perforan), the sclera will distend more than normal resulting in false low readings because the scleral rigidity changes significantly after distending (or false high reading in cases of more rigid sclera [e.g., scleral buckles]). Therefore, most people use applanation methods to measure intraocular pressure because the intraocular pressure usually will be determined more accurately.

Since the sclera has one-quarter the concentration of proteoglycans (scleral swelling pressure of 20 to 30 g/cm) between collagen fibrils than the cornea, it is not surprising that it contains less water (68%) than the cornea (78%).²⁵³ However, if the normal water content of sclera is reduced to about 40%, it will become somewhat translucent. This is a common observation made during long surgical procedures on the sclera, when scleral flaps are dissected and sometimes inadvertently allowed to dry. Similarly, if the water content is increased to about 80%, the sclera again becomes somewhat translucent due to the hydration of scleral proteoglycans.

AGE CHANGES

In elderly individuals, the sclera often becomes somewhat yellowish due to a fine deposition of fat. Another common finding is a small rectangular area of grayish-blue translucency just anterior to the insertion of the medial and lateral rectus muscles. These changes are known as senile scleral plaques and are associated with deposition of calcium in scleral regions that are under strain and exposed to the environment.^{252,253,254,255} They are almost never found adjacent to the superior or inferior rectus muscles.

WOUND HEALING

Superficial lacerations of the sclera typically heal because episcleral fibrovascular granulation tissue migrates

and fills the wound.²⁵⁵ Similarly, lacerations involving the inner portion of the sclera also heal through fibrovascular granulation tissue, which grows outward from the choroid.²⁵⁵ Penetrating scleral lacerations typically heal because fibrovascular granulation tissue grows from both these areas. Such healing is usually very strong because it is accompanied by myofibroblastic differentiation and fibrosis. As time passes, a gradual remodeling, or organization, occurs to this fibrovascular scar; however, it can always be identified histologically by the abrupt change in scleral collagen fibril orientation, the persistent vascularity, and the disorganization of the surrounding tissue architecture.

PERMEABILITY

Although most of the bulk transport of fluid out of the eye takes place through the conventional pathway (*i.e.*, trabecular meshwork/Schlemm's canal system) or the nonconventional pathway (*i.e.*, uveoscleral flow), it is known that an appreciable amount is also drained transretinally through the choroidal vessels, transsclerally, or both. This transscleral route is interesting to researchers and clinicians because it serves as a potential route to deliver medications into the eye without invasively entering the eye. The principal route for local ophthalmic drug delivery still remains the topical application of solutions to the surface of the eye as drops. Because of the significant barrier to solute flux provided by the corneal epithelium and precorneal drug loss that occurs by way of tear drainage and tear fluid turnover, typically less than 5% of a topically-applied drug actually permeates the cornea and eventually reaches intraocular tissues. The major portion of a topically-instilled dose is absorbed systemically by way of the conjunctiva, through the highly vascular conjunctival stroma, and through the lid margin vessels. Despite the relatively small proportion of a topically-applied drug dose that ultimately reaches intraocular tissues, these formulations can achieve therapeutic concentrations in anterior segment tissues, largely because of the very high concentrations of drugs that are administered.

Currently, the treatment of posterior segment disease is limited to a large extent by the difficulty in delivering effective doses of drugs to target tissues in the posterior vitreous, retina, or choroid. The traditional topical route of ophthalmic drug delivery does not yield therapeutic drug levels in the posterior tissues of the eye. Although systemic administration can deliver drugs to the posterior eye, the large systemic doses necessary are often associated with side effects and toxicities. Intravitreal injection and sustained-release vitreal implants, such as the sustained-release ganciclovir implant, deliver agents directly to the posterior eye. These methods, however, are invasive. Intravitreal injections need to be repeated, often frequently. These procedures are often poorly tolerated by patients and they can pose significant risk, including retinal detachment, endophthalmitis, and cataract.

An alternative approach to the delivery of drugs to the tissues of the posterior eye involves placing the drug, typically by injection, into the tissues surrounding the posterior segment of the eye—a peribulbar or sub-Tenon's injection. Corticosteroid preparations are the most common pharmacologic delivered by this route. The feasibility of using these approaches for drug delivery to posterior segment tissues depends, to a large extent, on the permeability of the sclera to the therapeutic solutes.

Initial animal studies by Barza were among the first to clearly establish that drugs can penetrate into various ocular tissues when they are administered by either subconjunctival or retrobulbar injection.^{260,261} Although the mechanisms by which solutes are transferred from the peribulbar location into the eye are not completely understood, it is clear that significant solute flux can occur through the sclera. Early experiments by Bill first demonstrated albumin or dextran injected into the suprachoroidal space of the rabbit eye, diffuse across the sclera and subsequently accumulate in the extraocular tissues.²⁶² *In vitro* permeability studies on bovine sclera by Maurice were the first to demonstrate that the tissue was permeable to a wide molecular weight range (285 to 69,000) of solutes.²⁶³ Edelhauser and Maren demonstrated that the *in vitro* permeability of human scleral tissue to carbonic anhydrase inhibitors was comparable to that of the corneal stroma.²⁶⁴ Although initial studies did suggest that the sclera was indeed quite permeable to a range of solutes, and Ahmed and Patton first suggested that it might be possible to exploit the scleral absorption route to promote site-specific delivery of

drugs to intraocular tissues in the back of the eye, it is only more recently that transscleral drug delivery has received significant interest.²⁶⁵

Steady-state permeability values of human sclera to a range of solutes are shown in Figure 36. The graph is a logarithmic plot of scleral permeability, expressed in K_{TRANS} (cm/sec) as a function of solute molecular weight.²⁶⁶ These data show the inverse relationship between solute size and scleral permeability, with the smallest molecular weight compound (5-FU, MW = 130) having the highest transscleral permeability. The transscleral permeability of the largest compound studied, dextran 70K (MW = 70,000), is nearly thirty-fold lower. These permeability values for human sclera are comparable to those of bovine tissue, if one considers the differences in thickness comparing the tissues of the two species.²⁶³ A number of permeability studies, using essentially comparable methods, have shown the sclera to be permeable to a wide range of solutes and that permeability seems to best correlate with molecular radius of the solute.^{267,268} The results of the *in vitro* permeability studies indicate that scleral permeability is comparable to that of the corneal stroma, with which the sclera shares a similar ultrastructure and composition.²⁶⁷ As in the corneal stroma, the primary route for solute movement through the sclera is by passive diffusion through the interfibrillar aqueous media of the gel-like proteoglycans.

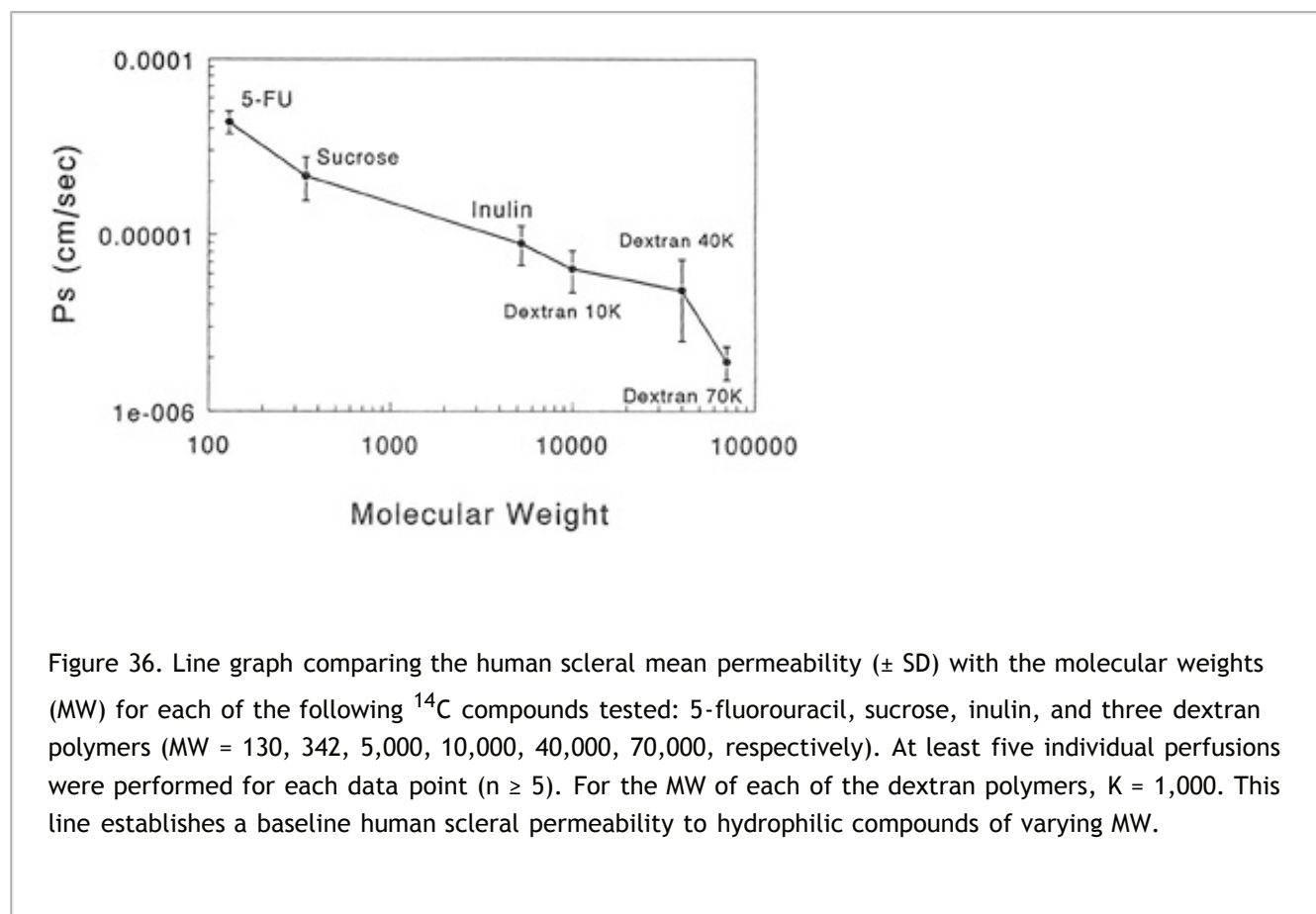


Figure 36. Line graph comparing the human scleral mean permeability (\pm SD) with the molecular weights (MW) for each of the following ^{14}C compounds tested: 5-fluorouracil, sucrose, inulin, and three dextran polymers (MW = 130, 342, 5,000, 10,000, 40,000, 70,000, respectively). At least five individual perfusions were performed for each data point ($n \geq 5$). For the MW of each of the dextran polymers, $K = 1,000$. This line establishes a baseline human scleral permeability to hydrophilic compounds of varying MW.

Although transscleral solute permeability has been shown to be affected by transscleral (intraocular) pressure, the effects of pressure on the transscleral permeability of solutes in the size range of commonly used drugs is relatively small.²⁶⁸ Because elevated intraocular pressure compresses the collagen fibers comprising the scleral stroma, narrowing the intracollagen diffusion pathways might be expected to affect the diffusion of larger molecules to a greater extent than smaller molecules.²⁶⁹ Thus, the effect of transscleral pressure on solute permeability may be considerably greater for solutes in the size range of macromolecules. These effects certainly must be considered as local genetic interventions for posterior segment disease are being investigated.

More recent *in vivo* studies have demonstrated that effective drug levels can be reached and maintained in posterior ocular tissues using transscleral delivery.^{270,271,272} Clinical studies by Weijtens measured dexamethasone concentrations in the vitreous and serum of 54 patients scheduled for vitrectomy who received 7.5 mg dexamethasone orally before surgery.^{273,274} These drug levels were compared to vitreous and serum concentrations measured in 61 patients scheduled for vitrectomy who had received a single peribulbar injection of 5 mg of dexamethasone at various intervals prior to surgery. The results of these studies demonstrate that following a peribulbar injection of dexamethasone, only a small portion of the administered dose reaches the vitreous through the systemic circulation, whereas most dexamethasone reaches the vitreous by diffusing directly through the sclera.

A more recent, randomized, masked, placebo-controlled clinical study has described the safety and efficacy of anecortave acetate, an angiostatic agent, depot suspension delivered by a posterior juxtасcleral depot application for the treatment of subfoveal choroidal neovascularization.²⁷⁵ Compared to placebo, the drug was found to be safe and effective in maintaining vision, preventing severe vision loss, and inhibiting further subfoveal neovascularization compared to placebo.

The sclera is permeable to a wide range of solutes, especially those in the molecular size range of drugs currently in use. Laboratory and clinical studies suggest that the relatively high permeability and the large surface area of the sclera could provide an excellent route for delivering drugs to the posterior segment of the eye. Based on recent studies, the transscleral route may be the drug delivery route of choice for posterior segment disease.

ACKNOWLEDGMENTS

This work was supported in part by National Institutes of Health Grants P30 EY06360 (Departmental Core Grant), T32EY07092 (DGD), R01EY00933 (HFE), the Scleroderma Foundation (MAW), and Research to Prevent Blindness, (New York, NY).

REFERENCES

1. von Bahr G: Measurements of the thickness of the cornea. *Acta Ophthalmol* 26:247, 1948
2. Mishima S: Corneal thickness. *Survey Ophthalmol* 13:57, 1968
3. Maurice DM, Giardini AA: A simple optical apparatus for measuring the corneal thickness and average thickness of the human cornea. *Br J Ophthalmol* 35:169, 1951
4. Martola EL, Baum JL: Central and peripheral corneal thickness: A clinical study. *Arch Ophthalmol* 79:28, 1968
5. Watsky MA, Jablonski MM, Edelhauser HF: Comparison of conjunctival and corneal surface areas in rabbit and human. *Curr Eye Res* 7:483, 1988
6. Klyce SD, Crosson CE: Transport processes across the rabbit corneal epithelium: A review. *Curr Eye Res* 4:323, 1985

7. McLaughlin BJ, Caldwell RB, Sasaki Y, Wood TO: Freeze fracture quantitative comparison of rabbit corneal epithelial and endothelial membranes. *Curr Eye Res* 4:951, 1985
8. Gipson IK, Yankauekas M, Spurr-Michaud JJ, et al: Characteristics of a glycoprotein in the ocular surface glycocalyx. *Invest Ophthalmol Vis Sci* 33:218, 1992
9. Nichols BA, Chiappini ML, Dawson CR: Demonstration of the mucous layer of the tear film by electron microscopy. *Invest Ophthalmol Vis Sci* 26:464, 1985
10. Argueso P, Gipson IK: Epithelial mucins of the ocular surface: Structure, biosynthesis, and function. *Exp Eye Res* 73:281; 2001
11. Friedenwald JS, Buscke W: Mitotic and wound healing activities of the corneal epithelium. *Arch Ophthalmol* 32:410, 1944
12. Hanna C, Bickness DS, O'Brien J: Cell turnover in the adult human eye. *Arch Ophthalmol* 65:695, 1961
13. Hanna C, O'Brien JE: Cell production and migration in the epithelium layer of the cornea. *Arch Ophthalmol* 64:536, 1960
14. Williams KK, Watsky MA: Gap junctional communication in the human corneal endothelium and epithelium. *Curr Eye Res* 25:29, 2002
15. Williams KK, Watsky MA: Bicarbonate promotes gap junctional intercellular communication in the epithelium and endothelium of the rabbit cornea. *Curr Eye Res* 28:109, 2004
16. Bam Y, Dota A, Cooper LJ, et al: Tight junction-related protein expression and distribution in human corneal epithelium. *Exp Eye Res* 76:663, 2003
17. Wang, Y, Zhang, J, Yi, X, Yu, FX: Activation of ERK1/2 MAP kinase pathway induces tight junction disruption in human corneal epithelial cells. *Exp Eye Res* 78:125, 2004
18. Buck RC: Measurement of centripetal migration of normal corneal epithelial cells in the mouse. *Invest Ophthalmol Vis Sci* 26:1296, 1985
19. Kinoshita S, Friend J, Thoft RA: Sex chromatin of donor corneal epithelium in rabbits. *Invest Ophthalmol Vis Sci* 21:434, 1981
20. Schermer A, Galvin S, Sun TT: Differentiation-related expression of a major 64k corneal keratin in vivo and in culture suggest a limbal location of corneal epithelial stem cells. *J Cell Biol* 103:49, 1986

21. Sharma A, Coles WH: Kinetics of corneal epithelial maintenance and graft loss. *Invest Ophthalmol Vis Sci* 30:1962, 1989
22. Thoft RA, Friend J: The X, Y, Z hypothesis of corneal epithelial maintenance. *Invest Ophthalmol Vis Sci* 24:1442, 1983
23. Dillon EC, Eagle RC, Laibson PR: Compensatory epithelial hyperplasia in human corneal disease. *Ophthalm Surg* 23:729, 1992
- 23A. Ubels JL, Edelhauser HF, Shaw D: Measurement of corneal epithelial healing rates and corneal thickness for evaluation of ocular toxicity of chemical substances *J Toxicol Cutan Ocular Toxicol* 1:133, 1982
24. Maumenee, AE: Repair in the cornea. In *Advances in Biology of Skin Wound Healing*. Montague WM, Billingham RA, Eds. Elmsford: Pergamon Press, 1964:208
25. Davanger M, Evensen A: Role of pericorneal papillary structure in renewal of corneal epithelium. *Nature* 229:560, 1971
26. Shapiro MS, Friend J, Thoft RA: Corneal re-epithelialization from the conjunctiva. *Invest Ophthalmol Vis Sci* 21:135, 1981
27. Thoft RA: Conjunctival transplantation. *Arch Ophthalmol* 95:1425, 1977
28. Schermer A, Galvin S, Sun TT: Differentiation-related expression of a major 64K corneal keratin in vivo and in culture suggests limbal location of corneal epithelial stem cells. *J Cell Biol* 103:49, 1986
29. Cotsarelis G, Cheng S, Dong S, et al: Existence of slow-cycling limbal epithelial basal cell that can be preferentially stimulated to proliferate: Implications on epithelial stem cells. *Cell* 57:201, 1989
30. Tseng SCG: Concept and application of limbal stem cells. *Eye* 3:141, 1989
31. Lavker RM, Tseng SCG, Sun TT: Corneal epithelial stem cells at the limbus: Looking at some old problems from a new angle. *Exp Eye Res* 78:433, 2004
32. Boulton M, Albon J: Stem cells in the eye. *Int J Biochem Cell Biol* 36:643, 2004
33. Candia OA: The flux rates of the Na-Cl cotransport mechanism in the frog corneal epithelium. *Curr Eye Res* 4:333, 1985

34. Donn A, Maurice DM, Mills NL: Studies in the living cornea in vitro. II. The active transport of sodium across the epithelium. *Arch Ophthalmol* 62:748, 1959
35. Klyce SD: Electrical profiles in the corneal epithelium. *J Physiol* 226:407, 1972
36. Zadunaisky J: Active transport of chloride across the cornea. *Nature* 209:1136, 1966
37. Bonano J: Regulation of corneal epithelial intracellular pH. *Optom Vis Sci* 68:682, 1991
38. Gillette TE, Chandler JW, Greiner JV: Langerhans cells of the ocular surface. *Ophthalmology* 89:700, 1982
39. Langerhans P: Uber die: nerven der meschlichen haut. *Virchows Arch Path Anat Physiol* 44:325, 1868
40. Steinman RM: The dendritic cell system and its role in immunogenicity. *Annu Rev Immunol* 9:271, 1991
41. Hamrah P, Zhang Q, Liu Y, Dana MR: Novel characterization of MHC class-negative population of resident corneal Langerhans cell-type dendritic cells. *Invest Ophthal Vis Sci* 43:639, 2002.
42. Kaye G: Stereologic measurement of cell volume fraction of rabbit corneal stroma. *Arch Ophthalmol* 82:792, 1969
43. Maurice DM: *The Eye: The Cornea and Sclera*, 3rd ed. New York: Academic Press, 1984:1
44. Hay ED: Development of the vertebrate cornea. *Int Rev Cytol* 63:263, 1979
45. Hedbys BO: The role of polysaccharides in corneal swelling. *Exp Eye Res* 1:81, 1961
46. Bettelheim FA, Plessy B: The hydration of proteoglycans of bovine cornea. *Biochimica et Biophysica Acta* 381:215, 1975
47. Scott JE: Proteoglycan: Collagen interactions and corneal ultrastructure. *Biochem Soc Trans* 19:877, 1991
48. Lerman S: Biophysical aspects of corneal and lenticular transparency. *Curr Eye Res* 3:3, 1984
49. Boettner EA, Wolter JR: Transmission of the ocular media. *Invest Ophthalmol Vis Sci* 6:776, 1962.
50. Farrell RA, McCally RL, Tatham P: Wave-length dependencies of light scattering in normal and cold

swollen rabbit corneas and their structural implications. *J Physiol* 233:589, 1973

51. Moller-Pedersen T: Keratocyte reflectivity and corneal haze. *Exp Eye Res* 78:553, 2004

52. Van de Berg TJ, Tan KE: Light transmittance of the human cornea from 320 nm to 700 nm for different ages. *Vis Res* 34:1453, 1994

53. Nakayasu K, Tanaka M, Konomi H, Hayashi T: Distribution of types I, II, III, IV, and V collagen in normal and keratoconus corneas. *Ophthalmic Res* 18:1, 1986

54. Cintron C, Hong B, Covington HI, Macarak EJ: Heterogeneity of collagens in rabbit cornea: type III collagen. *Invest Ophthalmol Vis Sci* 29:767, 1988

55. Maurice DM: The structure and transparency of the cornea. *J Physiol* 136:263, 1957

56. Cho J, Covington HI, Cintron C: Immunolocalization of type VI collagen in developing and healing rabbit cornea. *Invest Ophthalmol Vis Sci* 31:1096, 1990

57. Hirsch M, Prenant G, Renard G: Three-dimensional supramolecular organization of the extracellular matrix in human and rabbit corneal stroma, as revealed by ultrarapid-freezing and deep-etching methods. *Exp Eye Res* 72:123, 2001

58. Hogan MJ, Alvarado JA, Weddell E: *Histology of the Human Eye*. Philadelphia: WB Saunders, 1971:55

59. Komai Y, Ushiki T: The three-dimensional organization of collagen fibrils in human cornea and sclera. *Invest Ophthalmol Vis Sci* 32:2244, 1991

60. Meek KM, Boote C: The organization of collagen in the corneal stroma. *Exp Eye Res* 78:503, 2004

61. Newton RH, Meek KM: Circumcorneal annulus of collagen fibrils in the human limbus. *Invest Ophthalmol Vis Sci* 39:1125, 1998

62. Newton RH, Meek KM: The integration of corneal and limbal fibrils in the human eye. *Biophys J* 75:2508, 1998

63. Scott JE: Proteoglycan histochemistry—a valuable tool for connective tissue biochemists. *Coll Relat Res* 5:541, 1985

64. Scott JE: Extracellular matrix, supramolecular organization, and shape. *J Anat* 187:259, 1995

65. Hassell JR: Proteoglycan gene families. *Adv Mol Cell Biol* 6:69, 1993
66. Scott JE, Bosworth TR: The comparative chemical morphology of the mammalian cornea. *Basic Appl Histochem* 34:35, 1990
67. Castoro JA, Bettelheim AA, Bettelheim FA: Water gradient across bovine cornea. *Invest Ophthalmol Vis Sci* 29:963, 1988
68. Watsky MA: Keratocyte gap junctional dye spread in normal and wounded rabbit corneas and human corneas. *Invest Ophthalmol Vis Sci* 36:S22, 1995
69. Muller LJ, Pels L, Vrensen GFJM: Novel aspects of the ultrastructural organization of human corneal keratocytes. *Invest Ophthalmol Vis Sci* 36:2557, 1995
70. Patel SV, McLaren JW, Hodge DO, Bourne WM: Normal human keratocyte density and corneal thickness measurement by using confocal microscopy in vivo. *Invest Ophthalmol Vis Sci* 42:333, 2001
71. Hamrah P, Liu Y, Zhang Q, Dana MR: The corneal stroma is endowed with a significant number of resident dendritic cells. *Invest Ophthalmol Vis Sci* 44:581, 2003
72. Poole CA, Brookes NH, Clover GM: Keratocyte networks visualized in the living cornea using vital dyes. *J Cell Sci* 106:685, 1993
73. Watsky MA, Rae JL: Initial characterization of wholecell currents from freshly dissociated corneal keratocytes. *Curr Eye Res* 11:127, 1992
74. Hedbys BO, Dohlman CH: A new method for determination of the swelling pressure of the corneal stroma in vitro. *Exp Eye Res* 2:122, 1963
75. Klyce SD, Dohlman CH, Tolpin DM: In vivo determination of corneal swelling pressure. *Exp Eye Res* 11:220, 1971
76. Hedbys BO, Mishima S, Maurice DM: The imbibition pressure of the corneal stroma. *Exp Eye Res* 2:99, 1963
77. Ytteborg J, Dohlman CH: Corneal edema and intraocular pressure: II—clinical results. *Arch Ophthalmol* 74:477, 1965
78. Van Horn DL, Doughman DJ, Harris JE, et al: Ultrastructure of human organ-cultured cornea. *Arch Ophthalmol* 93:275, 1975

79. Meek KM, Dennis S, Khan S: Changes in the refractive index of the stroma and its extrafibrillar matrix when the cornea swells. *Biophys J* 85:2205, 2003
80. Muller LJ, Pels E, Vrensen GFJM: The specific architecture of the anterior stroma accounts for maintenance of corneal curvature. *BJO* 85:437, 2001
81. Kangis TA, Edelhauser HF, Twining SS, O'Brien WJ: Loss of stromal glycosaminoglycans during corneal edema. *Invest Ophthalmol Vis Sci* 31:1994, 1990
82. Cristol SM, Edelhauser HF, Lynn MJ: A comparison of corneal stroma edema induced from the anterior or the posterior surface. *Refract Corneal Surg* 8:224, 1992
83. Connon CJ, Meek KM: The structure and swelling of corneal scar tissue in penetrating full-thickness wounds. *Cornea* 23:165, 2004
84. Hatton MP, Perez VL, Dohlman CH: Corneal oedema in ocular hypotony. *Exp Eye Res* 78:549, 2004
85. Edelhauser HF: Castroviejo Lecture: The resiliency of the corneal endothelium to refractive and intraocular surgery. *Cornea* 19:263, 2000
86. Yee RW, Matsuda M, Schultz RO, Edelhauser HF: Changes in the normal corneal endothelial cellular pattern as a function of age. *Curr Eye Res* 4:671, 1985
87. Amann J, Holley GP, Lee S, Edelhauser HF: Increased endothelial cell density in the paracentral and peripheral regions of the human cornea. *Am J Ophthalmol* 135:584, 2003
88. Maurice DM: The cornea and sclera. In *The Eye*, 3rd ed. : Davson H, Ed. Orlando: Academic Press, 1984:85
89. Watsky MA, McDermott ML, Edelhauser HF: In vitro corneal endothelial permeability in rabbit and human: The effect of age, cataract surgery, and diabetes. *Exp Eye Res* 49:751, 1989
90. Stiemke MM, McCartney MP, Cantu-Crouch D, Edelhauser HF: Maturation of the corneal endothelial tight junction. *Invest Ophthalmol Vis Sci* 32:2757, 1991
91. Harris JE: Symposium on the cornea. Introduction: factors influencing corneal hydration. *Invest Ophthalmol* 1:151; 1962
92. Kaye GI, Tice LW: Studies on the cornea. V. Electron microscope localization of adenosine triphosphatase activity in the rabbit cornea in relation of transport. *Invest Ophthalmol* 5:22, 1966

93. Lim JJ: Na⁺ transport across the rabbit corneal epithelium. *Curr Eye Res* 1:225, 1981.
94. Lim JJ, Ussing HH: Analysis of presteady-state Na⁺ fluxes across the rabbit corneal endothelium. *J Membrane Biol* 65:197, 1982
95. Geroski DH, Matsuda M, Yee RW, Edelhauser HF: Pump function of the human corneal endothelium. Effects of age and corneal guttata. *Ophthalmol* 92:759, 1984
96. Stiemke MM, Edelhauser HF, Geroski DH: The developing corneal endothelium: Correlation of morphology, hydration, and Na/K ATPase pump site density. *Curr Eye Res* 10:145, 1991
97. Burns RR, Bourne WM, Burbaker RF: Endothelial function in patients with corneal guttata. *Invest Ophthalmol Vis Sci* 20:77, 1981
98. Mishima S: Clinical investigations on the corneal endothelium. XXXVIII Edward Jackson Memorial Lecture. *Am J Ophthalmol* 93:1, 1982
99. Bonanno JA: Identity and regulation of ion transport mechanisms in the corneal endothelium. *Prog Retinal Eye Res* 22:69, 2003
100. Stiemke MM, Roman RJ, Palmer M, Edelhauser HF: Na⁺ activity in the aqueous humor and corneal stroma of the rabbit. *Exp Eye Res* 55:425, 1992
101. Jentsch TJ, Korbmacher C, Janicke I, et al: Regulation of cytoplasmic pH of cultured bovine corneal endothelial cells in the absence and presence of bicarbonate. *J Membr Biol* 103:29, 1988
102. Rae JL, Watsky MA: Ion channels in corneal endothelium. *Am J Physiol* 270:C975, 1996
103. Bonanno JA, Giasson C: Intracellular pH regulation in fresh and cultured bovine corneal endothelium. II. Na⁺/HCO₃⁻ cotransport and Cl⁻/HCO₃⁻ exchange. *Invest Ophthalmol Vis Sci* 33:3068, 1992
104. Bonanno JA, Giasson C: Intracellular pH regulation in fresh and cultured bovine corneal endothelium. I. Na⁺/H⁺ exchange in the absence and presence of HCO₃⁻. *Invest Ophthalmol Vis Sci* 33:3058, 1992
105. Lane JR, Wigham CG, Hodson SA: Determination of Na⁺/Cl⁻, Na⁺/HCO₃⁻, and Na⁺/K⁺/2Cl⁻ cotransporter activity in corneal endothelial cell plasma membrane vesicles. *Biochim Biophys Acta* 1328:237, 1997
106. Jelamskii S, Sun XC, Herse P, Bonanno JA: Basolateral Na⁺-K⁺-2Cl⁻ cotransport in cultured and fresh

bovine corneal endothelium. Invest Ophthalmol Vis Sci 41:488, 2000

107. Watsky MA, Rae JL: Ion channel involvement in the temperature sensitive response of the rabbit corneal endothelial cell resting membrane potential. J Membrane Biol 135:61, 1993

108. Sun XC, Bonanno JA: Expression, localization and evaluation of CFTR in bovine corneal endothelial cells. Am J Physiol (Cell Physiol) 282:C673, 2002

109. Zhang Y, Xie Q, Sun XC, Bonanno JA: Enhancement of HCO₃ permeability across the apical membrane of bovine corneal endothelium by multiple signaling pathways. Invest Ophthalmol Vis Sci 43:1146, 2002

110. Kreuziger GO: Lateral membrane morphology and gap junction structure in rabbit corneal endothelium. Exp Eye Res 23: 285, 1976

111. Rae JL, Lewno AW, Cooper K, Gates P: Dye and electrical coupling between the cells of the rabbit corneal endothelium. Curr Eye Res 8:859, 1989

112. Watsky MA, Rae JL: Dye coupling in the corneal endothelium: The effects of ouabain and extracellular calcium removal. Cell Tissue Res 269:57, 1992

113. Williams KK, Watsky MA: Gap junctional communication in the human corneal endothelium and epithelium. Curr Eye Res 25:29, 2002

114. Bourne WM: Biology of the corneal endothelium in health and disease. Eye 17:912, 2003

115. Bourne RR, Minnassian DC, Dart JK, et al: Effect of cataract surgery on the corneal endothelium. Ophthalmol 111:679, 2004

116. Whitehart DR, Parikh CH, Lowe AV, Edelhauser HF: Evidence of stem-like cells for the human corneal endothelium. Submitted.

117. Bourne WM: Cellular changes in transplanted human corneas. Cornea 20:560, 2001

118. Johnson DH, Bourne WM, Campbell RJ: The ultrastructure of Descemet's membrane. I. Changes with age in normal corneas. Arch Ophthalmol 100:1942, 1982

119. Waring III GO: Posterior collagenous layer of the cornea. Ultrastructural classification of abnormal collagenous tissue posterior to Descemet's membrane in 30 cases. Arch Ophthalmol 100:122, 1982

120. Mapstone R: Measurement of corneal temperature. Exp Eye Res 7:237, 1968

121. Friend J: Biochemistry of ocular surface epithelium. *Int Ophthalmol Clin* 19:73, 1979
122. Reim M, Lax F, Lichte H, Turss R: Steady state levels of glucose in the different layers of corneal, aqueous humor, blood, and tears in vivo. *Ophthalmologica* 154:39, 1967
123. Thoft RA, Friend J: Corneal epithelial glucose utilization. *Arch Ophthalmol* 88:58, 1971
124. Thoft RA, Friend J: Biochemical transformation of regenerating ocular surface epithelium. *Invest Ophthalmol Vis Sci* 16:14, 1977
125. Friend J, Thoft RA: The diabetic cornea. *Int Ophthalmol Clin* 24:111, 1985
126. Kinoshita JH, Fukushi S, Kador P, Merola LO: Aldose reductase in diabetic complications of the eye. *Metabolism* 28:462, 1979
127. Mandrell RB, Fatt I: Thinning of the human cornea on awakening. *Nature* 208:292, 1965
128. Graymore CN: *Biochemistry of the Eye*. New York: Academic Press, 1970:103
129. Weissman BA, Fatt I, Rasson J: Diffusion of oxygen in human corneas in vivo. *Invest Ophthalmol Vis Sci* 20:123, 1981
130. Kinoshita JH: Some aspects of the carbohydrate metabolism of the cornea. *Invest Ophthalmol* 1:178, 1962
131. Klyce SD: Stromal lactate accumulation can account for corneal edema osmotically following epithelial hypoxia in the rabbit. *J Physiol* 321:49, 1981
132. Holden BA, Sweeney DF, Vannas A, et al: Effects of long-term extended contact lens wear on the human cornea. *Invest Ophthalmol Vis Sci* 26:1489, 1985
133. Madigan MC, Holden BA: Reduced epithelial adhesion after extended contact lens wear correlates with reduced hemidesmosome density in cat cornea. *Invest Ophthalmol Vis Sci* 33:314, 1992
134. Masferrer JC, Laniado-Schwartzman M: Novel cytochrome P450-dependent arachidonic acid metabolites and their ocular effects. *Prog Clin Biol Res* 312:85, 1989.
135. Schwartzman ML, Balazy M, Masferrer J, et al: 12(R)hydroxyeicosatetraenoic acid: A cytochrome P450-dependent arachidonate metabolite that inhibits Na⁺-K⁺ ATPase in the cornea. *Proc Natl Acad Sci USA*

136. Edelhauser HF, Geroski DH, Woods WD, et al: Swelling in the isolated perfused cornea induced by 12(R)-hydroxyeicosatetraenoic acid. *Invest Ophthalmol Vis Sci* 34:2953, 1993
137. Masferrer JL, Rimarchin JA, Gerritsen ME: 12(R)-hydroxyeicosatrienoic acid: A potent chemotactic and angiogenic factor produced by the cornea. *Exp Eye Res* 52:417, 1991
138. MacRae S, Matsuda M, Shellans S, Rich LF: The effects of hard and soft contact lens wear on the corneal endothelium. *Am J Ophthalmol* 102:50, 1986
139. Riley MV: Transport of ions and metabolites across the corneal endothelium. In *Cell Biology of the Eye*. McDevitt DS, Ed. New York: Academic Press, 1982:53
140. Davis KL, Conners MS, Dunn MW, Schwartzman ML: Induction of corneal epithelial cytochrome P-450 arachidonate metabolism by contact lens wear. *Invest Ophthalmol Vis Sci* 33:291, 1992
141. Pulse K, Brand R, Cohen S, Guillon M: Hypoxic effects on corneal morphology and function. *Invest Ophthalmol Vis Sci* 31:1542, 1990
142. Geroski DH, Edelhauser HF, O'Brien WJ: Hexose-monophosphate shunt response to diamide in the component layers of the cornea. *Exp Eye Res* 26:611, 1978
143. Whitehart DR, Zagrod ME: Adenosine-stimulated production of sugar-phosphate in bovine corneal endothelium. *Invest Ophthalmol Vis Sci* 26:1475, 1985
144. Bode AM, Vanderpool SS, Carlson EC, et al: Ascorbic acid uptake and metabolism by corneal endothelium. *Invest Ophthalmol Vis Sci* 32:2266, 1991
145. Crosson CE, Klyce SD, Beuerman RW: Epithelial wound closure in the rabbit cornea. *Invest Ophthalmol Vis Sci* 27:464, 1986
146. Kuwabara T, Perkins DG, Cogan DG: Sliding of the epithelium in experimental corneal wounds. *Invest Ophthalmol* 15:4, 1976
147. Matsuda M, Ubels JL, Edelhauser HF: A larger corneal epithelial wound closes at a faster rate. *Invest Ophthalmol Vis Sci* 26:897, 1985
148. Pfister RR: The healing of corneal epithelial abrasions in the rabbit: A scanning electron microscope study. *Invest Ophthalmol* 14:648, 1975

149. Dua HS, Gomes JA, Singh A: Corneal epithelial wound healing. *BJO* 78:401, 1994
150. Hanna C: Proliferation and migration of epithelial cells during corneal wound repair in the rabbit and the rat. *Am J Ophthalmol* 61:55, 1966
151. Gipson IK, Anderson RA: Actin filaments in normal and migrating corneal epithelial cells. *Invest Ophthalmol Vis Sci* 16:161, 1977
152. Soong HK, Cintron C: Disparate effects of calmodulin inhibitors on corneal epithelial migration in rabbit and rat. *Ophthalmic Res* 17:27, 1985
153. Dua HS, Watson NJ, Mathur RM, Forrester JV: Corneal epithelial cell migration in humans: hurricane and blizzard keratopathy. *Eye* 7:53, 1993
154. Tervo T, van Setten G-B, Beuerman RW, et al: Appearance of immunohistochemically detectable cellular fibronectin and tenascin in the experimental rabbit keratectomy wound. *Invest Ophthalmol Vis Sci* 30:149, 1989
155. Soong HK: Vinculin in focal cell-to-substrate attachments of spreading corneal epithelial cells. *Arch Ophthalmol* 105:1129, 1987
156. Zieske JD, Bukusoglu G, Gipson IK: Enhancement of vinculin synthesis by migrating stratified squamous epithelium. *J Cell Biol* 109:571, 1989
157. Zieske JD, Gipson IK: Protein synthesis during corneal epithelial wound healing. *Invest Ophthalmol Vis Sci* 27:1, 1986
158. Khodadoust AA, Silverstein AM, Kenyon KR, Dowling JE: Adhesion of regenerating corneal epithelium. *Am J Ophthalmol* 65:339, 1968
159. Soong HK, Cintron C: Different corneal epithelial healing mechanisms in rat and rabbit: Role of actin and calmodulin. *Invest Ophthalmol Vis Sci* 26:838, 1985
160. Beuerman RW, Schimmelpfennig B: Sensory denervation of the rabbit cornea affects epithelial properties. *Exp Neurol* 69:196, 1980
161. Elliott JH: Epidermal growth factor: In vivo ocular studies. *Trans Am Ophthalmol Soc* 78:629, 1980
162. Kandarakis AS, Page C, Kaufman HE: The effect of epidermal growth factor on epithelial healing after penetrating keratoplasty in human eyes. *Am J Ophthalmol* 98:411, 1984

163. Kawaba T, Nakayasu K, Kanai A: Effect of human EGF and plasma fibronectin on corneal epithelial regeneration. *Acta Soc Ophthalmol Jpn* 88:1237, 1984
164. Ubels JL, Edelhauser HF, Foley KM: The efficacy of retinoic acid ointment for treatment of xerophthalmia and corneal epithelial wounds. *Curr Eye Res* 4:1049, 1985
165. Friedenwald, JS: Growth pressure and metaplasia of conjunctival and corneal epithelium. *Doc Ophthalmol* 5-6:184, 1951
166. Thoft RA, Friend J, Murphy HS: Ocular surface epithelium and corneal vascularization in rabbits I. The role of wounding. *Invest Ophthalmol Vis Sci* 18:85, 1979
167. Shapiro MS, Friend J, Thoft RA: Corneal re-epithelialization from the conjunctiva. *Invest Ophthalmol Vis Sci* 21:135, 1981
168. Harris TM, Berry ER, Pakurar AS, Sheppard LB: Biochemical transformation of bulbar conjunctiva into corneal epithelium: an electrophoretic analysis. *Exp Eye Res* 41:597, 1985
169. Thoft RA, Friend J: Biochemical transformation of regenerating ocular surface epithelium. *Invest Ophthalmol Vis Sci* 16:14, 1977
170. Tseng, SCG, Hirst, LW, Farazdaghi, M, Green, WR: Goblet cell density and vascularization during conjunctival transdifferentiation. *Invest Ophthalmol Vis Sci* 25:1168, 1984
171. Kenyon KR, Tseng SCG: Limbal autograft transplantation for ocular surface disorders. *Ophthalmol* 96:709, 1989
172. Shimazaki J, Yang HY, Tsubota K: Amniotic membrane transplantation for ocular surface reconstruction in patients with chemical and thermal burns. *Ophthalmol* 104:2068, 1997
173. Tseng SCG, Barton K, Gray T, Meller D: Amniotic membrane transplantation with or without limbal allografts for corneal surface reconstruction in patients with stem cell deficiency. *Arch Ophthalmol* 116:431, 1998
174. Pellegrini G, Traverso CE, Franzi AT, et al: Long-term restoration of damaged corneal surfaces with autologous cultivated corneal epithelium. *Lancet* 349:1556, 1997
175. Kinoshita S, Koizumi N, Nakamura T: Transplantable cultivated mucosal epithelial sheet for ocular surface reconstruction. *Exp Eye Res* 78:483, 2004
176. Pires RTF, Tseng SCG, Prabhasawat P, et al: Amniotic membrane transplantation for symptomatic

bullous keratopathy. Arch Ophthalmol 117:1291, 1999

177. Meller D, Pires RTF, Mack RJS, et al: Amniotic membrane transplantation for acute chemical and thermal burns. Ophthalmol 107:980, 2000

178. Wolter JR: Reactions of the cellular elements of the corneal stroma. Arch Ophthalmol 59:873, 1958

179. Cintron C, Hassinger LC, Kublin CL, Cannon DJ: Biochemical and ultrastructural changes in collagen during corneal wound healing. J Ultrastruct Res 65:13, 1978

180. Hassell JR, Cintron C, Kublin C, Newsome DA: Proteoglycan changes during restoration of transparency in corneal scars. Arch Biochem Biophys 222:362, 1983

181. Cintron C, Covington HI, Kublin CL: Morphologic analyses of proteoglycans in rabbit corneal scars. Invest Ophthalmol Vis Sci 31:1789, 1990

182. Funderburgh JL, Cintron C, Covington HI, Conrad GW: Immunoanalysis of keratan sulfate proteoglycan from corneal scars. Invest Ophthalmol Vis Sci 29:1116, 1988

183. Binder PS, Wickham MG, Zavala EY, Akers PH: Corneal anatomy and wound healing . In Symposium on Medical and Surgical Diseases of the Cornea, Transactions of the New Orleans Academy of Ophthalmology. St. Louis, MO: CV Mosby, 1980:1

184. Mohan RR, Hutcheon AEK, Choi R, et al: Apoptosis, necrosis, proliferation, and myofibroblast generation in the stroma following LASIK and PRK. Exp Eye Res 76:71, 2003

185. Jester JV, Petroll WM, Cavanagh HD: Corneal stromal wound healing in refractive surgery: the role of myofibroblasts. Prog Retinal Eye Res 18:311, 1999

186. Zhao J, Nagasaki T, Maurice DM: Role of tears in kerocyte loss after epithelial removal in mouse cornea. Invest Ophthalmol Vis Sci 42:1743, 2001

187. Soong HK, Parkinson WC, Bafna S, et al: Movements of cultured corneal epithelial cells and stromal fibroblasts in electric fields. Invest Ophthalmol Vis Sci 31:2278, 1990

188. Watsky MA: Loss of keratocyte ion channels during wound healing in the rabbit cornea. Invest Ophthalmol Vis Sci 36:1095, 1995

189. Watsky MA: Lysophosphatidic acid, serum and hyposmolarity activate Cl^- currents in corneal keratocytes. Am J Physiol 38:C1385, 1995

190. Watsky MA, Griffith M, Xiaojuan X, et al: Lipid growth factors and wound healing. *Annals N Y Acad Sci* 905:142, 2000
191. Wang J, Carbone LD, Watsky MA: Receptor-mediated activation of a depolarizing Cl⁻ current by lysophosphatidic acid and sphingosine-1-phosphate in cultured corneal keratocytes. *Invest Ophthalmol Vis Sci* 43:3202, 2002
192. Wang D, Du H, Jaggar JH, et al: Expression and characterization of S1P and LPA receptors following rabbit corneal wound healing. *Am J Physiol* 283:C1646, 2002
193. Liliom K, Guan Z, Tseng JL, et al: Growth factor-like phospholipids generated following corneal injury. *Am J Physiol* 274:C1065, 1998
194. Jester JV, Barry-Lane PA, Cavanagh HD, Petroll WM: Induction of alpha-smooth muscle actin expression and myofibroblastic transformation in cultured corneal keratocytes. *Cornea* 15:505, 1996
195. Smith RS, Smith LA, Rich L, Weimar V: Effects of growth factors on corneal wound healing. *Invest Ophthalmol Vis Sci* 20:222, 1981
196. Weimar VL: Activation of initial wound healing responses in rat corneas in organ culture by mesodermal growth factor. *Invest Ophthalmol Vis Sci* 18:532, 1979
197. Hecquet C, Morisset S, Lorans G: Effects of acidic and basic fibroblast growth factors on the proliferation of rabbit and corneal cells. *Curr Eye Res* 9:429, 1990
198. Girard MT, Matsubara M, Fini ME: Transforming growth factor-β and interleukin-1 modulate metalloproteinase expression by corneal stromal cells. *Invest Ophthalmol Vis Sci* 32:2441, 1991
199. Woost PG, Brightwell J, Eiferman RA, Schultz GS: Effect of growth factors with dexamethasone on healing of rabbit corneal stromal incisions. *Exp Eye Res* 40:47, 1985
200. Kenney MC, Shih LM, Labermeir U, Satterfield D: Modulation of rabbit keratocyte production of collagen, sulfated glycosaminoglycans, and fibronectin by retinol and retinoic acid. *Acta Biochim Biophys* 889:156, 1986
201. Kirschmer SE, Ciaccia A, Ubels JL: The effect of retinoic acid on thymidine incorporation and morphology of corneal stromal fibroblasts. *Curr Eye Res* 9:1121, 1990
202. Johnson MK, Gebhardt BM, Berman MB: Appearance of collagenase in pneumolysin-treated fibroblast cultures. *Curr Eye Res* 7:951, 1988

203. Kenney MC, Chwa M, Escobar M, Brown D: Altered gelatinolytic activity by keratoconus corneal cells. *Biochem Biophys Res Commun* 161:353, 1989
204. Fujita H, Ueda A, Nishida T, Otori T: Uptake of india ink particles and latex beads by corneal fibroblasts. *Cell Tissue Res* 250:251, 1987
205. Mishima H, Yasumoto K, Nishida T, Otori T: Fibronectin enhances the phagocytic activity of cultured rabbit keratocytes. *Invest Ophthalmol Vis Sci* 28:1521, 1987
206. Mondino BJ, Sunda-Raj CV, Brady KJ: Production of first component of complement by corneal fibroblasts in tissue culture. *Arch Ophthalmol* 100:478, 1982
207. Taylor JL, O'Brien WJ: Interferon production and sensitivity of rabbit corneal epithelial and stromal cells. *Invest Ophthalmol Vis Sci* 26:1502, 1985
208. Taylor L, Menconi M, Leibowitz HM, Polgar P: The effect of ascorbate, hydroperoxides, and bradykinin on prostaglandin production by corneal and lens cells. *Invest Ophthalmol Vis Sci* 23:378, 1982
209. Awata T, Nishida T, Nakagawa S, Manabe R: Differential regulation of fibronectin synthesis in three different types of corneal cells. *Jpn J Ophthalmol* 33:132, 1989
210. Church RL: Procollagen and collagen produced by normal bovine corneal stroma fibroblasts in cell culture. *Invest Ophthalmol Vis Sci* 19:192, 1980
211. Conrad GW: Collagen and mucopolysaccharide biosynthesis in mass cultures of clones of chick corneal fibroblasts in vitro. *Dev Biol* 21:611, 1970
212. Klintworth GK, Smith CF: Difference between the glycosaminoglycans synthesized by corneal and cutaneous fibroblasts in culture. *Lab Invest* 44:553, 1981
213. Poschl A, Von Der Mark K: Synthesis of type V collagen by chick corneal fibroblasts in vivo and in vitro. *FEBS Lett* 115:110, 1980
214. Stoesser TR, Church RL, Brown SI: Partial characterization of human collagen and procollagen secreted by human corneal stromal fibroblasts in cell culture. *Invest Ophthalmol Vis Sci* 17:264, 1978
215. Yue TYJT, Hsieh P, Baum JL: Effects of corneal extracts on rabbit corneal stromal cells in culture. *Invest Ophthalmol Vis Sci* 27:14, 1986
216. Wilson SE, Liu JJ, Mohan RR: Stromal-epithelial interaction in the cornea. *Prog Retinal Eye Res* 18:293, 1999

217. Lemp MA: Cornea and sclera. Arch Ophthalmol 94:473, 1976.
218. Maurice DM: Castroviejo Lecture: The biology of wound healing in the corneal stroma. Cornea 6:162, 1987
219. Binder PS: Barraquer Lecture: What we have learned about corneal wound healing from refractive surgery. Refract Corneal Surg 5:98, 1989
220. Assil KK, Quantock AJ: Wound healing in response to keratorefractive surgery. Surv Ophthalmol 38:289, 1993
221. Jester JV, Moller-Pedersen T, Huang J, et al: The cellular basis of corneal transparency: evidence for corneal crystallins. J Cell Sci 112:613, 1999
222. Christensen L: Cataract-wound closure and healing. In Symposium on Cataracts. St. Louis, MO: CV Mosby, 1965:179
223. Flaxel JT, Swan KC: Limbal wound healing after cataract extraction: a histologic study. Arch Ophthalmol 81:653, 1969
224. Flaxel JT: Histology of cataract extraction. Arch Ophthalmol 83:436, 1970
225. Lang GK, Green WR, Maumenee AE: Clinicopathologic studies of keratoplasty eyes obtained post mortem. Am J Ophthalmol 101:28, 1986
226. Deg JK, Binder PS: Wound healing after astigmatic keratotomy in human eyes. Ophthalmol 94:1290, 1987
227. Melles GRJ, Binder PS: A comparison of wound healing in sutured and unsutured corneal wounds. Arch Ophthalmol 108:1460, 1990
228. Melles GRJ, Binder PS, Anderson JA: Variation in healing throughout the depth of long-term, unsutured, corneal wounds in human autopsy specimens and monkeys. Arch Ophthalmol 112:100, 1994
229. Melles GRJ, Binder PS, Moore MN, Anderson JA: Epithelial-stromal interactions in human keratotomy wound healing. Arch Ophthalmol 113:1124, 1995
230. Jester JV, Villasenor RA, Schanzlin DJ, Cavanaugh HD: Variations in corneal wound healing after radial keratotomy: possible insights into mechanisms of clinical complications and refractive effects. Cornea 11:191, 1992

231. Wu WC, Stark WJ, Green WR: Corneal wound healing after 193-nm excimer laser keratectomy. Arch Ophthalmol 109:1426, 1991
232. Taylor DM, L'Esperance FA, Del Pero RA, et al: Human excimer laser lamellar keratectomy: a clinical study. Ophthalmol 96:654, 1989
233. Anderson NJ, Edelhauser HF, Sharara N, et al: Histologic and ultrastructural findings in human corneas after successful laser in situ keratomileusis. Arch Ophthalmol 120:288, 2002
234. Kramer TR, Dawson DG, Chuckpaiwong V, et al: Pathologic findings in the cornea after successful LASIK surgery. Cornea 24:92, 2005
235. Dawson DG, Kramer TR, Grossniklaus HE, et al: Histologic, ultrastructural, and immunofluorescent evaluation of human laser in situ keratomileusis corneal wounds. Arch Ophthalmol, 123:741, 2005
236. Honda H, Higuchi OS, Kani K, Ogita Y: Cell movements in a living mammalian tissue: Long-term observation of individual cells in wounded endothelia of cats. J Morphol 174:25, 1982
237. Matsuda M, Sawa M, Edelhauser HF, et al: Cellular migration and morphology in corneal endothelial wound repair. Invest Ophthalmol Vis Sci 26:443, 1985
238. Yee RW, Geroski DH, Matsuda M, et al: Correlation of corneal endothelial pump site density, barrier function, and morphology in wound repair. Invest Ophthalmol Vis Sci 26:1191, 1985
239. Ling T, Vannas A, Holden BA: Long-term changes in corneal endothelial morphology following wounding in the cat. Invest Ophthalmol Vis Sci 29:1407, 1988
240. Landshman N, Ben-Hanan I, Assia E, et al: Relationship between morphology and functional ability of regenerated corneal endothelium. Invest Ophthalmol Vis Sci 29:1100, 1988
241. Griffith M, Osborne R, Munger R, et al: A functional human corneal equivalent from cell lines. Science 286:2169, 1999
242. Doillon C, Watsky MA, Munger R, et al: A stabilized collagen-based scaffold for a tissue engineered cornea: Physical and physiological properties. Int J Artificial Organs 26:764, 2003
243. Suuronen EJ, Nakamura M, Stys PK, et al: Innervated human corneal equivalents as *in vitro* models for nerve-target interactions. FASEB J 18:17, 2004
244. Schimmelpfennig B: Nerve structures in human central corneal epithelium. Graefes Arch Clin Exp

245. Muller LJ, Marfurt CF, Kruse F, Tervo TMT: Corneal nerves: structure, contents, and function. *Exp Eye Res* 76:521, 2003

246. Magendie J: De la influencia de la cinquieme paire nerfts surla nutrition et les fonctions de loeil. *J Physiol* 4:176, 1824

247. Wilson SE, Ambrosio R: Laser in situ keratomileusis-induced neurotrophic epitheliopathy. *Am J Ophthalmol* 132:405, 2001

248. Kauffman T, Bodanowitz S, Hesse L, Kroll P: Corneal reinnervation after photorefractive keratectomy and laser in situ keratomileusis: An in vivo study with a confocal videomicroscope. *Ger J Ophthalmol* 5:508, 1996

249. Millodot M: Objective measurement of corneal sensitivity. *Acta Ophthalmol* 51:325, 1973

250. Boberg-Ans J: On the corneal sensitivity. *Acta Ophthalmol* 34(suppl):149, 1976

251. Kumano MH, Zushi I, Yamada T, et al: Corneal sensation after correction of myopia by photorefractive keratectomy and laser in situ keratomileusis. *J Cataract Refract Surg* 27:370, 2001

252. Watson PG, Young RD: Scleral structure, organization, and diseases. A review. *Exp Eye Res* 78:609, 2004

253. Foster CS, de la Maza MS: *The Sclera*. New York, NY: Springer-Verlag, 1994

254. Hogan MJ, Zimmerman LE: *Ophthalmic pathology. An atlas and textbook*. Philadelphia: WB Saunders, 1962

255. Hogan MJ, Alvarado JA, Weddell JE: *Histology of the Human Eye. An Atlas and Textbook*. Philadelphia: WB Saunders, 1971: 183

256. Olsen TW, Aaberg T, Edelhauser HF: Thickness of human sclera. *Am J Ophthalmol* 125:237, 1998

257. Borcharding MS, Blacik LJ, Sittig RA, et al: Proteoglycans and collagen fibre organization in human corneoscleral tissue. *Exp Eye Res* 21:59, 1975

258. Meyer PAR, Watson PG: Low dose fluorescein angiography of the conjunctiva and episclera. *BJO* 71:2, 1987

259. St. Helen R, McEwen W: Rheology of human sclera: I. Anelastic behavior. *Am J Ophthalmol* 52:539, 1961
260. M. Barza, Kane A, Baum JL: Regional differences in ocular concentration of gentamicin after subconjunctival and retrobulbar injection in the rabbit. *Am J Ophthalmol* 83:407, 1977
261. Barza M, Kane A, Baum JL: Intraocular penetration of gentamicin after subconjunctival and retrobulbar injection. *Am J Ophthalmol* 85:541, 1978
262. Bill A: Movement of albumin and dextran through the sclera. *Arch Ophthalmol* 72:248, 1965
263. Maurice DM, Polgar J: Diffusion across the sclera. *Exp Eye Res* 25:577, 1977
264. Edelhauser HF, Maren TH: Permeability of human cornea and sclera to sulfonamide carbonic anhydrase inhibitors. *Arch Ophthalmol* 106:1110, 1988
265. Ahmed I, Patton TF: Importance of the noncorneal absorption route in topical ophthalmic drug delivery. *Invest Ophthalmol Vis Sci* 26:584, 1985
266. Olsen TW, Edelhauser HF, Lim JI, Geroski DH: Human scleral permeability: Effects of age, cryotherapy, transscleral diode laser, and surgical thinning. *Invest Ophthalmol Vis Sci* 36:1893, 1995
267. Prausnitz MR, Noonan JS: Permeability of cornea, sclera, and conjunctiva: A literature analysis for drug delivery to the eye. *J Pharm Sci* 87:1479, 1998
268. Ambati J, Canakis CS, Miller JW, et al: Diffusion of high molecular weight compounds through sclera. *Invest Ophthalmol Vis Sci* 41:1181, 2000
269. Rudnick DE, Noonan JS, Geroski DH, et al: The effect of intraocular pressure on human and rabbit scleral permeability. *Invest Ophthalmol Vis Sci* 40:3054, 1999
270. Ambati J, Gragoudas ES, Miller JW, et al: Transscleral delivery of bioactive protein to the choroid and retina. *Invest Ophthalmol Vis Sci* 41:1186, 2000.
271. Simpson AE, Gilbert JA, Rudnick DE, et al: Transscleral diffusion of carboplatin: An in vitro and in vivo study. *Arch Ophthalmol* 120:1069, 2002
272. Gilbert JA, Simpson AE, Rudnick DE, et al: In vivo transscleral permeability and in vivo intraocular concentrations of cisplatin from a collagen matrix. *J Controlled Release* 89:409, 2003

273. Weijtens O, Schoemaker RC, Lentjes EGWM, et al: High concentration of dexamethasone in aqueous and vitreous after subconjunctival injection. *Am J Ophthalmol* 128:192, 1999

274. Weijtens O, Schoemaker RC, Lentjes EGWM, et al: Dexamethasone concentration in the subretinal fluid after a subconjunctival injection, a peribulbar injection, or an oral dose. *Am J Ophthalmol* 107:1932, 2000

275. Anecortave Acetate Clinical Study Group: Anecortave acetate as monotherapy for treatment of subfoveal neovascularization in age-related macular degeneration. *Ophthalmol* 110:2372, 2003